



UNIVERSITA' DEGLI STUDI ROMA TRE
Department of Mathematics

Doctoral School in Mathematical and Physical Sciences
XXII Cycle A.Y. 2009

Doctorate Thesis
Università Roma Tre - Université de la Méditerranée
Co-tutorship agreement

Semiclassical analysis of Loop Quantum Gravity

Dr. Claudio Perini

Director of the Ph.D. School:

prof. Renato Spigler
Roma Tre University, Department of Mathematics, Rome

Supervisors:

prof. Fabio Martinelli
Roma Tre University, Department of Mathematics, Rome

prof. Carlo Rovelli
Université de la Méditerranée, Centre de Physique Théorique de Luminy, Marseille

Contents

1	Introduction	4
2	Hamiltonian General Relativity	8
2.1	<i>Canonical formulation of General Relativity in ADM variables</i>	8
2.2	<i>Lagrangian and ADM Hamiltonian</i>	9
2.3	<i>Triad formalism</i>	11
2.4	<i>Ashtekar-Barbero variables</i>	11
2.5	<i>Constraint algebra</i>	12
2.6	<i>The holonomy</i>	14
3	The structure of Loop Quantum Gravity	16
3.1	<i>Kinematical state space</i>	16
3.2	<i>Solution to the Gauss and diffeomorphism constraints</i>	18
3.3	<i>Electric flux operator</i>	22
3.4	<i>Holonomy-flux algebra and the C^*-algebraic viewpoint</i>	24
3.5	<i>Area and volume operators</i>	25
3.6	<i>Physical interpretation of quantum geometry</i>	26
3.7	<i>Dynamics</i>	27
4	Covariant formulation: Spin Foam	30
4.1	<i>Path integral representation</i>	30
4.2	<i>Regge discretization</i>	32
4.3	<i>Quantum Regge calculus and spinfoam models</i>	34
4.4	<i>BF theory</i>	36
4.5	<i>Barret-Crane model</i>	37
5	A new model: EPRL vertex	40
5.1	<i>The goal of the model: imposing weakly the simplicity constraints</i>	40
5.2	<i>Description of the model</i>	41
6	Asymptotics of LQG fusion coefficients	47
6.1	<i>Analytical expression for the fusion coefficients</i>	47
6.2	<i>Asymptotic analysis</i>	49
6.3	<i>Semiclassical behavior</i>	53
6.4	<i>The case $\gamma = 1$</i>	55
6.5	<i>Summary of semiclassical properties of fusion coefficients</i>	56
6.6	<i>Properties of $9j$-symbols and asymptotics of $3j$-symbol</i>	57
7	Numerical investigations on the semiclassical limit	58
7.1	<i>Wave-packets propagation</i>	58
7.2	<i>The semi-analytic approach</i>	63
7.3	<i>Physical expectation values</i>	64

7.4	<i>Improved numerical analysis</i>	65
8	Semiclassical states for quantum gravity	66
8.1	<i>Livine-Speziale coherent intertwiners</i>	68
8.2	<i>Coherent tetrahedron</i>	70
8.3	<i>Bianchi-Magliaro-Perini coherent spin-networks</i>	72
8.4	<i>Resolution of the identity and holomorphic representation</i>	77
9	Graviton propagator in Loop Quantum Gravity	80
9.1	<i>n-point functions in generally covariant field theories</i>	81
9.2	<i>Compatibility between of radial, Lorenz and harmonic gauges</i>	83
9.2.1	<i>Maxwell theory</i>	85
9.2.2	<i>Linearized General Relativity</i>	87
10	LQG propagator from the new spin foams	90
10.1	<i>Semiclassical boundary state and the metric operator</i>	91
10.2	<i>The new spin foam dynamics</i>	96
10.3	<i>LQG propagator: integral formula</i>	97
10.4	<i>Integral formula for the amplitude of a coherent spin-network</i>	97
10.5	<i>LQG operators as group integral insertions</i>	98
10.6	<i>LQG propagator: stationary phase approximation</i>	100
10.7	<i>The total action and the extended integral</i>	100
10.8	<i>Asymptotic formula for connected two-point functions</i>	101
10.9	<i>Critical points of the total action</i>	102
10.10	<i>Hessian of the total action and derivatives of the insertions</i>	103
10.11	<i>Expectation value of metric operators</i>	105
10.12	<i>LQG propagator: the leading order</i>	106
10.13	<i>Comparison with perturbative quantum gravity</i>	109
11	Conclusions and outlook	111

1 Introduction

In the last century, General Relativity and Quantum Mechanics revolutionized the physics and demolished two deep-rooted prejudices about Nature: the determinism of physical laws and the absolute, inert character of space and time. At the same time they explained most of the phenomena that we observe. In particular the microscopic observations of nuclear and subnuclear physics have been explained within the Quantum Field Theory (QFT) called Standard Model of particle physics, and, on the other side, the large scale phenomena of the Universe have been explained within General Relativity (GR). QM and GR are the two conceptual pillars on which modern physics is built. GR has modified the notion of space and time; QM the notion of causality, matter and measurements, but these modified notions do not fit together easily. The basic assumptions of each one of the two theories are contradicted by the other. On the one hand QM is formulated in a Newtonian absolute, fixed, non-dynamical space-time, while GR describes spacetime as a dynamical entity: it is no more an external set of clocks and rods, but a physical interacting field, namely the gravitational field. Moreover the electromagnetic, weak and strong interactions, unified in the language of Quantum Field Theory, obeys the laws of quantum mechanics, and on the other side the gravitational interaction is described by the classical deterministic theory of General Relativity. Both theories work extremely well at opposite scales but this picture is clearly incomplete [1] unless we want to accept that Nature has opposite foundations in the quantum and in the cosmological realm. QM describes microscopic phenomena involving fundamental particles, ignoring completely gravity, while GR describes macroscopic systems, whose quantum properties are in general (safely) neglected. This is not only a philosophical problem, but assumes the distinguishing features of a real scientific problem as soon as one considers measurements in which both quantum and gravitational effects cannot be neglected. The search for a theory which merges GR and QM in a whole coherent picture is the search for a theory of Quantum Gravity (QG). If one asks the question:

why do we need Quantum Gravity?

the answers are many. It is worth recalling that the theory describing the gravitational interaction fails in giving a fully satisfactory description of the observed Universe. General relativity, indeed, leads inevitably to space-time singularities as a number of theorems mainly due to Hawking and Penrose demonstrate. The singularities occur both at the beginning of the expansion of our Universe and in the collapse of gravitating objects to form black holes. Classical GR breaks completely down at these singularities, or rather it results to be an incomplete theory. On the quantum mechanical side, we can ask what would happen if we managed to collide an electron-positron pair of energy (in the center of mass) greater than the Planck energy. We are unable to give an answer to this question. The reason of this failure is related to the fact that, in such an experiment, we cannot neglect the gravitational properties of the involved particles at the moment of the collision. But, we do not have any scientific information on how taking into account such an effect in the framework of QFT. In other words, when the gravitational field is so intense that space-time geometry evolves on a very short time scale, QFT cannot be consistently applied any longer. Or, from another perspective, we can say that when the gravitational effects are so strong to produce the emergence of spacetime singularities, field theory falls into troubles.

A possible attempt for quantizing gravity is the one that leads to perturbative Quantum Gravity, the conventional quantum field theory of gravitons (spin 2 massless particles) propagating over Minkowski

spacetime. Here the metric tensor is splitted in

$$g_{\mu\nu} = \eta_{\mu\nu} + h_{\mu\nu}$$

and η is treated as a background metric (in general any solution to Einstein equations) and h is a dynamical field representing self-interacting gravitons. This theory gives some insights but cannot be considered a good starting point because it brakes the general covariance of General Relativity, and (more practically) it is non-renormalizable. It is remarkable that it *is* possible to construct a quantum theory of a system with an infinite number of degrees of freedom, without assuming a fixed background causal structure; this is the framework of modern background independent theories of quantum General Relativity, called Loop Quantum Gravity.

The energy regime where we expect quantum gravity effects to become important (Planck scale) is outside our experimental or observational capabilities. But we emphasize that it could be not necessary to reach the Planck energy to see some QG effects. In this respect, we recall that a class of extremely energetic phenomena called Gamma Ray Bursts could represent a really important laboratory to test QG predictions [2, 3, 4, 5, 6], in fact they seem to be the natural candidates to verify whether the fundamental hypothesis about a discrete structure of space-time will be confirmed by experiments. The peculiar features which make Gamma Ray Bursts relevant for QG is the extremely wide range of the emitted energies and the cosmological distance of the explosive events.

Loop quantum gravity has the main objective to merge General Relativity and quantum mechanics. Its major features [7] are resumed in the following.

- LQG is the result of “canonical” quantization of Hamiltonian General Relativity.
- It implements the teachings of General Relativity. First, the physical laws are relational: only events independent from coordinates are meaningful; physics must be described by generally covariant theories. Second, the gravitational field is the geometry of spacetime. The spacetime geometry is dynamical: the gravitational field defines the geometry on top of which its own degrees of freedom and those of matter fields propagate. GR is not a theory of fields moving on a curved background geometry, GR is a theory of fields moving on top of each other, namely it is background independent.
- It assumes QM, suitably formulated to be compatible with general covariance, to be correct; also the Einstein equations, though they can be modified at high energy, are assumed to be correct, and are the starting point of the quantization process.
- It is non perturbative: the metric is *not* split in a Minkowskian background plus a dynamical perturbation. The full metric tensor is dynamical.
- There are not extra-dimensions: it is formulated in four spacetime dimensions. We can say more: the whole framework works only for a 4-dimensional spacetime!
- The major physical prediction is the discrete and combinatorial structure for quantum spacetime: the spectra of geometrical observables, such as the length, the area and the volume operator, are discrete [8] and the quantum states of geometry have a relational character. Discreteness and the appearance of a fundamental Plankian length scale, renders the theory UV finite.

- Its application in cosmology gave rise to Loop Quantum Cosmology [9]. Some of the main results achieved by this theory are the explanation of the Bekenstein-Hawking formula for black-hole entropy [10, 11, 12, 13] and the absence of the initial Big Bang singularity [14]. Instead of a singularity, the theory predicts a “bouncing”.

In the following we present the research line carried out during the PhD, which come together in this thesis.

The kinematics of LQG is well understood, mathematically rigorous and almost without quantization ambiguities. Conversely, even if still well-defined, the dynamics of the theory is plagued by quantization ambiguities. The Hamiltonian quantum constraint defined by Thiemann is the most popular realization of the LQG dynamics, but many others are possible; a natural requirement is that the quantum dynamics should not give rise to anomalies, namely it should respect the classical algebra of constraints. This non-trivial requirement is satisfied by Thiemann’s Hamiltonian. Nevertheless, because of the complicated form of the Hamiltonian, we do not have control on which kind of quantum evolution it generates, in particular if the correct semiclassical dynamics is reproduced. In other words, it is technically difficult to understand the link (if any) between classical and quantum dynamics. Like in ordinary QFT, a covariant formulation could help to find an answer.

Spin foams provide a non-perturbative and background independent definition of the path integral for General Relativity, and at the same time they are an attempt to define the covariant version of LQG. In this context it is easier to implement the dynamics. The hope is to find a clear-cut connection between spin foam models and Loop Quantum Gravity. The “new spin foam models” (both the Euclidean and the Lorentzian ones) realize the kinematical equivalence between canonical and covariant approaches [15], while the full equivalence has been proven only in three dimensions [16]. In this thesis we will analyze the LQG dynamics through spin foams, hoping that one day the equivalence of the two formalisms will be proven also in four dimensions.

The recovering of the right semiclassical limit is perhaps the most important test for a quantum theory. A possible way of studying the semiclassical limit of LQG is the comparison of n -point functions computed in LQG with the ones of standard perturbative quantum gravity. The main issue with this approach is even to formally *define* n -point functions which are background independent: the dependence on the n points seems indeed to disappear if we implement diffeomorphism invariance in the path integral. We can go over this difficulty using the general boundary formalism for background independent field theories [17]. Using this general boundary framework and the “new” spin foam models we computed the connected 2-point function, or graviton propagator, in LQG finding an exact matching with the standard propagator. More specifically, we recovered the right scaling behavior of all tensorial components; moreover the full tensorial structure matches with the standard one in a particular limit, and in a particular gauge. This non trivial result shows that the new models are an improvement of the previous Barret-Crane spin foam model, since there, as shown in [18], some components of the propagator had the wrong scaling.

The second original result presented in this thesis is a simple asymptotic formula for the fusion coefficients [19], which are a building block of the vertex amplitude of the new models. A consequence of our asymptotic analysis is the following remarkable semiclassical property of the fusion coefficient: they map semiclassical $SO(3)$ tetrahedra into semiclassical $SO(4)$ tetrahedra; this peculiar property sheds light on the semiclassical limit of the “new” models.

Another criterion to select the good semiclassical behavior is the stability under evolution of coherent wave-packets. The introduction of this approach [20] and its improvement [21] are another original con-

tribution to the subject of semiclassical analysis in LQG. The main idea is as old as quantum physics: a theory has the correct semiclassical limit only if semiclassical wave-packets follow the trajectory predicted by classical equations of motion. The equations of motion of any dynamical system can be expressed as constraints on the set formed by the initial, final and (if it is the case) boundary variables. For instance, in the case of the evolution of a free particle in the time interval t , the equations of motion can be expressed as constraints on the set $(x_i, p_i; x_f, p_f)$. These constraints are of course $m(x_f - x_i)/t = p_i = p_f$ (for the general logic of this approach to dynamics, see [7]). In General Relativity, Einstein equations can be seen as constraints on boundary variables; we can construct in LQG semiclassical wave packets centered on the classical value of conjugate geometric quantities (intrinsic and extrinsic curvature, analogous to x and p). It follows immediately from these considerations that a boundary wave packet centered on these values must be correctly propagated by the propagation kernel, if the vertex amplitude is to give the Einstein equations in the classical limit. We studied numerically the propagation of some degrees of freedom of LQG, finding preliminary indications on the good semiclassical behavior. The propagation of semiclassical equilateral tetrahedra in the boundary of a 4-simplex is “rigid”, that is four Gaussian wavepackets evolve into one Gaussian wavepacket with the same shape, except for a flip in the phase. This is in agreement with the geometry of one flat 4-simplex, the most simple instance of Einstein equations in the discretized setting. This result was the first, though preliminary, indication of the good semiclassical properties of the new spin foam models.

The semiclassical states used in the calculation of the propagator are put by hand but nevertheless are motivated by geometrical intuition and by the requirement that they fit well with the spin foam dynamics in order to reproduce the classical limit of the amplitudes computed, e.g. expectation values of geometric operators and correlation functions. In this thesis we give a beautiful top-down derivation of those states, as states centered on a point in the phase space of General Relativity, as captured by a graph. More precisely we recover the states used in spin foam calculations in the large spin limit, so that the latter can be viewed as approximate coherent states; the exact coherent states are here called *coherent spin-networks*, and are candidate semiclassical states for full Loop Quantum Gravity. Their geometrical interpretation is the following. A space-time metric (e.g. Minkowski or deSitter space-time) induces an intrinsic and extrinsic geometry of a spatial slice Σ . A graph Γ embedded in Σ is dual to a cellular decomposition of Σ . The graph captures a finite amount of geometrical data: in fact we can smear the Ashtekar-Barbero connection on links of the graph and the gravitational electric field on surfaces dual to links. These smeared quantities are the labels for the coherent spin-networks. An interesting fact about these labels is that for each edge of the graph they are in correspondence with elements in $SL(2, \mathbb{C})$, that can be viewed as the cotangent bundle of $SU(2)$ and carries a natural phase space (symplectic) structure. For this reason the labels of coherent spin-networks live on the phase space of GR as captured by a single graph.

2 Hamiltonian General Relativity

In this chapter we briefly summarize the Hamiltonian formulation of General Relativity. It turns out that the Hamiltonian is a linear combination of first class constraints, in the terminology of Dirac [22]; these constraints generate gauge transformations and define the dynamics of General Relativity with respect to the arbitrarily chosen time parameter. In order to quantize the theory, we perform a suitable change of variables: we introduce the Ashtekar-Barbero connection. Then we express the constraints in these new variables and write their commutation algebra. We conclude introducing the concept of holonomy which will play a major role in the quantum theory.

2.1 Canonical formulation of General Relativity in ADM variables

The Hamiltonian formulation of a field theory requires the splitting of the spacetime in space and time [23, 24, 25, 26, 27]. The first step is the choice of a time function t and a vector field t^μ over the spacetime manifold such that the hypersurfaces Σ_t at constant t are Cauchy spacelike surfaces and $t^\mu \nabla_\mu t = 1$. The second step is the definition of a configuration space of fields q over Σ_t and conjugate momenta Π . The last step is the introduction of a Hamiltonian: a functional $H[q, \Pi]$ of the form

$$H[q, \Pi] = \int_{\Sigma_t} \mathcal{H}(q, \Pi), \quad (1)$$

where \mathcal{H} is the Hamiltonian density; the Hamilton equations $\dot{q} = \frac{\delta \mathcal{H}}{\delta \Pi}$ and $\dot{\Pi} = -\frac{\delta \mathcal{H}}{\delta q}$ are equivalent to the field equations of Lagrangian theory. Given the Lagrangian formulation there is a standard prescription to obtain the Hamiltonian one by the Legendre transformation

$$\mathcal{H}(q, \Pi) = \Pi \dot{q} - \mathcal{L}, \quad (2)$$

where $\dot{q} = \dot{q}(q, \Pi)$ and $\Pi = \frac{\partial \mathcal{L}}{\partial \dot{q}}$.

Now consider General Relativity [28] on a globally hyperbolic spacetime $(M, g_{\mu\nu})$. This spacetime can be foliated in Cauchy surfaces Σ_t , parametrized by a global time function $t(x^0, x^1, x^2, x^3)$. Take n^μ the unitary vector field normal to Σ_t . The spacetime metric induces a spatial metric $h_{\mu\nu}$ on every Σ_t given by the formula

$$h_{\mu\nu} = g_{\mu\nu} + n_\mu n_\nu. \quad (3)$$

The metric $h_{\mu\nu}$ is spatial in the sense that $h_{\mu\nu} n^\mu = 0$. Take t^μ a vector field on M satisfying $t^\mu \nabla_\mu t = 1$; we decompose it in its tangent and normal components to Σ_t

$$t^\mu = N^\mu + N n^\mu, \quad (4)$$

where

$$N = -t^\mu n_\mu = (n^\mu \nabla_\mu t)^{-1}, \quad (5)$$

$$N_\mu = h_{\mu\nu} t^\nu. \quad (6)$$

We can interpret the vector field t^μ as the “flux of time” across spacetime, in fact we “move forward in time” with the parameter t starting from the surface Σ_0 and reaching the surface Σ_t . If we identify the

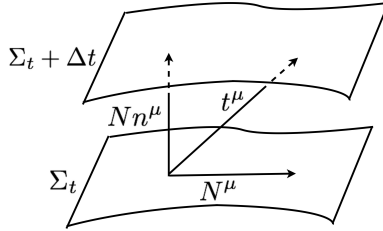


Figure 1: ADM foliation

hypersurfaces Σ_0 and Σ_t through the diffeomorphism obtained by following the integral curves of t^μ , we can reinterpret the effect of moving through time as a changing spatial metric on a *fixed* 3-dimensional manifold Σ from $h_{ab}(0)$ to $h_{ab}(t)$. Hence we can view a globally hyperbolic spacetime as the representation of a time evolution of a Riemannian metric on a fixed 3-dimensional manifold. The quantity N is called lapse function and measures the flow of proper time with respect to the time coordinate t when we move in a direction normal to Σ_t . N^μ is called shift vector and it measures the shift of t^μ in direction tangent to Σ_t . The fields N and N^μ are not dynamical as they only describe the way of moving through time. Suitable initial data of the Cauchy problem for General Relativity are the spatial metric $h_{\mu\nu}$ on Σ_0 and its “time derivative”. The notion of time derivative of a spatial metric on Σ_t is provided by the extrinsic curvature

$$K_{\mu\nu} \equiv \nabla_\mu \xi_\nu, \quad (7)$$

where ξ_ν is the unitary timelike vector field tangent to the timelike geodesics normal to Σ_t (ξ^μ is equal to n^μ on Σ_t). $K_{\mu\nu}$ is purely spatial; it can be expressed as a Lie derivative

$$K_{\mu\nu} = \frac{1}{2} \mathcal{L}_\xi g_{\mu\nu} = \frac{1}{2} \mathcal{L}_\xi h_{\mu\nu}. \quad (8)$$

If we choose $N^\mu = 0$, then the extrinsic curvature is simply

$$K_{\mu\nu} = \frac{1}{2} \frac{\partial h_{\mu\nu}}{\partial t}. \quad (9)$$

In terms of general N , N^μ and t^μ , the metric is given by

$$g^{\mu\nu} = h^{\mu\nu} - n^\mu n^\nu = h^{\mu\nu} - N^{-2} (t^\mu - N^\mu)(t^\nu - N^\nu), \quad (10)$$

where we have used the identity $n^\mu = N^{-1}(t^\mu - N^\mu)$.

2.2 Lagrangian and ADM Hamiltonian

The Lagrangian density for General Relativity in empty space is $\mathcal{L}_{\text{GR}} = (2\kappa)^{-1} \sqrt{-g} R$, with R the Ricci scalar and $\kappa = 8\pi G/c^3$. G is Newton’s gravitational constant, and c the speed of light. The action of

General Relativity is then

$$S_{\text{GR}} = \frac{1}{2\kappa} \int d^4x \sqrt{-g} R. \quad (11)$$

The Hamiltonian analysis is made passing to the variables N , N^μ , $h_{\mu\nu}$. In terms of these variables the Lagrangian density reads

$$\mathcal{L}_{\text{GR}} = \frac{1}{2\kappa} \sqrt{h} N [{}^{(3)}R + K_{\mu\nu} K^{\mu\nu} - K^2], \quad (12)$$

where $K_{\mu\nu}$ can be written as

$$K_{\mu\nu} = \frac{1}{2N} [\dot{h}_{\mu\nu} - D_\mu N_\nu - D_\nu N_\mu], \quad (13)$$

D_μ is the covariant derivative with respect to $h_{\mu\nu}$, ${}^{(3)}R$ is the Ricci scalar calculated with respect to $h_{\mu\nu}$, and $\dot{h}_{\mu\nu} = h_\mu{}^\rho h_\nu{}^\sigma \mathcal{L}_t h_{\rho\sigma}$.

The momentum conjugate to $h_{\mu\nu}$ is

$$\Pi^{\mu\nu} = \frac{\delta L}{\delta \dot{h}_{\mu\nu}} = \frac{1}{2\kappa} \sqrt{h} (K^{\mu\nu} - K h^{\mu\nu}). \quad (14)$$

The Lagrangian does not contain any temporal derivative of N and N^a , so their conjugate momenta are zero. As anticipated, the fields N and N^a are not dynamical, so they can be considered as Lagrange multipliers in the Lagrangian. Variation of the action (11) w.r.t. shift and lapse produces the following constraints:

$$V^\nu[h, \Pi] \equiv -2D_\mu (h^{-1/2} \Pi^{\mu\nu}) = 0, \quad (15)$$

$$S[h, \Pi] \equiv -(h^{1/2} [{}^{(3)}R - h^{-1} \Pi_{\rho\sigma} \Pi^{\rho\sigma} + \frac{1}{2} h^{-1} \Pi^2]) = 0. \quad (16)$$

The first is called vector constraint, and the second scalar constraint. These constraints, together with the Hamilton equations

$$\dot{h}_{\mu\nu} = \frac{\delta H}{\delta \Pi^{\mu\nu}}, \quad (17)$$

$$\dot{\Pi}^{\mu\nu} = -\frac{\delta H}{\delta h_{\mu\nu}}, \quad (18)$$

define the dynamics of General Relativity, i.e. they are equivalent to vacuum Einstein equations. Finally, the Hamiltonian density is

$$\mathcal{H}_{\text{GR}} = \frac{1}{2\kappa} h^{1/2} \{ N [-{}^{(3)}R + h^{-1} \Pi_{\mu\nu} \Pi^{\mu\nu} - \frac{1}{2} h^{-1} \Pi^2] - 2N_\nu [D_\mu (h^{-1/2} \Pi^{\mu\nu})] \}. \quad (19)$$

We deduce that the Hamiltonian is a linear combination of (first class) constraints, i.e. it vanishes identically on the solutions of equations of motion. This is a general property of generally covariant systems.

The variables chosen in this formulation are called ADM (Arnowitt, Deser and Misner) [29] variables. Notice that ADM variables are tangent to the surface Σ_t , so we can use equivalently the genuinely 3-dimensional quantities h_{ab} , Π^{ab} , N^a , N ($a, b = 1, 2, 3$); these are the pull back on Σ_t of the 4-dimensional ones.

2.3 Triad formalism

The spatial metric h_{ab} can be written as

$$h_{ab} = e_a^i e_b^j \delta_{ij} \quad i, j = 1, 2, 3, \quad (20)$$

where $e_a^i(x)$ is a linear transformation which permits to write the metric in the point x in flat diagonal form. The index i of e_a^i is called internal and e_a^i is called a triad, or better co-triad, because it defines a set of three 1-forms. The triad can be seen as a map from the co-tangent bundle to the Euclidean space, preserving the scalar product. We can introduce the densitized inverse triad

$$E_a^i \equiv \frac{1}{2} \epsilon_{abc} \epsilon^{ijk} e_b^j e_c^k; \quad (21)$$

using this definition, the inverse 3-metric h^{ab} is related to the densitized triad as follows:

$$h^{ab} = E_i^a E_j^b \delta^{ij}. \quad (22)$$

We also define

$$K_a^i \equiv \frac{1}{\sqrt{\det(E)}} K_{ab} E_j^b \delta^{ij}. \quad (23)$$

It is not difficult to see that E_i^a and K_a^i are conjugate Hamiltonian variables, so the symplectic structure is

$$\{E_j^a(x), K_b^i(y)\} = \kappa \delta_b^a \delta_j^i \delta(x, y), \quad (24)$$

$$\{E_j^a(x), E_i^b(y)\} = \{K_a^j(x), K_b^i(y)\} = 0. \quad (25)$$

We can write the vector and the scalar constraint (15-16) in terms of the new conjugate variables E_i^a and K_a^i . However these variables are redundant; in fact we are using the nine E_i^a to describe the six independent components of h^{ab} . This is clear also from a geometrical point of view: we can choose different triads e_a^i acting by local $SO(3)$ rotations on the internal index i without changing the metric:

$$R_m^i(x) R_n^j(x) e_a^m(x) e_b^n(x) \delta_{ij} = e_a^i e_b^j \delta_{ij}. \quad (26)$$

Hence if we want to formulate General Relativity in terms of these redundant variables we have to impose an additional constraint that makes the redundancy manifest. The missing constraint is:

$$G_i(E_j^a, K_a^j) \equiv \epsilon_{ijk} E^{aj} K_a^k = 0. \quad (27)$$

For a review on the triad formalism, see e.g. [30].

2.4 Ashtekar-Barbero variables

We can now introduce the Ashtekar-Barbero connection [31, 32, 33, 34, 35], defined in terms of the previous canonically conjugate variables (E_i^a, K_a^i) as follows:

$$A_a^i = \Gamma_a^i(E) + \gamma K_a^i, \quad (28)$$

where $\Gamma_i^a(E)$ is the spin connection, that is the unique solution to the Cartan structure equation

$$\partial_{[a}e_{b]}^i + \epsilon^i{}_{jk}\Gamma_{[a}^j e_{b]}^k = 0 \quad (29)$$

and γ is any non zero real number, called Barbero-Immirzi parameter. Explicitly, the solution of (29) is

$$\Gamma_a^i(E) = -\frac{1}{2}\epsilon^{ij}{}_{k}e_j^b(\partial_{[a}e_{b]}^k + \delta^{kl}\delta_{ms}e_l^m\partial_b e_c^s). \quad (30)$$

By an explicit computation, the Poisson brackets between the new variables are

$$\{E_j^a(x), K_b^i(y)\} = \kappa\gamma\delta_b^a\delta_j^i\delta(x, y), \quad (31)$$

$$\{E_j^a(x), E_i^b(y)\} = \{A_a^i(x), A_b^j(y)\} = 0. \quad (32)$$

This non trivial fact is remarkable, because it means that

$$(E_i^a, \Gamma_a^i) \longrightarrow (\frac{1}{\gamma}E_i^a, A_a^i) \quad (33)$$

is a canonical transformation. The new variables put classical General Relativity in a form which closely resembles an $SU(2)$ Yang-Mills theory. Indeed A_a^i and E_i^a are the components of a connection and of an electric field respectively. This follows from their transformation properties under local $SU(2)$ gauge transformations. Writing

$$A_a = A_a^i\tau_i \in su(2) \quad (34)$$

$$E^a = E_i^a\tau^i \in su(2) \quad (35)$$

where τ^i are $su(2)$ generators, the transformation rules are

$$A'_a = gA_ag^{-1} + g\partial_ag^{-1}, \quad E'^a = gE^ag^{-1}, \quad (36)$$

that is the standard transformation rules for connections and electric fields of Yang-Mills theories. We can push the analogy even further looking at the constraints. This is done in the next section.

2.5 Constraint algebra

As we have seen, General Relativity can be formulated in terms of a real $su(2)$ connection¹ $A_a^i(x)$ and a real momentum field $E_i^a(x)$, called electric field, both defined on a 3-dimensional differential manifold Σ_t . The theory is defined by the Hamiltonian system constituted by the three constraints (27), (15), (16), and the Hamilton equations. In terms of the new variables the full set of constraints is

$$G_i \equiv D_a E_i^a = 0, \quad (37)$$

$$V_b \equiv E_i^a F_{ab}^i - (1 + \gamma^2)K_b^i G_i = 0, \quad (38)$$

$$S \equiv \frac{E_i^a E_j^b}{\sqrt{\det(E)}} (\epsilon^{ij}{}_{k} F_{ab}^k - 2(1 + \gamma^2)K_{[a}^i K_{b]}^j) = 0, \quad (39)$$

¹The groups $SO(3)$ and $SU(2)$ have the same Lie algebra, so we can speak equivalently about connections with values in $su(2)$ or $su(3)$.

where D_a and F_{ab}^i are respectively the covariant derivative and the curvature of the connection A_a^i defined by

$$D_a v_i = \partial_a v_i - \epsilon_{ijk} A_a^j v^k, \quad (40)$$

$$F_{ab}^i = \partial_a A_b^i - \partial_b A_a^i + \epsilon^i_{jk} A_a^j A_b^k. \quad (41)$$

As anticipated, the electric field satisfies the Gauss law, whose differential version is exactly the first constraint (37). This Gauss constraint is also present in the Hamiltonian formulation of Yang-Mills theories.

The system (37-39) generates gauge transformations. To see this, define the smeared constraints

$$G(\alpha) \equiv \int_{\Sigma} d^3x \alpha^i G_i = \int_{\Sigma} d^3x \alpha^i D_a E_i^a = 0, \quad (42)$$

$$V(f) \equiv \int_{\Sigma} d^3x f^a V_a = 0, \quad (43)$$

$$S(N) \equiv \int_{\Sigma} d^3x N S. \quad (44)$$

The “test” functions α^i , f^a , N are an internal vector field, a tangent vector field and a scalar field respectively. A direct calculation implies

$$\delta_{\alpha} A_a^i = \{A_a^i, G(\alpha)\} = -D_a \alpha^i \quad \text{and} \quad \delta_{\alpha} E_i^a = \{E_i^a, G(\alpha)\} = [E^a, \alpha]_i \quad (45)$$

which are the infinitesimal version of the $SU(2)$ gauge transformations (36) (the square brackets in (45) are the vector field commutator). The constraint (37) is in the form of the Gauss law of Yang-Mills theories. For the smeared vector constraint we have

$$\delta_f A_a^i = \{A_a^i, V(f)\} = \mathcal{L}_f A_a^i = f^b F_{ab}^i \quad \text{and} \quad \delta_f E_i^a = \{E_i^a, V(f)\} = \mathcal{L}_f E_i^a, \quad (46)$$

so $V(f)$ acts as the infinitesimal diffeomorphism associated to the vector field f , namely as a Lie derivative \mathcal{L} . Finally, one can show that the scalar constraint S generates time evolution w.r.t. the time parameter t . In fact the Hamiltonian of General Relativity is the sum of the smeared constraints (42-44):

$$H[\alpha, N^a, N] = G(\alpha) + V(N^a) + S(N), \quad (47)$$

and the Hamilton equations of motion are therefore

$$\dot{A}_a^i = \{A_a^i, H[\alpha, N^a, N]\} = \{A_a^i, G(\alpha)\} + \{A_a^i, V(N^a)\} + \{A_a^i, S(N)\}, \quad (48)$$

$$\dot{E}_i^a = \{E_i^a, H[\alpha, N^a, N]\} = \{E_i^a, G(\alpha)\} + \{E_i^a, V(N^a)\} + \{E_i^a, S(N)\}. \quad (49)$$

These equations define the action of $H[\alpha, N^a, N]$ on observables (phase space functions), that is their time evolution up to diffeomorphisms and $SU(2)$ gauge transformations. In General Relativity coordinate time evolution has no physical meaning; it is analogous to a $U(1)$ gauge transformation of QED.

Next, we can compute all possible Poisson brackets between the smeared constraints, obtaining the following constraint algebra:

$$\{G(\alpha), G(\beta)\} = G([\alpha, \beta]), \quad (50)$$

$$\{G(\alpha), V(f)\} = G(\mathcal{L}_f \alpha), \quad (51)$$

$$\{G(\alpha), S(N)\} = 0, \quad (52)$$

$$\{V(f), V(g)\} = V([f, g]), \quad (53)$$

$$\{S(N), V(f)\} = -S(\mathcal{L}_f N), \quad (54)$$

$$\{S(N), S(M)\} = V(\tilde{f}) + \text{terms proportional to Gauss law}, \quad (55)$$

where $\tilde{f}^a = h^{ab}(N\partial_b M - \partial_b N)$. We can also give the Hamilton-Jacobi system by writing

$$E_i^a(x) = \frac{\delta \mathcal{S}[A]}{\delta A_a^i(x)} \quad (56)$$

in (37-39). The constraints (37) and (38) require the invariance of $\mathcal{S}[A]$ under local $SU(2)$ transformations and 3-dimensional diffeomorphisms. The last one, (39), is the Hamilton-Jacobi equation for General Relativity. A preferred solution to the Hamilton-Jacobi equation is the Hamilton functional. This is defined as the value of the action of a bounded region, computed on a solution of the field equations determined by the boundary configuration A_a^i .

2.6 The holonomy

The concept of holonomy has a major role in the quantization of General Relativity. It is a group element giving the parallel transport of vectors along curves. Consider a Lie(G)-valued connection A defined on a vector bundle with base manifold M and structure group G (the gauge group), and a curve γ on the base manifold parametrized as

$$\gamma : [0, 1] \rightarrow M \quad (57)$$

$$s \mapsto x^\mu(s). \quad (58)$$

The holonomy $H[A, \gamma]$ of the connection A along the curve γ is the element of G defined as follows. Consider the differential equation

$$\frac{d}{ds} h(s) + \dot{x}^\mu(s) A_\mu(\gamma(s)) h(s) = 0, \quad (59)$$

with initial data

$$h(0) = \mathbb{1}, \quad (60)$$

where $h(s)$ is a G -valued function of the parameter s . The solution to this Cauchy problem is

$$h(s) = \mathcal{P} \exp \int_0^s d\tilde{s} A^i(\tilde{s}) \tau_i, \quad (61)$$

where τ_i is a basis of the Lie algebra of the group G and $A^i(s) \equiv \dot{\gamma}^\mu(s) A_\mu^i(\gamma(s))$. The path ordered exponential $\mathcal{P} \exp$ is defined through the series

$$\mathcal{P} \exp \int_0^s d\bar{s} A(\gamma(\bar{s})) \equiv \sum_{n=0}^{\infty} \int_0^s ds_1 \int_0^{s_1} ds_2 \dots \int_0^{s_{n-1}} ds_n A(\gamma(s_n)) \dots A(\gamma(s_1)). \quad (62)$$

Finally, the holonomy of the connection A along γ is defined as

$$H[A, \gamma] \equiv \mathcal{P} \exp \int_0^1 ds A^i(s) \tau_i = \mathcal{P} \exp \int_\gamma A. \quad (63)$$

Intuitively, the connection A is the rule that defines the meaning of infinitesimal parallel transport of an internal vector from a point of M to another near point: the vector v in x is defined parallel to the vector $v + A_\mu dx^\mu v$ in $x + dx$. The holonomy gives the parallel transport for points at finite distance. A vector is parallel transported along γ into the vector $H[A, \gamma]v$. Notice that even if there is a finite set of points where γ is not smooth and A is not defined, the holonomy of a curve γ is well-defined; we can break γ in smooth pieces and define the holonomy as the product of holonomies associated to the smooth pieces. For the applications to quantum gravity, we will be concerned with a base manifold given by the spatial slice Σ_t and with $SU(2)$ as gauge group. In Spin Foams, we will consider $SO(4)$ or $SO(1,3)$ holonomies over the 4-dimensional spacetime manifold.

3 The structure of Loop Quantum Gravity

In this section review the “canonical” quantization of Hamiltonian General Relativity; in other words we introduce Loop Quantum Gravity (LQG). We exhibit the states satisfying some of the quantum constraints, and construct the basic geometric operators. We show that length, area and volume operators have a discrete (quantized) spectrum. The quantum dynamics is defined by the quantization of the scalar constraint. The main physical prediction of Loop Quantum Gravity is that spacetime is fundamentally discrete, the minimal quanta being of size of the order of the Planck length.

3.1 Kinematical state space

At the intuitive level, the quantum states of Hamiltonian General Relativity in Ashtekar-Barbero variables are Schrödinger wave functionals $\Psi[A]$ of the classical configuration variable, like in the Schrödinger representation of ordinary quantum mechanics. The classical Hamilton function $\mathcal{S}[A]$ is interpreted as \hbar times the phase of $\Psi[A]$, i.e. we interpret the classical Hamilton-Jacobi equation as the iconal approximation of the quantum wave equation. This can be obtained substituting the derivative of the Hamilton functional (the electric field) with derivative operators. The quantization of the first two constraints require the invariance of $\Psi[A]$ under $SU(2)$ gauge transformations and 3-dimensional diffeomorphisms. Imposing the scalar constraint leads to the Wheeler-DeWitt equation that governs the quantum dynamics of spacetime.

Cylindrical functions: $\text{Cyl}(\mathcal{A})$ Consider the set \mathcal{A} of smooth 3-dimensional real connections A_a^i defined everywhere (except, possibly isolated points) on a 3-dimensional surface Σ with the topology of the 3-sphere. Consider also an ordered collection Γ (graph) of L smooth oriented paths γ_l ($l = 1, \dots, L$), called links of the graph, and a smooth complex valued function $f(g_1, \dots, g_L)$ of L group elements; smoothness of f is with respect to the standard differential structure on $SU(2)$. A couple (Γ, f) defines the complex functional of A

$$\Psi_{\Gamma, f}[A] \equiv f(H[A, \gamma_1], \dots, H[A, \gamma_L]) \quad (64)$$

where $H[A, \gamma]$ is the holonomy of the connection along the path. We call functionals of this form “cylindrical functions”; their linear span (vector space of their finite linear combinations) is denoted with $\text{Cyl}(\mathcal{A})$.

Scalar product on the space of cylindrical functions If two functionals $\Psi_{\Gamma, f}[A]$ and $\Psi_{\Gamma, h}[A]$ are supported on the same oriented graph Γ , we define the inner product

$$\langle \Psi_{\Gamma, f}, \Psi_{\Gamma, h} \rangle \equiv \int dg_1, \dots, dg_L \overline{f(g_1, \dots, g_L)} h(g_1, \dots, g_L), \quad (65)$$

where dg is the Haar measure over $SU(2)$ (the unique normalized bi-invariant regular Borel measure over a compact group). The previous definition extends to functionals supported on different graphs. If Γ and Γ' are two disjoint graphs with n and n' curves respectively, define the union graph $\tilde{\Gamma} = \Gamma \cup \Gamma'$ with $n + n'$ curves. If we define

$$\tilde{f}(g_1, \dots, g_n, g_{n+1}, \dots, g_{n+n'}) \equiv f(g_1, \dots, g_n), \quad (66)$$

$$\tilde{h}(g_1, \dots, g_n, g_{n+1}, \dots, g_{n+n'}) \equiv h(g_{n+1}, \dots, g_{n+n'}); \quad (67)$$

then we put

$$\langle \Psi_{\Gamma, f}, \Psi_{\Gamma', h} \rangle \equiv \langle \Psi_{\tilde{\Gamma}, \tilde{f}}, \Psi_{\tilde{\Gamma}, \tilde{h}} \rangle. \quad (68)$$

If Γ and Γ' are not disjoint, we can break $\Gamma \cup \Gamma'$ into the two disjoint pieces Γ and $\Gamma' - (\Gamma \cap \Gamma')$, so we are in the previous case. Notice that cylindrical functions do not live on a single graph but rather on all possible graphs embedded in Σ_t , so we can already envisage the profound difference with lattice Yang-Mills theories, which are defined over a fixed lattice. In quantum GR we are not cutting any short (or large) scale degree of freedom.

Kinematical Hilbert space The kinematical Hilbert space \mathcal{H}_{kin} of quantum gravity is the completion of $\text{Cyl}(\mathcal{A})$ w.r.t. the previous inner product:

$$\mathcal{H}_{\text{kin}} = \overline{\text{Cyl}(\mathcal{A})}. \quad (69)$$

In order to have at our disposal also distributional states, we consider the topological dual of $\text{Cyl}(\mathcal{A})$ to build the Gelfand triple

$$\mathcal{S} \subset \mathcal{K} \subset \mathcal{S}' \quad (70)$$

which constitutes the kinematical rigged Hilbert space. The kinematical Hilbert space can be viewed as an L^2 space

$$\mathcal{H}_{\text{kin}} = L^2(\overline{\mathcal{A}}, d\mu_{\text{AL}}) \quad (71)$$

where $\overline{\mathcal{A}}$ is a suitable distributional extension of \mathcal{A} and $d\mu_{\text{AL}}$ the Ashtekar-Lewandowski measure [36]. The key to construct a basis in \mathcal{H}_{kin} is the Peter-Weyl theorem, which states that an orthonormal basis for the Hilbert space $L^2(G, \text{dg})$, where G is a compact group, is given by the matrix elements of unitary irreducible representations. The unitary irreducible representations of $SU(2)$

$$SU(2) \longrightarrow \text{Hom}(\mathcal{H}_j) \quad (72)$$

$$g \longrightarrow \overset{j}{\Pi}(g) \quad (73)$$

are labeled by non-negative half-integers $j \in \mathbb{N}/2$ called spins, in analogy with the theory of angular momentum in quantum mechanics. The carrying Hilbert space is $\mathcal{H}_j \equiv \mathbb{C}^{2j+1}$. Thus an orthonormal basis for \mathcal{H}_{kin} is

$$\Psi_{\Gamma, j_l, \alpha_l, \beta_l}[A] \equiv \sqrt{\dim(j_1) \dots \dim(j_L)} \overset{j}{\Pi}_{\beta_1}^{\alpha_1}(H[A, \gamma_1]) \dots \overset{j_L}{\Pi}_{\beta_L}^{\alpha_L}(H[A, \gamma_L]), \quad (74)$$

where $\dim(j) = (2j + 1)$ is the dimension of the representation space of spin j . These functions, called open spin-networks, are labeled by an oriented graph embedded in Σ , a spin for each link (or edge) of the graph, and the matrix indices (two for each link). Since graphs embedded in the 3-manifold Σ are uncountable, it follows from the definition of the scalar product that the kinematical Hilbert space is clearly non separable.

An interesting class of states are the traces of holonomies over a single closed loop α :

$$\Psi_{\alpha, j}[A] = \text{Tr} \overset{j}{\Pi}[A, \alpha] \quad (75)$$

These are the most simple gauge invariant states, as we will see in the next section. For historical reasons, Loop Quantum Gravity takes its name from the loop states.

Intuitively, the Hilbert space \mathcal{H}_{kin} is formed by Schrödinger wave functions of the connection. Then, at least formally, the connection itself must be quantized as a multiplication operator, and the electric field as a functional derivative operator:

$$\widehat{A}_a^i(x)\Psi[A] = A_a^i(x)\Psi[A], \quad (76)$$

$$\widehat{E}_i^a(x)\Psi[A] = -i\hbar\kappa\gamma\frac{\delta}{\delta A_a^i(x)}\Psi[A]. \quad (77)$$

3.2 Solution to the Gauss and diffeomorphism constraints

The quantum Gauss and vector constraints impose the invariance of kinematical states under local $SU(2)$ transformations and 3-dimensional diffeomorphisms of the spatial slice Σ . Let us see how.

Under local $SU(2)$ gauge transformations $g : \Sigma \rightarrow SU(2)$, connection and holonomy transform as

$$A_g = gAg^{-1} + g dg^{-1}, \quad (78)$$

$$U[A_g, \gamma] = g(x_f)U[A, \gamma]g(x_i)^{-1}, \quad (79)$$

where $x_i, x_f \in \Sigma$ are the initial and final points of the oriented path γ . We can define the action of the Gauss constraint on a cylindrical function $\Psi_{\Gamma, f} \in \text{Cyl}(\mathcal{A})$:

$$U(g)\Psi_{\Gamma, f}[A] \equiv \Psi_{\Gamma, f}[A_g^{-1}] = f(g(x_f^{\gamma_1})g_1g(x_i^{\gamma_1})^{-1}, \dots, g(x_f^{\gamma_L})g_Lg(x_i^{\gamma_L})^{-1}). \quad (80)$$

From the definition (65) of scalar product, it follows that it is invariant under gauge transformations. It is easy to prove that the transformation law (80) extends to a unitary representation of gauge transformations over the whole \mathcal{H}_{kin} . Now consider an invertible function $\phi : \Sigma \rightarrow \Sigma$ such that the function and its inverse are smooth everywhere, except possibly in a finite number of isolated points where they are only continuous. Call the set of these functions extended diffeomorphisms Diff^* . Under an extended diffeomorphism the connection transforms as a 1-form:

$$A \mapsto \phi^*A, \quad (81)$$

where ϕ^* is the push-forward map, and the holonomy transforms as

$$U[A, \gamma] \mapsto U[\phi^*A, \gamma] = U[A, \phi^{-1}\gamma], \quad (82)$$

that is applying a diffeomorphism ϕ to A is equivalent to applying the diffeomorphism to the curve γ . The action of $\phi \in \text{Diff}^*$ on cylindrical functions $\Psi_{\Gamma, f}$ is then defined as:

$$U(\phi)\Psi_{\Gamma, f}[A] = \Psi_{\Gamma, f}[(\phi^*)^{-1}A] = \Psi_{\phi^{-1}\Gamma, f}[A]. \quad (83)$$

It is immediate to verify that the scalar product is Diff^* -invariant, and that (83) also extends to a unitary representation on \mathcal{H}_{kin} .

In this way we have easily implemented at the quantum level the classical kinematical gauge symmetries which are the (semi-direct) product of local gauge transformations and diffeomorphisms; most importantly, no anomalies arise.

Intertwiners The space solution to the Gauss constraint is easily expressed by first introducing the objects called *intertwiners*. Consider N irreducible representations of $SU(2)$, labeled by spins j_1, \dots, j_N , and their tensor product which act on the space

$$\mathcal{H}_{j_1 \dots j_N} \equiv \mathcal{H}_{j_1} \otimes \dots \otimes \mathcal{H}_{j_N} \quad (84)$$

where $\mathcal{H}_j \simeq \mathbb{C}^{2j+1}$. The tensor product (84) decomposes into a direct sum of irreducible subspaces. In particular

$$\mathcal{H}_{j_1 \dots j_N}^0 \equiv \text{Inv } \mathcal{H}_{j_1 \dots j_N} \subset \mathcal{H}_{j_1 \dots j_N} \quad (85)$$

is the subspace formed by invariant tensors, called N -valent *intertwiners*. The k -dimensional space of intertwiners decomposes in the k 1-dimensional irreducible subspaces. Choosing a basis for each \mathcal{H}_j , we can use an index notation: intertwiners are N -index objects $v^{\alpha_1 \dots \alpha_N}$ with an index for each representation, invariant under the joint action of $SU(2)$:

$$\prod_{\beta_1}^{j_1 \alpha_1} (g) \dots \prod_{\beta_N}^{j_N \alpha_N} (g) v^{\beta_1 \dots \beta_N} = v^{\alpha_1 \dots \alpha_N} \quad \forall g \in SU(2). \quad (86)$$

We will use the notation $v_i^{\alpha_1 \dots \alpha_N}$ with $i = 1, \dots, k$ to denote a set of k such invariant tensors, orthonormal w.r.t. the standard scalar product in $\mathcal{H}_{j_1 \dots j_N}$:

$$\overline{v_i^{\alpha_1 \dots \alpha_N}} v_{i'}^{\alpha_1 \dots \alpha_N} = \delta_{ii'}. \quad (87)$$

Solution to the Gauss constraint: spin-network states Spin-network [37, 38] states are labeled by an embedded oriented graph Γ , a set of spin labels j_l (one for each link l), and a set of intertwiners i_n (one for each node n). They are obtained by contraction of the open spin-network states (74) with the intertwiners:

$$\Psi_{\Gamma, j_l, i_n} [A] = \sum_{\alpha_l \beta_l} v_{i_1}^{\beta_1 \dots \beta_{n_1}} \alpha_1 \dots \alpha_{n_1} v_{i_2}^{\beta_{n_1+1} \dots \beta_{n_2}} \alpha_{n_1+1} \dots \alpha_{n_2} \dots v_{i_N}^{\beta_{n_{N-1}+1} \dots \beta_L} \alpha_{n_{N-1}+1} \dots \alpha_L \Psi_{\Gamma, j_l, \alpha_l, \beta_l} [A]. \quad (88)$$

The pattern of contraction of the indices is dictated by the topology of the graph itself: the index α_l (β_l) of the link l is contracted with the corresponding index of the intertwiner v_{i_n} of the node n where the link l begins (ends). To an N -valent node it is associated an N -valent intertwiner between the spins meeting at the node. $SU(2)$ indices are raised and lowered with the ϵ tensor, which is the intertwiner between a representation and its dual. In the fundamental $1/2$ representation, its matrix form is

$$\epsilon^{1/2} = \begin{pmatrix} 0 & 1 \\ -1 & 0 \end{pmatrix}. \quad (89)$$

The importance of spin-network states is that they form an orthonormal basis of the subspace of \mathcal{H}_{kin} solution of the Gauss constraint, namely the gauge-invariant subspace. Gauge invariance follows immediately from the invariance of the intertwiners and from the transformation properties (80).

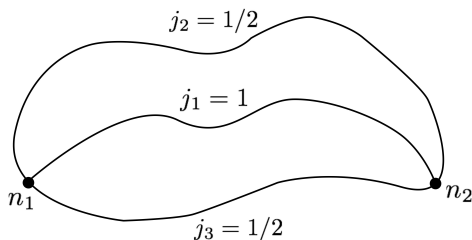


Figure 2: A spin-network with two trivalent nodes

Examples The most simple example of (gauge invariant) spin-network state is the loop state (75). Another more complicated example is given in figure 2. We have to associate to each node an intertwiner between two fundamental (i.e. $j = 1/2$) and one adjoint (i.e. $j = 1$) irreducible representations. Since their tensor product contains a single 1-dimensional (i.e. $j = 0$) representation,

$$\frac{1}{2} \otimes \frac{1}{2} \otimes 1 = (0 \oplus 1) \otimes 1 = 1 \oplus 0 \oplus 1 \oplus 2, \quad (90)$$

there is a unique normalized intertwiner, represented by the triple of Pauli matrices: $v_{AB}^i = \frac{1}{\sqrt{3}}\sigma_{AB}^i$; hence the spin-network state associated to the graph in figure 2 is:

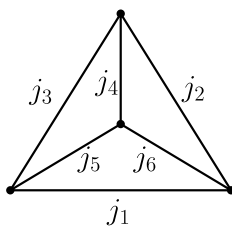
$$\Psi[A] = \prod (H[A, \gamma_2])_B^A \sigma_i^B \prod (H[A, \gamma_1])_j^i \sigma^{j,D} \prod (H[A, \gamma_3])_D^C. \quad (91)$$

Four-valent intertwiners: virtual links In the case of 3-valent nodes (like in the previous example) there is only one possible (normalized) intertwiner, namely the 3-valent intertwiner space is 1-dimensional. If the node is instead 4-valent, the normalized intertwiner is no more unique. A possible basis is obtained by decomposition in virtual links, that is writing the intertwiner as the contraction of two 3-valent intertwiners. Explicitly, the virtual basis $\{v_i^{abcd}\}$ is

$$v_i^{abcd} = v^{dae} v_e^{bc} = \sqrt{2i+1} \begin{array}{c} j_4 \quad j_3 \\ \diagdown \quad \diagup \\ i \\ \diagup \quad \diagdown \\ j_1 \quad j_2 \end{array} \quad (92)$$

where a dashed line has been used to denote, in the language of Feynman diagrams, the virtual link associated to the coupling channel; the index e is in the representation i and each node represents Wigner $3j$ -symbols (related in a simple way to the Clebsh-Gordan coefficients). The link labeled by i is called virtual link, and the open links labeled by j_1, j_4 are said to be *paired*, or *coupled*. Two other choices of pairing (coupling channels) are possible, giving two other bases:

$$\tilde{v}_i^{abcd} = \sqrt{2i+1} \begin{array}{c} j_4 \quad j_3 \\ \diagdown \quad \diagup \\ i \\ \diagup \quad \diagdown \\ j_1 \quad j_2 \end{array}, \quad \tilde{\tilde{v}}_i^{abcd} = \sqrt{2i+1} \begin{array}{c} j_4 \quad j_3 \\ \diagdown \quad \diagup \\ i \\ \diagup \quad \diagdown \\ j_1 \quad j_2 \end{array}. \quad (93)$$


 Figure 3: $6j$ -symbol

The formula for the change of pairing, called recoupling theorem, is

$$\begin{array}{c} d \\ \diagdown \\ \text{---} \\ \diagup \\ c \\ \text{---} \\ \text{---} \\ \diagup \\ a \\ \diagdown \\ b \end{array} = \sum_m \dim(m) (-1)^{b+c+f+m} \left\{ \begin{array}{ccc} a & c & m \\ d & b & f \end{array} \right\} \begin{array}{c} a \\ \diagdown \\ \text{---} \\ \diagup \\ d \\ \text{---} \\ \text{---} \\ \diagup \\ c \\ \diagdown \\ b \end{array}, \quad (94)$$

where

$$\left\{ \begin{array}{ccc} j_1 & j_2 & j_3 \\ j_4 & j_5 & j_6 \end{array} \right\} \quad (95)$$

is the Wigner $6j$ -symbol. The $6j$ -symbol is defined as the contraction of four $3j$ -symbols, according to the tetrahedral pattern in figure 3.

Solution to the diffeomorphism constraint Spin-network states are not invariant under diffeomorphisms, because a generic diffeomorphism changes the underlying graph; it can also modify the link ordering and orientation. Diffeomorphism-invariant states must be searched in \mathcal{S}' , the distributional extension of \mathcal{H}_{kin} . Recall that \mathcal{S}' is formed by all the continuous linear functionals over the space of cylindrical functions. The action of the extended diffeomorphism group is defined in \mathcal{S}' by duality

$$U_\phi \Phi(\Psi) \equiv \Phi(U_{\phi^{-1}} \Psi), \quad \forall \Psi \in \mathcal{S} \quad (96)$$

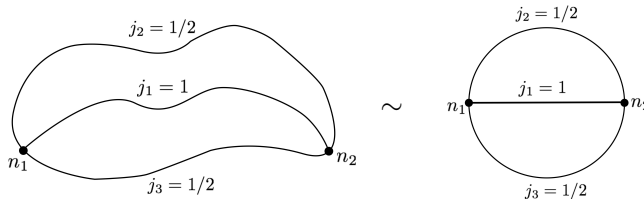
where U_ϕ is the action (83), so a diffeomorphism invariant state Φ is such that

$$\Phi(U_\phi \Psi) = \Phi(\Psi). \quad (97)$$

We can define formally [39, 40] a “projection” map onto the solutions of the diffeomorphism constraint

$$\begin{aligned} P_{\text{Diff}} : \mathcal{S} &\rightarrow \mathcal{S}' \\ (P_{\text{Diff}} \Psi)(\Psi') &= \sum_{\Psi''=U_\phi \Psi} \langle \Psi'', \Psi' \rangle \end{aligned} \quad (98)$$

The sum is over all the states $\Psi'' \in \mathcal{S}$ for which there exist a diffeomorphism $\phi \in \text{Diff}^*$ such that $\Psi'' = U_\phi \Psi$; the main point is that this sum is effectively over a finite set, because a diffeomorphism acting on a cylindrical function can either transform it in an orthogonal state, or leave it unchanged, or



change the link ordering and orientation, but these latter operations are discrete and contribute only with a multiplicity factor. We shall write $\mathcal{S}'_{\text{Diff}}$ for the space of solutions of the diffeomorphism *and* Gauss constraint. Clearly $P_{\text{Diff}^*}\Psi$ and the image of P_{Diff^*} is $\mathcal{H}_{\text{Diff}}$. The scalar product on $\mathcal{S}_{\text{Diff}^*}$ is naturally defined as

$$\langle \Phi, \Phi' \rangle_{\text{Diff}^*} = \langle P_{\text{Diff}^*}\Psi, P_{\text{Diff}^*}\Psi' \rangle_{\text{Diff}^*} \equiv P_{\text{Diff}^*}\Psi(\Psi'). \quad (99)$$

Denote $\phi_k\Psi_\Gamma$ the state obtained from a spin-network Ψ_Γ by a diffeomorphism ϕ_k , where the maps $\{\phi_k\}$ form the discrete subgroup of diffeomorphisms which change only ordering and orientation of the graph Γ . For any two spin-networks supported on Γ and Γ' respectively, it is clear that

$$\langle P_{\text{Diff}^*}\Psi_\Gamma, P_{\text{Diff}^*}\Psi_{\Gamma'} \rangle = \begin{cases} 0 & \Gamma \neq \phi\Gamma' \text{ for all } \phi \in \text{Diff}^* \\ \sum_k \langle \Psi_\Gamma, \phi_k\Psi_{\Gamma'} \rangle & \Gamma = \phi\Gamma' \text{ for some } \phi \in \text{Diff}^* \end{cases} \quad (100)$$

An equivalence class under extended diffeomorphisms of non oriented graphs is called a knot; two spin-networks Ψ_Γ and $\Psi_{\Gamma'}$ define orthogonal states in $\mathcal{S}'_{\text{Diff}^*}$ unless they are in the same equivalence class. So states in $\mathcal{S}'_{\text{Diff}^*}$ are labeled by a knot and they are distinguished only by the coloring of links and nodes. The orthonormal states obtained coloring links and nodes are called spin-knot states, or abstract spin-networks, and, very often, simply spin-networks.

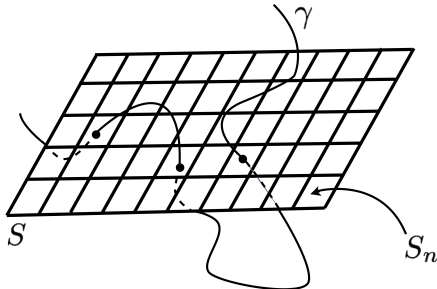
3.3 Electric flux operator

The operators (76) and (77) are not well defined in \mathcal{H}_{kin} . The situation is quite similar to the quantum mechanics of a particle on the real line, where the position and momentum operators are not well-defined on $L^2(\mathbb{R}, dx)$, but a suitable regularization, or smearing, of them is well defined. The smearing of the connection A along a path γ gives nothing else then the holonomy; the corresponding operator $\widehat{H}[A, \gamma]$ is a well-defined self-adjoint multiplication operator on \mathcal{H}_{kin} . It is defined as

$$\widehat{H}[A, \gamma]^A{}_B \Psi[A] = H[A, \gamma]^A{}_B \Psi[A] \quad (101)$$

where $H[A, \gamma]$ is intended in the fundamental, spin 1/2, representation of $SU(2)$. Also the electric field must be smeared. In fact it is a densitized vector, which is naturally smeared over surfaces. Before doing this passage, it is instructive to write the action of the electric field operator \widehat{E} on spin-networks, at formal level, using distributions. In particular, its action on a single holonomy functional in the fundamental representation (the generalization to arbitrary representations is trivial) is:

$$\frac{\delta}{\delta A_a^i(y)} H[A, \gamma] = \int ds \dot{x}^a(s) \delta^3(x(s), y) (H[A, \gamma_1] \tau_i H[A, \gamma_2]), \quad (102)$$


 Figure 4: A partition of \mathbf{S}

where s is an arbitrary parametrization of the curve γ , $x^a(s)$ are the coordinates along the curve, γ_1 and γ_2 are the two parts in which γ is splitted by the point $x(s)$, and δ^3 is a Dirac delta distribution. Its effect is to insert $SU(2)$ generators τ_i between the splitted holonomies, an operation called *grasping* of holonomies. Note that the r.h.s. of (3.3) is a two-dimensional distribution (δ^3 is integrated over a curve), hence also from this “quantum” point of view it is natural to look for a well-defined operator smearing \hat{E} over a 2-dimensional surface.

Consider a two-dimensional surface S embedded in the 3-dimensional manifold Σ ; be $\sigma = (\sigma^1, \sigma^2)$ coordinates on S . The embedding is defined by $S : (\sigma^1, \sigma^2) \mapsto x^a(\sigma^1, \sigma^2)$. Classically, the quantity we are going to quantize is the electric flux:

$$E_i(S) \equiv -i\hbar\kappa\gamma \int_S d\sigma^1 d\sigma^2 n_a(\sigma) E_i^a(\sigma), \quad (103)$$

where

$$n_a(\sigma) = \epsilon_{abc} \frac{\partial x^b(\sigma)}{\partial \sigma^1} \frac{\partial x^c(\sigma)}{\partial \sigma^2} \quad (104)$$

is the 1-form normal to S . The observable $E_i(S)$ is quantized with the replacement $E_i^a \rightarrow \hat{E}_i^a$ inside (103). If we now compute the action of $\hat{E}_i(S)$ on the holonomy, using we obtain

$$\hat{E}_i(S)H[A, \gamma] = -i\hbar\kappa\gamma \int_S \int_\gamma d\sigma^1 d\sigma^2 ds \epsilon_{abc} \frac{\partial x^a}{\partial \sigma^1} \frac{\partial x^b}{\partial \sigma^2} \frac{\partial x^c}{\partial s} \delta^3(x(\sigma), x(s)) H(A, \gamma_1) \tau_i H(A, \gamma_2). \quad (105)$$

This integral vanishes unless the curve γ and the surface S intersect. In the case they have a single intersection, the result is

$$\hat{E}_i(S)H(A, \gamma) = \pm i\hbar\kappa\gamma H(A, \gamma_1) \tau_i H(A, \gamma_2), \quad (106)$$

where the sign is dictated by the relative orientation of γ w.r.t. the surface. The electric flux operator simply act *grasping* the holonomies. When many intersections p are present (like in figure 4) the result is

$$\hat{E}_i(S)H(A, \gamma) = \sum_p \pm i\hbar\kappa\gamma H(A, \gamma_1^p) \tau_i H(A, \gamma_2^p), \quad (107)$$

and the sum is over intersections. The action on an arbitrary representation of the holonomy is

$$\widehat{E}_i(S) \overset{j}{R}(H[A, \gamma]) = \sum_p \pm \hbar \kappa \gamma \overset{j}{\Pi}(H[A, \gamma_1^p]) \overset{j}{\tau}_i \overset{j}{\Pi}(H[A, \gamma_2^p]), \quad (108)$$

where τ are now generators of a generic representation j . It is easy to extend the electric flux to a self-adjoint operator on the whole Hilbert space \mathcal{H}_{kin} , in particular on its $\text{SU}(2)$ gauge-invariant subspace.

3.4 Holonomy-flux algebra and the C^* -algebraic viewpoint

We have found a well-defined quantization of holonomies and electric fluxes over a suitable Hilbert space of Schrödinger wave functionals. Now we just have to solve the scalar constraint (we have already solved the Gauss and diffeomorphism constraints), then start posing physical questions about quantum geometry, the semiclassical limit of the theory and so on. Before attempting to do this, it is of great interest to ask how much this construction is unique: which are the hypothesis bringing to the Loop Quantum Gravity representation?

We answer (partially) sketching the recipes of algebraic quantization, and then enunciating the LOST uniqueness theorem. The first step is to choose a basic set of classical observables \mathcal{P} (a Poisson algebra) and then considering the corresponding abstract $*$ -algebra (algebra of quantum observables) obtained by identifying ($i\hbar$ times) Poisson brackets with commutators and complex conjugation with involution operation $*$. It is the free tensor algebra $T(\mathcal{P})$ over \mathcal{P} modulo the 2-sided ideal generated by elements of the form

$$fg - gf - i\hbar\{f, g\}. \quad (109)$$

The representation theory on Hilbert spaces of the abstract $*$ -algebra defines the quantum theory. If the classical theory have first class constraints which generate gauge transformations, these should be well (unitarily) implemented as operators in the quantum theory. Recall that if we give a state ω (positive linear functional) on a $*$ -algebra \mathcal{A} which is invariant under a group of automorphisms G , we can construct the corresponding GNS representation (ξ, π, \mathcal{H}) , where $\pi(a)$ ($a \in \mathcal{A}$) is the representation of a as a bounded linear operator on the Hilbert space \mathcal{H} , and ξ is a cyclic vector, i.e. its image under π is dense. The cyclic vector is such that $\langle \xi, \pi(a)\xi \rangle = \omega(a)$; moreover, the group of automorphisms acts as a group of unitary operators on the Hilbert space. Now we can see what happens when we apply this quantization programme to GR.

In General Relativity, electric fluxes and holonomies are natural basic observables to start with the quantization process. From the fundamental Poisson bracket between the Ashtekar-Barbero connection and the electric field we derive easily

$$\{E^i(S), H[\gamma, A]\} = \gamma \kappa \tau^i H[\gamma, A] \quad (110)$$

in the case the path γ have a single intersection with S and starts on an interior point on the surface. The most general rule can be given, but we skip the details. The abstract $*$ -algebra, called holonomy-flux algebra, is formed by the “words” made from letters $E^i(S)$ and $H(\gamma, A)$, subject to the commutation rules like (110). The basic abstract $*$ -operations can be read off from

$$H[\gamma, A]^* = \overline{H[\gamma, A]} = H[\gamma^{-1}, A]^T \quad (111)$$

and the trivial

$$E^i(S)^* = \overline{E^i(S)} = E^i(S). \quad (112)$$

$SU(2)$ gauge transformations and diffeomorphisms act as automorphisms of the *-algebra. Now we can state the uniqueness result, due to Lewandowski, Okolow, Sahlmann and Thiemann:

1. There exist a unique gauge and diffeomorphism invariant state on the holonomy-flux *-algebra. This is the analogous of the vacuum state in algebraic quantum field theory, being the state annihilated by all the momenta.
2. The GNS representation associated to the vacuum state is given by the Hilbert space $L^2(\overline{A}, d\mu_{AL})$ with the holonomy and flux operators acting on it, namely it gives the kinematics of Loop Quantum Gravity!

3.5 Area and volume operators

The electric field flux $E^i(S)$ is not gauge invariant (it has an $SU(2)$ index), but its norm is gauge invariant. Now consider the operator $E^2 = \sum_{i=1}^3 E^i(S)E^i(S)$ and compute its action on a spin-network Ψ_Γ whose graph has a single intersection with S . Let j be the spin of the link intersecting the surface. Since

$$-\sum_{i=1}^3 \tau_i^j \tau_i^j = j(j+1)\mathbb{1} \quad (113)$$

is the Casimir operator of $SU(2)$ in the j representation, using the grasping rule (106) we have simply:

$$\widehat{E}^2(S)\Psi_\Gamma = (\hbar\kappa\gamma)^2 j(j+1)\Psi_\Gamma. \quad (114)$$

Now we are ready to quantize the area [8, 41, 42, 43]: in classical General Relativity the physical area of a surface S is

$$A(S) = \int_S d^2\sigma \sqrt{n_a E_i^a n_b E_i^b} = \lim_{n \rightarrow \infty} \sum_n \sqrt{E^2(S_n)}, \quad (115)$$

where S_n are N smaller surfaces in which S is partitioned. For N large enough, the operator associated to $A(S)$, acting on a spin-network, is such that every S_n is punctured at most once by the links of the spin-network. So we have immediately

$$\widehat{A}(S)\Psi_\Gamma = \hbar\kappa\gamma \sum_p \sqrt{j_p(j_p+1)} \Psi_\Gamma. \quad (116)$$

This beautiful result tells us that \widehat{A} is well defined on \mathcal{H}_{kin} and that spin-networks are eigenvectors of this operator. So far we have tacitly supposed that the spin-network has no nodes on S . The result of the complete calculation in the general case is:

$$\widehat{A}(S)\Psi_\Gamma = \hbar\kappa\gamma \sum_{u,d,t} \sqrt{\frac{1}{2}j_u(j_u+1) + \frac{1}{2}j_d(j_d+1) + \frac{1}{2}j_t(j_t+1)} \Psi_\Gamma, \quad (117)$$

where u labels the outgoing parts of the links, d the incoming and t the tangent links with respect to the surface. We must stress again that the classical observable $A(S)$ is the physical area of the surface S , hence we have also a precise physical prediction: every measure of area can give only a result in the spectrum of the operator $\widehat{A}(S)$, so the area is quantized. The quantum of area carried by a link in the fundamental representation $j = 1/2$ is the smallest eigenvalue (area gap); it is of order of the Planck area:

$$A_0 \approx 10^{-66} \text{cm}^2 \quad (\gamma = 1). \quad (118)$$

Analogously, we can define an operator $V(\mathcal{R})$ corresponding to the volume of a region \mathcal{R} . The physical volume of a 3-dimensional region is given by the expression [8, 44, 45, 46, 47, 48]

$$V(\mathcal{R}) = \int_{\mathcal{R}} d^3x \sqrt{\frac{1}{3!} |\epsilon_{abc} E_i^a E_j^b E_k^c \epsilon^{ijk}|} = \lim_{N \rightarrow \infty} \sum_n \sqrt{\epsilon_{abc} E_i(S^a) E_j(S^b) E_k(S^c) \epsilon^{ijk}}, \quad (119)$$

where the sum is over the N cubes in which the region \mathcal{R} has been partitioned, and S^a are three sections of the n -th coordinate cube. Now consider the quantization of the right hand side of (119) and consider its action on a spin-network. Definitely, for large N , each coordinate cube contains at most one node. It turns out that, as for the area, spin-networks are eigenstates of the volume operator and the corresponding eigenvalues receive one contribution from each node. The explicit calculation shows that nodes with valence $V \leq 3$ do not contribute to the volume and that the spectrum is discrete.

3.6 Physical interpretation of quantum geometry

Since each node of a spin-network Ψ_Γ contribute to the volume eigenvalue, the volume of the region \mathcal{R} is a sum of terms, one for each node contained in \mathcal{R} . We can then identify nodes with quanta of volume; these quanta are separated by surfaces whose area is measured by the operator $\widehat{A}(S)$. All the links of the graph which intersect the surface S contribute to the area spectrum. Two space elements, or chunks, or volume quanta, or nodes, are contiguous if they are connected by a link l ; in this case they are separated by a surface of area $A_l = \hbar \kappa \gamma G \sqrt{j_l(j_l + 1)}$, where j_l is the spin label of the link l . The intertwiners, the labels of the nodes, are the quantum numbers of volume and the spins associated to the links are quantum numbers of area. The graph Γ determines the contiguity relations between the chunks of space, and can be interpreted as the dual graph of a cellular decomposition of the physical space. A spin-network state represents a quantized metric, and a discretized space.

Abstract spin-networks, the diffeomorphism equivalence class of embedded spin-networks have to be regarded as more fundamental, because they solve the kinematical constraints of the theory; they have a precise physical interpretation. Passing from an embedded spin-network state to its equivalence class, we preserve all the information except for its localization in the 3-dimensional manifold; this is precisely the implementation of the diffeomorphism invariance also in the classical theory, where the physical geometry is an equivalence class of metrics under diffeomorphisms. A spin-network is a discrete quantized geometry, formed by abstract quanta of space not living somewhere on a 3-dimensional manifold, they are only localized one respect to another. This a remarkable result in LQG, which predicts a Planck scale discreteness of space, on the basis of a standard quantization procedure, in the same manner in which the quantization of the energy levels of an atom is predicted by nonrelativistic Quantum Mechanics.

3.7 Dynamics

The quantization of the scalar constraint S is a more difficult task mainly for two reasons: first of all it is highly non linear, not even polynomial in the fundamental fields A and E . This gives origin to quantization ambiguities and possible ultraviolet divergences; most importantly, it is difficult to have a clear geometrical interpretation of the transformation generated by S (it contains Einstein equations!). Remarkably, a quite simple quantization recipe has been found by Thiemann [49, 50], and we sketch some details of its construction.

The scalar constraint is the sum of two terms:

$$S(N) = S^E(N) - 2(1 + \gamma^2)T(N), \quad (120)$$

where E stands for Euclidean, for historical reasons. The procedure found by Thiemann consists in rewriting S in such a way that the complicated non-polynomial structure gets hidden in the volume observable. For example, the first Euclidean term can be rewritten as

$$S^E(N) = \frac{\kappa\gamma}{4} \int_{\Sigma} d^3x N \epsilon^{abc} \delta_{ij} F_{ab}^j \{A_c^i, V\}. \quad (121)$$

The main point is that a suitably regulated version of the last expression is easy to quantize. Indeed given an infinitesimal loop α_{ab} in the coordinate ab -plane, with coordinate area ϵ^2 , the curvature tensor F_{ab} can be regularized observing that

$$H_{\alpha_{ab}}[A] - H_{\alpha_{ab}}^{-1}[A] = \epsilon^2 F_{ab}^i \tau_i + \mathcal{O}(\epsilon^4). \quad (122)$$

Similarly, the Poisson bracket $\{A_a^i, V\}$ is regularized as

$$H_{e_a}^{-1}[A] \{H_{e_a}[A], V\} = \epsilon \{A_a, V\} + \mathcal{O}(\epsilon^2), \quad (123)$$

where e_a is a path along the a -coordinate of coordinate length ϵ . Using this we can write the scalar constraint $S_E(N)$ as a limit of Riemann sums

$$\begin{aligned} S^E(N) &= \lim_{\epsilon \rightarrow 0} \sum_I N_I \epsilon^3 \epsilon^{abc} \text{Tr}[F_{ab}[A] \{A_c, V\}] = \\ &= \lim_{\epsilon \rightarrow 0} \sum_I N_I \epsilon^{abc} \text{Tr}[(H_{\alpha_{ab}^I}[A] - H_{\alpha_{ab}^I}[A]^{-1}) H_{e_c^I}^{-1}[A] \{H_{e_c^I}, V\}], \end{aligned} \quad (124)$$

where in the first equality we have replaced the integral in (121) by a limit of a sum over cells, labeled with the index I , of coordinate volume ϵ^3 . The loop α_{ab}^I is a small closed loop of coordinate area ϵ^2 in the ab -plane associated to the I -th cell, while the edge e_a^I is the corresponding edge of coordinate length ϵ , dual to the ab -plane. If we quantize the last expression in (124) we obtain the quantum scalar constraint

$$\widehat{S}^E(N) = \lim_{\epsilon \rightarrow 0} \sum_I N_I \epsilon^{abc} \text{Tr}[(\widehat{H}_{\alpha_{ab}^I}[A] - \widehat{H}_{\alpha_{ab}^I}[A]^{-1}) \widehat{H}_{e_c^I}^{-1}[A] [\widehat{H}_{e_c^I}, \widehat{V}]]. \quad (125)$$

The regulated quantum scalar constraint, that is before taking the limit in (125), acts only at spin-network nodes; this is a consequence of the very same property of the volume operator. By this we mean that

the terms in (125) corresponding to cells which do not contain nodes annihilates the spin-network state. Like the volume operator, it acts only at nodes of valence $V > 3$. Due to the action of infinitesimal loop operators representing the regularized curvature, the scalar constraint modify spin-networks by creating new links around nodes, so creating a triangle in which one vertex is the node, a fact exemplified in the following picture:

$$\widehat{S}_\epsilon^n \text{ (node } j \text{ with links } k, l, m \text{ and triangle on } k, l) = \sum_{op} S_{jklm,opq} \text{ (node } j \text{ with links } k, l, m, o \text{ and triangle on } k, l, o) +$$

$$+ \sum_{op} S_{jlmk,opq} \text{ (node } j \text{ with links } k, l, m, o \text{ and triangle on } l, m, o) + \sum_{op} S_{jmk,opq} \text{ (node } j \text{ with links } k, l, m, o \text{ and triangle on } m, k, o)$$
(126)

A similar quantization can be given for the other term of the scalar constraint (120). To remove the regulator ϵ we note that the only dependence on ϵ is in the position of the extra link in the resulting spin-network. This suggests to define the quantum scalar constraint at the diffeomorphism invariant level, that is to take the limit $\epsilon \rightarrow 0$ weakly in the space $\mathcal{S}'_{\text{Diff}^*}$. If we do that, the position of the new link is irrelevant. Hence the limit

$$\langle \Phi, \widehat{S}(N)\Psi \rangle = \lim_{\epsilon \rightarrow 0} \langle \Phi, \widehat{S}_\epsilon(N)\Psi \rangle \quad (127)$$

exists trivially for any $\Psi, \Phi \in \mathcal{S}'_{\text{Diff}^*}$. In the language of particle physics, we have avoided any UV singularity in taking away the regulator; this is a benefit of the diffeomorphism invariance of Loop Quantum Gravity. We now point out some properties of the quantum scalar constraint.

There is a non trivial consistency condition on the quantum scalar constraint: it must satisfy the quantum analog of the classical identity (55). The correct commutator algebra is recovered, in the sense that

$$\langle \Phi | [\widehat{S}(N), \widehat{S}(M)] | \Psi \rangle = 0 \quad (128)$$

for any Φ and Ψ in $\mathcal{S}'_{\text{Diff}^*}$, and we can say that the loop quantization of GR does not give rise to anomalies. Similar techniques can be applied to the case of (possibly supersymmetric) matter coupled to GR. We should also point out that there is a rich space of rigorous solutions to the scalar constraint and a precise algorithm for their construction has been developed [51, 52, 53]. The Hamiltonian constraint acts by annihilating and creating spin degrees of freedom and therefore the dynamical theory obtained could be called “Quantum Spin Dynamics in analogy to Quantum Chromodynamics in which the Hamiltonian acts by creating and annihilating color degrees of freedom. In fact we could draw a crude analogy to Fock space terminology as follows: the (perturbative) excitations of QCD carry a continuous label, the mode number $k \in \mathbb{R}^3$ and a discrete label, the occupation number $n \in \mathbb{N}$ (and others). In Loop Quantum Gravity the continuous labels are the links of the abstract graphs and the discrete ones are spins j (and others).

Next, when solving the Hamiltonian constraint, that is, when integrating the quantum Einstein equations, one realizes that one is not dealing with a (functional) partial differential equation but rather with a (functional) partial *difference* equation. Therefore, when understanding coordinate time as measuring how for instance volumes change, we conclude that also time evolution is necessarily discrete. Such discrete time evolution steps driven by the Hamiltonian constraint assemble themselves into what is known as a spin foam. A spin foam is a four dimensional complex of two dimensional surfaces where each surface is to be thought of as the world sheet of a link of a spin-network and it carries the spin that the link was carrying before it was evolved.

In summary, there is no mathematical inconsistency, however, there are doubts about the physical correctness of the scalar constraint operator although no proof exists so far that it is necessarily wrong. In the next section we introduce spin foam models, as an alternative, probably equivalent way to define the dynamics of Loop Quantum Gravity.

4 Covariant formulation: Spin Foam

Spin Foam Models (SFM) are proposals for the covariant Lagrangian (path integral) formulation of non-perturbative quantum gravity. There are some indications that actually Spin Foam Models could be the covariant implementation of the dynamics of Loop Quantum Gravity. A quite strong contact between the two formalisms has been established for 3-dimensional Riemannian pure gravity by Reisenberger, Perez and Noui in [54, 16]. In the 4-dimensional more physical case the New Spin Foam Models (NSFM) [55, 15, 56, 57] realized a beautiful bridge with the kinematics of LQG, and remarkably the spectra of geometric operators are the same of LQG, even in the Lorentzian signature version of the models. The spin foam formulation is based on a path integral “à la Feynmann” that implements the idea of sum over geometries; more precisely, the sum is over colored 2-complexes (like in fig. 4.1), i.e. collections of faces, edges and vertices combined together and labeled (or colored) using the representation theory of the gauge group. As we mentioned in the end of the last section, we can think to this formalism as a way to represent the time evolution of spin-networks: we can interpret a spin foam as an history of spin-networks. The two formulations of nonperturbative quantum gravity, LQG and SFM, have different properties: Lagrangian formalism is more transparent and keeps symmetries and covariance manifest. The Hamiltonian formalism is more rigorous but calculations involving dynamics are cumbersome. Even if simpler and often euristically constructed, Spin Foam Models allow to compute explicitly transition amplitudes in quantum gravity between two quantum states geometry, in particular between semiclassical states. In this section we give a general definition of a SFM and we motivate at an intuitive level the reasons and the sense in which they are the path integral representation of the action of the LQG scalar constraint. It is easier to start in three dimensions, following an historical path, and introduce the topological Ponzano-Regge model of 3d pure gravity; this is based on the triangulation “à la Regge” of a 3-dimensional manifold. Then we extend this model to four dimensions obtaining the topological quantum BF theory. BF theory is currently the main starting point for the construction of physical, non topological models for quantum gravity. The reason is that BF theory becomes General Relativity under the imposition of some constraints in the path integral. It is just the way those constraints are imposed that brought to the well known Barrett-Crane SFM, and more recently to the New Spin Foam Models.

4.1 Path integral representation

A spin foam σ is a 2-complex Γ with a representation j_f of the gauge group G associated to each face and an intertwiner i_e associated to each edge [58]. The gauge group can be either $SO(4)$ or $SO(1, 3)$ for the 4-dimensional models; it is $SO(1, 2)$ or $SO(3)$ in 3 spacetime dimensions; usually they are replaced with the corresponding universal covering groups. A Spin Foam Model [59] is defined, at least formally, by the partition function

$$Z = \sum_{\Gamma} w(\Gamma) Z[\Gamma] \quad (129)$$

where the amplitude associated to the spin foam Γ is

$$Z[\Gamma] = \sum_{j_f, i_e} \prod_f A_f(j_f) \prod_e A_e(j_f, i_e) \prod_v A_v(j_f, i_e). \quad (130)$$

The weight $w(\Gamma)$ is a possible multiplicity factor, A_f , A_e and A_v are the amplitudes associated to faces, edges and vertices of Γ respectively. For most models the face amplitude $A_f(j_f)$ is just the dimension of

the representation $\dim(j_f) = 2j_f + 1$. So a spinfoam model is defined by:

- 1) a set of 2-complexes, and associated weights;
- 2) a set of representations and intertwiners;
- 3) a vertex and an edge amplitude.

There is a close relation between LQG dynamics and spin foams [60, 61, 62]. In the context of LQG, there is an implicit way to solve the scalar constraint. We can define a “projection” operator P from the kinematical Hilbert space \mathcal{H}_{kin} to the kernel $\mathcal{S}'_{\text{phys}} \subset \mathcal{S}'_{\text{Diff}^*}$ of the scalar constraint. Formally we can write P as

$$P = \int D[N] e^{i \int_{\Sigma} N \hat{S}}, \quad (131)$$

where the functional integration is over all lapse functions N . Indeed (4.1) represents a sort of infinite dimensional δ distribution:

$$P \sim \prod_x \delta(\hat{S}(x)). \quad (132)$$

Expressions like (132) and were the starting point for a rigorous construction of the projector in 3d pure gravity and 4d topological BF theory [16, 63]. For any state $\Psi \in \mathcal{H}_{\text{kin}}$, $P\Psi$ is a formal solution to the scalar constraint \hat{S} . Moreover P naturally defines the *physical scalar product*

$$\langle \Psi, \Psi' \rangle_{\text{phys}} \equiv \langle P\Psi, \Psi' \rangle_{\text{kin}}. \quad (133)$$

The main importance of the physical scalar product is that it represents the probability amplitude for a process involving quantum states of geometry. Following a quite standard derivation of the path integral from the Hamiltonian theory, in analogy with nonrelativistic quantum mechanics and QFTs, one can see that the physical scalar product of spin-networks states can be represented as a sum over spin-network histories [64, 65], or spin foams (see fig. 5) which are bounded by the given spin-networks

$$\langle \Psi, \Psi' \rangle_{\text{phys}} = \sum_{\partial\Gamma = \Psi \cup \Psi'} w(\Gamma) Z[\Gamma]. \quad (134)$$

Imagine that the ‘nitial’ spin-network moves upward along a time coordinate of spacetime, sweeping a worldsheet, changing at each discrete time step under the action of \hat{S} . The worldsheet defines a possible history. An history from Ψ to Ψ' is a 2-complex with boundary given by the graphs of the spin-networks, whose *faces* f are the worldsheets of the links of the initial graph, and whose *edges* e are the worldlines of the nodes. Since the scalar constraint acts on nodes, the individual steps in the history can be represented as the *branching off* of the edges. We call *vertices* v the points where edges branch. We obtain in this manner a collection of faces, meeting at edges, in turn meeting at vertices; the set of those elements and their adjacency relations defines a 2-complex Γ . Moreover the 2-complex is colored with the irreducible representations and intertwiners inherited from spin-networks, namely it is a spin foam.

The underlying discreteness discovered in LQG is crucial to have a well-defined physical scalar product. Indeed the functional integral for gravity is replaced by a discrete sum over quantum amplitudes associated to combinatorial objects with a foam-like structure. A spin foam represents a possible quantum history of the gravitational field. Boundary data in the path integral are given by quantum states of 3-geometry, namely spin-networks.

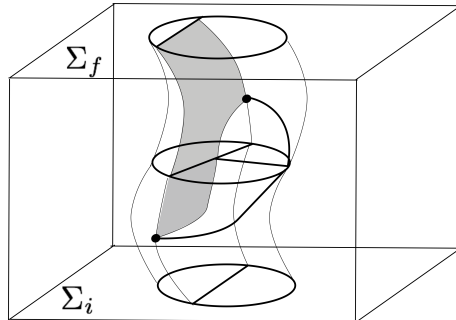


Figure 5: A spin foam seen as evolution of spin-networks

Deriving Spin Foam Models from the canonical theory can be a difficult task; for this reason they are derived directly from the Lagrangian of General Relativity. The most common setting is a discretization of the topological BF field theory: given a simplicial decomposition of spacetime one defines a discretized version of BF theory and then quantize it. The result of the quantization is a recipe for spin foam amplitudes on a *fixed* triangulation of spacetime. This is a bad feature, because we expect from the canonical theory that the Feynmann path integral contains, besides a sum over quantum numbers, also a sum over graphs. The most common tool used to recover (maybe partially) the full state sum is an auxiliary field theory called Group Field Theory (GFT) [66, 67, 68, 69]. Since every SFM has its GFT twin, we have:

$$Z[\Gamma] = Z_{\text{GFT}}[\Gamma], \quad (135)$$

where the GFT amplitude $Z_{\text{GFT}}[\Gamma]$ is defined inside a Feynman expansion

$$Z_{\text{GFT}} = \sum_{\Gamma} \frac{\lambda^{v[\Gamma]}}{\text{sym}[\Gamma]} Z_{\text{GFT}}[\Gamma]. \quad (136)$$

The sum (136) is over a certain class of triangulations, and possibly also over spacetime topologies, and $v[\Gamma]$ is the number of vertices in the triangulation Γ . The physical origin of the sum over graphs is the following: in a realistic model for quantum gravity, the sum over 2-complexes, or at least over simplicial triangulations, must be present in order to capture the infinite number of degrees of freedom of General Relativity: General Relativity is a field theory with local degrees of freedom. This is also what we expect from the canonical theory, from expression like (134).

4.2 Regge discretization

Historically, the first SFM was the one introduced by Ponzano and Regge. This is the quantization of a discretization of classical GR introduced by Regge himself in the early 1960's and called Regge calculus [70]. Regge calculus is a natural way to approximate General Relativity by means of a discrete lattice theory. We illustrate the construction for Euclidean (i.e. Riemannian) General Relativity in any

dimension. A Riemannian manifold (M, g) , where M is a smooth manifold and g its metric tensor, can be “approximated” with a *piecewise flat* manifold (Δ, g_Δ) , formed by flat simplices (triangles in 2d, tetrahedra in 3d, 4-simplices in 4d...) glued together in such a way that the geometry of their shared boundaries matches. Here Δ is the abstract triangulation, and the discretized metric g_Δ assumes a constant value on the edges of simplices and is determined by the size of simplices. For instance, a curved 2d surface can be approximated by a surface obtained by gluing together flat triangles along their sides: curvature is then concentrated on the points where triangles meet, possibly forming “the top of a hill”. With a sufficient number N of simplices, we can (fixing the abstract triangulation and varying the size of the individual n -simplices) approximate sufficiently well any given Riemannian manifold with a Regge triangulation. Thus, over a fixed Δ we can define an approximation of GR, in a manner analogous to the way a given Wilson lattice defines an approximation to Yang-Mills field theory, or the approximation of a partial differential equation with finite differences defines a discretization of the equation. Therefore the Regge theory over a fixed triangulation Δ defines a cut-off version of GR.

The meaning of Regge cut-off There is an important and fundamental difference between this kind of discretization and lattice Yang-Mills theories: the Regge cut-off is neither ultraviolet nor infrared. In lattice QCD, the number N of elementary cells of the lattice defines an infrared cut-off: long wavelength degrees of freedom are recovered by increasing N . On the other hand, the physical size a of the individual cells enters the action of the theory, and short wavelength degrees of freedom are recovered in lattice QCD by decreasing a . Hence a is an ultraviolet cut-off. In Regge GR, on the contrary, there is no fixed background size of the cells that enters the action. A fixed Δ can carry both a very large or a very small geometry, depending on the (discrete) metric we put on it. The cut-off implemented by Δ is therefore of a different nature than the one of lattice QFT. It is not difficult to see that it is a cut-off in the *ratio* between the smallest allowed wavelength and the overall size of the spacetime region considered. Thus, fixing Δ is equivalent to cutting-off the degrees of freedom of GR that have much smaller wavelength than the arbitrary size L of the region one considers. Since the quantum theory has no degrees of freedom below the Planck scale, it follows that a Regge approximation is good for L small, and it is a low-energy approximation for L large.

Geometrical construction Consider a 4d triangulation. This is formed by oriented 4-simplices (v), tetrahedra (e), triangles (f), segments and points. The notation refers to the dual triangulation (v for vertices, e for edges and f for faces) that will be useful when dealing with spin foams. The metric is flat within each 4-simplex v . All the tetrahedra and triangles are flat. The geometry induced on a given tetrahedron from the geometry of the two adjacent 4-simplices is the same. In d dimensions, a $(d-2)$ -simplex is surrounded by a cyclic sequence of d -simplices, separated by the $(d-1)$ -simplices that meet at the $(d-2)$ -simplex. This cyclic sequence is called the *link* of the $(d-2)$ -simplex. For instance, in dimension 2, a point is surrounded by a link of triangles, separated by the segments that meet at the point; in dimension 3, it is a segment which is surrounded by a link of tetrahedra, separated by the triangles that meet at the segment; in dimension 4, a triangle f is surrounded by a link of 4-simplices v_1, \dots, v_n , separated by the tetrahedra that meet at the triangle f . In Regge calculus, curvature is concentrated on the $(d-2)$ -simplices. In dimension 4, curvature is therefore concentrated on the triangles f . It is generated by the fact that the sum of the dihedral angles of the 4-simplices in the link around the triangle may be different from 2π . We can always choose Cartesian coordinates covering one 4-simplex, or two adjacent

4-simplices; but in general there are no continuous Cartesian coordinates covering the region formed by all the 4-simplices in the link around a triangle. The variables used by Regge to describe the geometry g_Δ of the triangulation Δ are given by the set of the lengths of all the segments of the triangulation. Regge has also written the Einstein action in this discretized context: in three dimensions the discretized Einstein-Hilbert action for a tetrahedron v is

$$S_v = \sum_f l_f \theta_f(l_f), \quad (137)$$

where θ_f is the dihedral angle associated to the segment f , that is the angle between the outward normals of the triangles incident to the segment. One can show that the action

$$S_{\text{Regge}} = \sum_v S_v, \quad (138)$$

called the Regge action, is an approximation to the integral of the Ricci scalar curvature, namely to the Einstein-Hilbert action.

4.3 Quantum Regge calculus and spinfoam models

Quantum Regge calculus is a quantization of discretized General Relativity [71]. Contrary to LQG, here the discretization is not derived, but imposed already in the classical theory. Consider the 3d Euclidean case, which is easier and is the one originally studied by Ponzano and Regge. The idea is to define a partition function as a sum over Regge geometries, using the Regge action as the weight in the Feynman path integral:

$$Z = \int dl_1 \dots dl_N e^{iS_{\text{Regge}}}; \quad (139)$$

this is a sum over the N edge lengths of a fixed triangulation. Regge discovered a surprising property of the Wigner $6j$ -symbol, a well-known combinatorial object in the theory of angular momentum: in the large spins j limit the following asymptotic formula holds, linking the symbol which depends on 6 spins to the Regge action (137):

$$\{6j\} \sim \frac{1}{\sqrt{12\pi V}} \cos\left(S_v(j_n) + \frac{\pi}{4}\right). \quad (140)$$

S_v is the Regge action for a single tetrahedron with edge lengths j_n . Expanding the cosine in two complex exponentials, the two resulting terms correspond to forward and backward propagation in coordinate time, and $\pi/4$ does not affect classical dynamics. V is the volume of the tetrahedron. So the $6j$ -symbol knows about quantum gravity: it is the right weight for the path integral! Under the assumption that the lengths are quantized multiples of a fundamental length, they proposed the following formula for 3d quantum gravity:

$$Z_{\text{PR}} = \sum_{j_1 \dots j_N} \prod_f \dim(j_f) \prod_v \{6j\}_v. \quad (141)$$

Formula (141) contains a sum over all possible spins and there is a product of $6j$'s, one per each dual vertex (tetrahedron) of the triangulation. This formula has the general form (130) where the set of two complexes summed over is formed by a single 2-complex (we are not summing over triangulations); the

representations summed over are the unitary irreducible of $SU(2)$, the intertwiners are the unique 3-valent ones and the vertex amplitude is $A_v = \{6j\}$. So (141) defines a spin foam model called the Ponzano-Regge model. This model can be obtained also by direct evaluation of a discrete path integral when we introduce appropriate variables. To this aim, consider the dual triangulation Δ^* defined as follows: place a *vertex* v inside each tetrahedron of Δ ; if two tetrahedra share a triangle e , we connect the two corresponding vertices by an *edge* e , dual to the triangle e ; for each segment (or edge, one has to be careful not to confuse with the dual edge) f of the triangulation we have a *face* f of Δ^* . Finally for each point of Δ we have a 3d region of Δ^* , bounded by the faces dual to the segments sharing the point (Table 1). Let

Δ_3	Δ_3^*	Δ_4	Δ_4^*
tetrahedron	<i>vertex</i> (4 edge, 6 faces)	4-simplex	<i>vertex</i> (5 edge, 10 faces)
triangle	<i>edge</i> (3 faces)	tetrahedron	<i>edge</i> (4 faces)
segment	<i>face</i>	triangle	<i>face</i>
point	<i>3d region</i>	segment	<i>3d region</i>
		point	<i>4d region</i>

Table 1: Relation between a triangulation and its dual, in three and four dimensions. In parenthesis: adjacent elements.

$h_e = \mathcal{P} \exp(\int_e \omega^i \tau_i)$ be the holonomy of the $SU(2)$ spin connection along each edge of Δ^* ; let l_f^i be the line integral of the triad (gravitational field) e^i along the segment f of Δ . The basic variables are h_e and l_f^i . The discretized Einstein-Hilbert action in these variables reads

$$S[l_f, h_e] = \sum_f l_f^i \text{Tr}[h_f \tau_i] = \sum_f \text{Tr}[h_f l_f], \quad (142)$$

where

$$h_f = h_{e_1^f} \dots h_{e_n^f} \quad (143)$$

is the product of group elements associated to the edges e_1^f, \dots, e_n^f bounding the face f . The l_f 's are elements in the Lie algebra $\mathfrak{su}(2)$ ($l_f \equiv l_f^i \tau_i$). If we vary this action w.r.t. the lengths l_f^i we obtain the simple equations of motion

$$h_f = \mathbb{1}, \quad (144)$$

namely the lattice connection is flat. Varying w.r.t. h_e , and using (144), we obtain the equations of motion $l_{f_1}^i + l_{f_2}^i + l_{f_3}^i = 0$ for the three sides f_1, f_2, f_3 of each triangle. This is the discretized version of the Cartan structure equation $De = 0$. Now we can define the path integral as

$$Z = \int dl_f^i dh_e \exp iS[l_f, h_e], \quad (145)$$

where dh_e is the Haar measure over $SU(2)$. Up to an overall normalization factor, we find

$$Z = \int dh_e \prod_f \delta(h_{e_1^f} \dots h_{e_n^f}) = \sum_{j_1 \dots j_N} \prod_f \dim(j_f) \int dh_e \prod_f \text{Tr} \Pi^{j_f}(h_{e_1^f} \dots h_{e_n^f}), \quad (146)$$

where we have expanded the Dirac δ distribution over the group manifold using the Plancherel expansion

$$\delta(h) = \sum_j \dim(j) \text{Tr} \overset{j}{\Pi}(h) \quad (147)$$

in which the sum is over all unitary irreducible representations of $SU(2)$. Since every dual edge is shared by three dual faces, the integrals over a single holonomy h_e are of the form

$$\int_{SU(2)} dg \overset{j_1}{\Pi}(g)^a_{a'} \overset{j_2}{\Pi}(g)^b_{b'} \overset{j_3}{\Pi}(g)^c_{c'} = v^{abc} v_{a'b'c'}, \quad (148)$$

where v^{abc} is the normalized intertwiner ($v^{abc} v_{abc} = 1$) between the representations of spin j_1, j_2, j_3 . Each of the two invariant tensors in the r.h.s. is associated to one of the two vertices that bounds the edge. In all we have four intertwiners for each vertex; these intertwiners get fully contracted among each other following a tetrahedral pattern. This contraction is precisely the Wigner $6j$ -symbol. Bringing all together we obtain the Ponzano-Regge partition function (141).

4.4 BF theory

Here we extend the above construction to four dimensions. As a first step we do not consider GR, but a much simpler 4d theory, called BF theory, which is topological and is a simple extension to 4 dimensions of the topological 3d GR. BF theory for the group $SU(2)$ is defined by two fields: an $\mathfrak{su}(2)$ -valued 2-form B^{IJ} (indices I, J are in the Lie algebra), and an $\mathfrak{su}(2)$ -valued spin connection Γ^{IJ} . The action is a direct generalization of the 3d one:

$$S[B, \Gamma] = \int B_{IJ} \wedge F^{IJ}[\Gamma]. \quad (149)$$

The wedge \wedge is the exterior product of differential forms, so we are integrating a 4-form over a 4-dimensional space. We discretize BF theory on a fixed triangulation; the discrete configuration variables are B_f^{IJ} , which are the integrals of the smooth 2-forms over triangles f (f stands for faces dual to triangles). The construction of the dual 4-dimensional triangulation is resumed in Table 1. Following the same procedure of the 3d model, we obtain an equation analog to (146), but now we are in four dimensions, and every edge bounds four faces; so we have to compute integrals of this form

$$\int_{SU(2)} dg \overset{j_1}{R}(g)^a_{a'} \overset{j_2}{R}(g)^b_{b'} \overset{j_3}{R}(g)^c_{c'} \overset{j_4}{R}(g)^d_{d'} = \sum_i v_i^{abcd} v_{a'b'c'd'}^i. \quad (150)$$

Here i labels an orthonormal basis v_i^{abcd} ($v_i^{abcd} v_{jabcd} = \delta_{ij}$) in the space of the intertwiners between the representations of spin j_1, j_2, j_3, j_4 ; we choose the virtual spin basis, and i is interpreted as a virtual spin. Now, each vertex bounds ten faces and so for each vertex we have ten representations. Analogously to the three dimensional case, where the vertex amplitude was given by a $6j$ -symbol, we find that here the vertex amplitude is the Wigner $15j$ -symbol

$$A(j_1, \dots, j_{10}, i_1, \dots, i_5) \equiv \sum_{a_1 \dots a_{10}} v_{i_1}^{a_1 a_6 a_9 a_5} v_{i_2}^{a_2 a_7 a_{10} a_1} v_{i_3}^{a_3 a_7 a_8 a_2} v_{i_4}^{a_4 a_9 a_7 a_3} v_{i_5}^{a_5 a_{10} a_8 a_4} = \{15j\}.$$

We have 15 spins because 10 of them are associated to faces, while 5 of them are the virtual spins labeling the interwiner basis. The pattern of the contraction of the indices reproduces the structure of a four simplex (fig 4.4). We can then write the full partition function

$$Z = \sum_{j_f, i_e} \prod_f \dim(j_f) \prod_v \{15j\}_v. \quad (151)$$

In conclusion, the spinfoam model of BF theory is defined by the following choices:

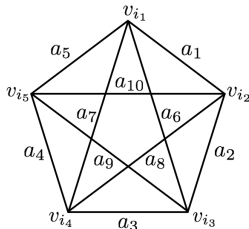


Figure 6: The Wigner 15j-symbol

- 1) the set of two complexes summed over is formed by a single 2-complex, given by the 2-skeleton of the dual triangulation;
- 2) the representations summed over are the unitary irreducibles of $SU(2)$;
- 4) the vertex amplitude is $A_v = \{15j\}$.

For the applications to gravity, BF theory must be formulated with the $SO(4)$ or $SO(3,1)$ gauge group. The fields B and F will have values in the respective Lie algebras. General Relativity can be obtained from $SO(3,1)$ BF theory substituting the field B^{IJ} with $\epsilon^{IJ} e^K \wedge e^L$, where e is a Lorentz tetrad, and this is the reason for which we describe BF theory as an intermediate step. We will describe the Euclidean version, where the gauge group is $SO(4)$.

The quantization of the discretized $SO(4)$ BF theory is straightforward, because of the decomposition $SO(4) \simeq SU(2) \times SU(2)/\mathbb{Z}_2$. $SO(4)$ unitary irreducible representations are then the tensor product of couples of $SU(2)$ representations. They are labeled by couples j_+, j_- . A basis for the 4-valent intertwiner space is given by the tensor product of the basis intertwiners of $SU(2)$; from this, also intertwiners can be labeled by a couple i_+, i_- of virtual spins. The resulting vertex amplitude is

$$A(j_1^\pm, \dots, j_{10}^\pm, i_1^\pm, \dots, i_5^\pm) \equiv \{15j^+\} \{15j^-\} \quad (152)$$

that is the product of two 15j-symbols. The full partition function is

$$Z = \sum_{j_f^\pm, i_e^\pm} \prod_f \dim(j_f^+) \dim(j_f^-) \prod_v \{15j^+\}_v \{15j^-\}_v. \quad (153)$$

4.5 Barret-Crane model

Now we are ready to look for a spinfoam model for quantum General Relativity. We restrict our attention on the Euclidean signature model, with gauge group $SO(4)$. As we have anticipated, to obtain GR from

the topological BF theory we must replace B^{IJ} with

$$B^{IJ} = \epsilon^{IJ}{}_{KL} e^K \wedge e^L, \quad (154)$$

where e_μ^I is a tetrad. Equation (154) is equivalent to the following constraint:

$$B^{IJ} \wedge B^{KL} = V \epsilon^{IJKL}, \quad (155)$$

where V is proportional to the volume element. Consider now the simplicial discretization of BF theory. For each tetrahedron, the discretized version of equation (155) is the following:

$$B_f^* \cdot B_f = 0, \quad (156)$$

$$B_f^* \cdot B_{f'} = 0, \quad f \text{ and } f' \text{ share an edge}, \quad (157)$$

$$B_f^* \cdot B_{f'} = \pm 2V(v) \quad f \text{ and } f' \text{ are opposite faces of } t, \quad (158)$$

where $V(v)$ is the volume of the 4-simplex v , and the $*$ is the Hodge dual w.r.t. the internal indices. In the quantum theory, as in the quantization of lattice Yang-Mills theories, the standard procedure is to quantize B_f^{IJ} as left-invariant or right-invariant vector fields of the $SO(4)$ Lie algebra, depending on the orientation of the face. It is immediate to see that the four bivectors associated to the four triangles of a single tetrahedron satisfy the closure relation

$$B_{f_1}^{IJ}(t) + B_{f_2}^{IJ}(t) + B_{f_3}^{IJ}(t) + B_{f_4}^{IJ}(t) = 0, \quad (159)$$

which is the discrete analog of Gauss constraint. Equation (156) is called diagonal simplicity constraint, and it becomes, in the quantum theory, a restriction on the representations summed over in the partition function. Recall indeed that irreducible representations of $SO(4)$ are labeled by couples of spins j_+, j_- . The quantum diagonal simplicity constraint expresses the vanishing of the pseudo-scalar Casimir operator:

$$\epsilon_{IJKL} \hat{B}_f^{IJ} \hat{B}_f^{KL} = \hat{B}_+^{IJ} \hat{B}_{+IJ} - \hat{B}_-^{IJ} \hat{B}_{-IJ} = [j_+(j_+ + 1) - j_-(j_- + 1)] \mathbb{1} = 0. \quad (160)$$

The quantities B_+^{IJ} and B_-^{IJ} are respectively the self-dual and antiself-dual parts of B^{IJ} :

$$B_\pm^{IJ} = B^{IJ} \pm B^*{}^{IJ}. \quad (161)$$

It follows that the representations have to be simple, that is $j_+ = j_-$. This suggests that quantum GR can be obtained by restricting the sum over representations in (153) to the sole simple representations. The other two constraints (157) and (158) are called off-diagonal and dynamical simplicity constraints respectively; the off-diagonal one selects the simple representations also in the intertwiner space. This singles out the Barrett-Crane intertwiner, defined as

$$i_{\text{BC}}^{(aa')(bb')(cc')(dd')} = \sum_i (2i + 1) v^{abg} v^{gcd} v^{a'b'g'} v^{g'c'd'}, \quad (162)$$

where the $SO(4)$ indices are couple of $SU(2)$ indices, and the indices g and g' are in the representation i . The BC intertwiner has the property of being formed by a simple virtual link in any decomposition

$$i_{\text{BC}} = \sum_{i^x} (2i^x + 1) \begin{array}{c} \diagup \quad \text{---} \quad \diagdown \\ \diagdown \quad \text{---} \quad \diagup \end{array} = \sum_{i^y} (2i^y + 1) \begin{array}{c} \diagdown \quad \diagup \\ \text{---} \quad \text{---} \\ \diagup \quad \diagdown \end{array}. \quad (163)$$

Note that the scalar Casimir $\hat{B}_f \cdot \hat{B}_f$ is the quantization of the area of the triangle f and its eigenvalues $j_f(j_f + 1)$ are the quantum numbers of area. The Barret-Crane vertex amplitude is:

$$\begin{array}{c}
 \begin{array}{c}
 \text{Diagram 1: 4-simplex with vertices } i_{BC} \text{ and edges } j_1 \dots j_{10} \\
 \text{Diagram 2: 4-simplex with vertices } i_1 \dots i_5 \text{ and edges } j_1 \dots j_{10} \\
 \text{Diagram 3: 4-simplex with vertices } i_1 \dots i_5 \text{ and edges } j_1 \dots j_{10}
 \end{array}
 \end{array}
 = \sum_{i_1 \dots i_5} \quad (164)$$

This combinatorial symbol is called $10j$ -symbol. The Barret-Crane spinfoam model [72, 73] is defined by the partition function constructed with the vertex amplitude (164):

$$Z_{BC} = \sum_{j_f} \prod_f \dim(j_f)^2 \prod_v \{10j\}_v. \quad (165)$$

A remarkable property of the $10j$ -symbol is its asymptotic expansion [74, 75]. Its large spin behavior is

$$\{10j\} \sim \sum_{\sigma} P(\sigma) \cos S_{\text{Regge}}(\sigma) + k \frac{\pi}{4} + D, \quad (166)$$

where

$$S_{\text{Regge}}(\sigma) = \sum_a j_a \theta_a \quad (167)$$

is the so-called *area Regge calculus* action for a 4-simplex; j_a is the area of the a -th triangle in the 4-simplex, and θ the exterior 4-dimensional dihedral angle between the two tetrahedra sharing the a -th triangle. The sum is over possible discrete degeneracies. The term $P(\sigma)$ is a non oscillating, slowly varying factor, like the volume factor in the Ponzano-Regge asymptotic formula; D is the contribution of the so-called degenerate configurations and k is an integer depending on σ . In [76] Baez, Christensen and Egan showed that the term D is in fact dominant in the asymptotics of the $10j$ -symbol, i.e. the leading order terms are contained in the set of degenerated configurations. This has later been confirmed by the results of Freidel and Louapre [77] and Barrett and Steele [78]. However, such degenerate terms do not contribute in the calculation of observables (e.g. the 2-point function) in the semiclassical limit.

There are some difficulties in interpreting the Barrett-Crane model as a model for quantum gravity. The first is that the low energy 2-point function is pathological: some components of the graviton propagator (the ones depending on the intertwiners d.o.f.) are suppressed. Another more structural problem is in the interpretation of the model as an amplitude for the LQG spin-networks. LQG spin-networks are based on the group $SU(2)$, while the covariant state space of spin foams is based on $SO(4)$. In principle, one could build a natural correspondence between the two state spaces, but in the case of the BC model, there is a mismatch between the linear structures of $SO(4)$ and $SO(3)$ in building up this correspondence. We refer to [79] for a short discussion on this subtle point.

5 A new model: EPRL vertex

Some time ago, J. Engle, R. Pereira and C. Rovelli [55] introduced a new spinfoam model. The main motivation was to find an improvement of the Barrett-Crane model. The difficulties with the BC model are related to the fact that the intertwiner quantum numbers are fully constrained; this has been traced back to the mistake of imposing the simplicity constraints as strong operator equations, even though they are second class constraints. In fact it is well known that imposing second class constraints strongly may lead to the incorrect elimination of physical degrees of freedom. The generalization of this model to arbitrary values of γ is performed in a paper by J. Engle, E.R. Livine, R. Pereira and C. Rovelli [15]. Here we describe this more general model, called shortly EPRL model. Its main characteristics are the following ones:

- The boundary quantum state space matches *exactly* the one of $SO(3)$ LQG: no degrees of freedom are lost.
- The asymptotic expansion of the vertex on a coherent state basis gives the exponential of the Regge action.
- As the degrees of freedom missing in BC are recovered, the vertex yields the correct low-energy n -point functions.
- The vertex is $SO(4)$ -covariant.
- The spectrum of area and volume operators coincides with the one of Loop Quantum Gravity, even in the Lorentzian version of the model.

5.1 *The goal of the model: imposing weakly the simplicity constraints*

The Barrett-Crane theory constrains entirely the intertwiner degrees of freedom. The reduction of the intertwiner space to the sole intertwiner i_{BC} comes from the strong imposition of the off-diagonal simplicity constraints, as we have seen in section 4.5. But these constraints do not commute with one another, and are therefore second class. Imposing second class constraints strongly is a well-known way of erroneously killing physical degrees of freedom in a quantum theory.

In order to illustrate the problems that follow from imposing second class constraints strongly, and a possible solution to this problem, consider a simple system that describes a single particle, but using twice as many variables as needed. The phase space is the doubled phase space for one particle, formed by the two couples (q_1, p_1) and (q_2, p_2) , and the symplectic structure is the one given by the commutator $\{q_a, p_b\} = \delta_{ab}$. We set the constraints to be

$$\begin{aligned} q_1 - q_2 &= 0, \\ p_1 - p_2 &= 0. \end{aligned} \tag{168}$$

To simplify the constraints we perform a change of variables $q_{\pm} = (q_1 \pm q_2)/2$ and $p_{\pm} = (p_1 \pm p_2)/2$, so now the system (168) reads: $q_- = p_- = 0$. They are clearly second class constraints.

Suppose we quantize this system on the Schrödinger Hilbert space $L^2(\mathbb{R}^2)$ formed by wave functions of the form $\psi(q_+, q_-)$. If we impose strongly the constraints we obtain the set of two equations

$$\begin{aligned} q_- \psi(q_+, q_-) &= 0, \\ i\hbar \frac{\partial}{\partial q_-} \psi(q_+, q_-) &= 0, \end{aligned} \tag{169}$$

which has no non trivial solutions. We have lost entirely the system.

There are several ways of dealing with second class systems. One possibility, which is employed for instance in the Gupta-Bleuler formalism for electromagnetism and in string theory, can be illustrated as follows in the context of the simple model above. Define the creation and annihilation operators $a_-^\dagger = (p_- + iq_-)/\sqrt{2}$ and $a_- = (p_- - iq_-)/\sqrt{2}$. The constraints now read $a_- = a_-^\dagger = 0$. Impose only one of these strongly: $a_-|\psi\rangle = 0$ and call the space of states solving this \mathcal{H}_{ph} . Notice that the other one holds weakly, in the sense that

$$\langle \phi | a_-^\dagger | \psi \rangle = 0 \quad \forall \phi, \psi \in \mathcal{H}_{\text{ph}}. \tag{170}$$

That is, a_-^\dagger maps the physical Hilbert space \mathcal{H}_{ph} into a subspace orthogonal to \mathcal{H}_{ph} . Similarly, in the Gupta-Bleuler formalism the Lorenz gauge condition (which forms a second class system with the Gauss constraint) holds in the form

$$\langle \phi | \partial^\mu A_\mu | \psi \rangle = 0 \quad \forall \phi, \psi \in \mathcal{H}_{\text{ph}}. \tag{171}$$

A general strategy to deal with second class constraints is therefore to search for a decomposition of the Hilbert space of the theory $\mathcal{H}_{\text{kin}} = \mathcal{H}_{\text{phys}} \oplus \mathcal{H}_{\text{sp}}$ (sp. for spurious) such that the constraints map $\mathcal{H}_{\text{phys}} \rightarrow \mathcal{H}_{\text{sp}}$. We then say that the constraints vanish weakly on $\mathcal{H}_{\text{phys}}$. This is the strategy we employ below for the off-diagonal simplicity constraints of BF theory. Since the decomposition may not be unique, we will have to select the one which is best physically motivated.

5.2 Description of the model

As in the BC model we discretize spacetime using as configuration variables the bivectors $B_f(t)^{IJ}$ associated to faces f , and the holonomy $U_f(t, t')$ along the tetrahedra sharing f , starting from the tetrahedron t and ending at t' ; $U_f(t) \equiv U_f(t, t)$ is the holonomy around the full link of tetrahedra. Discretized GR results from imposing constraints on the B variables as seen for the BC model. They are:

- 1) simplicity constraints (diagonal (156), off-diagonal (157), dynamical (158));
- 2) closure constraint.

The dynamical simplicity constraint is automatically satisfied when the other constraints are satisfied. The closure constraint will be automatically implemented in the quantum theory; its effect, as known, is to restrict the states of the quantum theory to the gauge invariant ones.

Classical theory In the EPRL model the the classical action one starts with is a slight modification of BF theory which includes the Immirzi parameter. This is the Holst action, obtained adding to the original action a term that does not change the equations of motion. Holst action is also the one used in LQG,

because it the one resulting from the Einstein-Hilbert action after the introduction of the Ashtekar-Barbero variables. A possible discretization of the the Holst action is

$$S = -\frac{1}{\kappa} \sum_{f \in \text{int}\Delta} \text{Tr} \left[B_f(t) U_f(t) + \frac{1}{\gamma} {}^* B_f(t) U_f(t) \right] - \frac{1}{\kappa} \sum_{f \in \partial\Delta} \text{Tr} \left[B_f(t) U_f(t, t') + \frac{1}{\gamma} B_f^*(t) U_f(t, t') \right]. \quad (172)$$

where the original variables have been integrated over paths and surfaces of a simplicial triangulation of spacetime. The boundary conjugate variables can be read off from the action. For each triangle f on the boundary, we have two tetrahedra t_L, t_R sharing it; to these tetrahedra are associated the holonomies $U_f(t_R)$ and $U_f(t_L)$, and the shifted fields

$$J_f(t) \equiv B_f^*(t) + \frac{1}{\gamma} B_f(t) \quad (173)$$

Holonomies and shifted fields are canonically conjugate variables, with Poisson brackets

$$\{J_f^{IJ}(t), U_f(t)\} = \tau^{IJ} U_f(t) \quad (174)$$

where τ^{IJ} are $SO(4)$ ($SO(1,3)$ in the Lorentzian) generators. Now constraints have to be imposed on these boundary variables. The constraints (156) and (157) have two sectors of solutions, one in which $B = {}^*e \wedge e$, and one in which $B = e \wedge e$. For finite Immirzi parameter both sectors in fact yield GR, but the value of the Newton constant and Immirzi parameter are different in each sector. In the $B = {}^*e \wedge e$ sector, the discrete Holst action becomes the Holst formulation of GR [80] with Newton constant G and Immirzi parameter γ . In the $B = e \wedge e$ sector, one *also* obtains the Holst formulation of GR, but this time with Newton constant $G\gamma$, and Immirzi parameter s/γ , where the signature s is $+1$ in the Euclidean theory and -1 in the Lorentzian theory. In order to select a single sector, the EPRL construction reformulate the simplicity constraints in such a way that these two sectors are distinguished. This was a crucial step for the construction of the new SFM. To this purpose, we replace the off-diagonal constraint (157) with the following stronger constraint: for each tetrahedron t there must exist a (timelike in the Lorentzian case) vector n^I such that

$$n_I B_f^{IJ}(t) = 0 \quad (175)$$

for every triangle f of the tetrahedron. This condition is stronger than (157) since it selects only the desired $B = e \wedge e$ sector.

For each tetrahedron t , define the gauge-fixed spatial and temporal components of $J(t)$ choosing a coordinate system such that the vector normal to t takes the standard form $(1, 0, 0, 0)$; then we can determine the ‘‘magnetic’’ and ‘‘electric’’ components of J :

$$L^i \equiv \frac{1}{2} \epsilon_{jk}^i J^{jk} \quad (176)$$

$$K^i \equiv J^{0i} \quad i, j, k = 1, 2, 3. \quad (177)$$

In terms of the shifted fields, the diagonal and off-diagonal simplicity constraints (156)-(175) read

$$\mathcal{C}_{ff} \equiv \left(1 + \frac{s}{\gamma^2}\right) *J_f \cdot J_f - \frac{2s}{\gamma} J_f \cdot J_f \approx 0 \quad (178)$$

$$\mathcal{C}_f^J \equiv n_I (*J_f^{IJ} - \frac{s}{\gamma} J_f^{IJ}) \approx 0 \Leftrightarrow \mathcal{C}_f^j \equiv L_f^j - \frac{s}{\gamma} K_f^j \approx 0. \quad (179)$$

The first constraint (178) commutes with the others, while the system of off-diagonal constraints (179) does not close a Poisson algebra. Thus we will impose strongly (178) and more weakly (179).

Quantization We quantize the discretized classical theory as in lattice QFT. We choose the unconstrained kinematical quantum state space to be

$$L^2(SO(4), dg)/SO(4) \quad (180)$$

where G is $SO(4)$ or $SO(1,3)$, dg is the Haar measure, and L is the number of links in the dual graph of the boundary triangulation (or the number of triangles in the boundary). Division by $SO(4)$ means that we took the gauge invariant subspace. We quantize the variable $J_f^{IJ}(t_R)$ as a right-invariant vector field over $SO(4)$, and $J_f^{IJ}(t_L)$ as a left-invariant vector field, acting on the portion of the Hilbert space associated to the link f . What is right or left is determined by the orientation of the graph.

The quantum diagonal and off-diagonal constraints now read

$$\widehat{\mathcal{C}}_{ff} \equiv \left(1 + \frac{s}{\gamma^2}\right) *\widehat{J}_f \cdot \widehat{J}_f - \frac{2s}{\gamma} \widehat{J}_f \cdot \widehat{J}_f \approx 0, \quad (181)$$

$$\widehat{\mathcal{C}}_f^j \equiv \widehat{L}_f^j - \frac{s}{\gamma} \widehat{K}_f^j \approx 0. \quad (182)$$

where the “electric” and “magnetic” fields become the generators of $SU(2)$ rotations (that leave n^I invariant) and boosts at the quantum level. The Gauss constraint, which in the discretized context means that the bivectors associated to a tetrahedron satisfy the closure relation

$$\sum_f B_f(t) = 0 \quad (183)$$

implements, as usual, the gauge invariance of quantum states.

Euclidean In the Euclidean version of EPRL model, consider a single link, and its associated Hilbert space $L^2(SO(4), dg)$. The $SO(4)$ scalar Casimir $\widehat{J} \cdot \widehat{J}$ acts diagonally on the (j_+, j_-) irreducible component of this Hilbert space; the associated eigenvalue is $j_+(j_+ + 1) + j_-(j_- + 1)$. The pseudo-scalar Casimir $*\widehat{J} \cdot \widehat{J}$ gives instead the eigenvalue $j_+(j_+ + 1) - j_-(j_- + 1)$. Then by a simple calculation we see that the diagonal constraint (182) restricts the self dual and anti-self dual quantum numbers to be related by

$$j_+ = \frac{\gamma + 1}{|\gamma - 1|} j_-. \quad (184)$$

Also in the BC model the diagonal constraint gives the relation between the two sectors, but here the two sectors are not balanced because of the finite value of γ . The system of off-diagonal constraints (182) must be imposed weakly. Alternatively, it can be replaced by the single “master” constraint

$$\sum_i (C^i)^2 = \sum_i \left(L^i - \frac{S}{\gamma} K^i \right)^2 \approx 0. \quad (185)$$

which is of course equivalent at the classical level. Using (181) the “master” constraint becomes simply

$$*\hat{J} \cdot \hat{J} - 4\gamma \hat{L}^2 \approx 0, \quad (186)$$

i.e. a simple relation between the pseudo-scalar Casimir and the generator of rotations. To see its effect, notice that the $SO(4)$ representation space labeled by (j_+, j_-) decomposes into the Clebsch-Gordan series of $SU(2)$ irreducible subspaces

$$|j_+ - j_-| \oplus \dots \oplus (j_+ + j_-) \quad (187)$$

labeled by a pure rotation quantum number k . The “master” constraint simply means that:

$$k = \begin{cases} j^+ + j^- & 0 < \gamma < 1, \\ j^+ - j^- & \gamma > 1. \end{cases} \quad (188)$$

For $\gamma < 1$ the constraint picks out the highest $SU(2)$ irreducible representation, for $\gamma > 1$ the lowest. The set of closure, diagonal, and “master” constraints selects a physical state space \mathcal{H}_{ph} , which is spanned by $SO(4)$ spin-networks (viewed as functions of holonomies, not of the connection) labeled by quantum numbers (j_+, j_-) satisfying an unbalanced relation. One can show that the effect of the full set of constraints on the intertwiner labels is to project onto the following highest (or lowest) weight intertwiner space:

$$\text{Inv } \mathcal{H}_{|j_{1+} \pm j_{1-}|} \otimes \dots \mathcal{H}_{|j_{4+} \pm j_{4-}|} \quad (189)$$

where the sign depends on γ as we have seen. Remarkably, \mathcal{H}_{ph} is isomorphic to

$$L^2(SU(2), dg)/SU(2) \quad (190)$$

which is the Hilbert space associated to a single graph! The isomorphism is realized identifying the label of rotations k with the $SU(2)$ label of LQG, while the intertwiner mapping can be defined in terms of *fusion coefficients* f :

$$|i\rangle \mapsto \sum_{i_+ i_-} f_{i_+ i_-}^i |i_+\rangle \otimes |i_-\rangle, \quad (191)$$

where

$$f_{i_+ i_-}^i(j_1, j_2, j_3, j_4) = \langle i_+ i_- | f | i \rangle = i^{abcd} C_a^{a+a-} C_b^{b+b-} C_c^{c+c-} C_d^{d+d-} i_{a_+ b_+ c_+ d_+}^+ i_{a_- b_- c_- d_-}^-. \quad (192)$$

The intertwiners $|i\rangle$, $|i_+\rangle \otimes |i_-\rangle$ form respectively an $SU(2)$ and $SO(4)$ orthonormal basis of intertwiners and

$$C_a^{a+a-} \equiv \langle j_1^+ j_2^-, a_+ a_- | j_1 a \rangle \quad (193)$$

are Clebsh-Gordan coefficients. The fusion coefficients (192) define a map

$$f : \text{Inv } \mathcal{H}_{j_1} \otimes \dots \otimes \mathcal{H}_{j_4} \longrightarrow \text{Inv } \mathcal{H}_{\left(\frac{|1-\gamma|j_1}{2}, \frac{(1+\gamma)j_1}{2}\right)} \otimes \dots \otimes \mathcal{H}_{\left(\frac{|1-\gamma|j_4}{2}, \frac{(1+\gamma)j_4}{2}\right)} \quad (194)$$

from the $SU(2)$ to the $SO(4)$ intertwiner space. The elementary objects which codes the dynamics is the vertex amplitude. The natural vertex amplitude associated to the physical Hilbert space we have constructed is the full contraction of five intertwiners of the kind (189), with contraction pattern given by the 4-simplex graph, namely:

$$A(\{j_{ab}\}, \{i^a\}) = \sum_{i_+^a i_-^a} 15j \left(\frac{j_{ab}(1+\gamma)}{2}; i_+^a \right) 15j \left(\frac{j_{ab} |1-\gamma|}{2}; i_-^a \right) \prod_a f_{i_+^a i_-^a}^{i^a}(j_{ab}). \quad (195)$$

It depends on 10 spins and 5 $SU(2)$ intertwiners.

Lorentzian With some modifications, we can repeat the previous construction for the Lorentzian signature. In this case we have to consider the $SL(2, \mathbb{C})$ Casimir operators for the representations of the Lorentz group in the so called principal series (n, ρ) . They are given by

$$\hat{J} \cdot \hat{J} = 2(\hat{L}^2 - \hat{K}^2) = \frac{1}{2}(n^2 - \rho^2 - 4)\mathbb{1}, \quad (196)$$

$$*\hat{J} \cdot \hat{J} = -4\hat{L} \cdot \hat{K} = n\rho\mathbb{1}. \quad (197)$$

The solutions of (181) are given by either $\rho = \gamma n$ or $\rho = -n/\gamma$. The existence of these two solutions reflects the two sectors mentioned previously with Immirzi parameter γ and $-1/\gamma$. BF theory cannot a priori distinguish between these two sectors. However, in our framework, the “master” constraint (185) breaks this symmetry and selects the first branch $\rho = \gamma n$. It further imposes that $k = n/2$, where k again labels the subspaces diagonalizing \hat{L}^2 . Therefore the constraints select the lowest $SU(2)$ irreducible representation in the decomposition of

$$\mathcal{H}_{(n,\rho)} = \bigoplus_{k \geq n/2} \mathcal{H}_k. \quad (198)$$

Notice also that the continuous label ρ becomes quantized, because n is discrete. It is because of this fact that any continuous spectrum depending on ρ comes out effectively discrete on the subspace satisfying the simplicity constraints.

As before, we have an embedding map of $SU(2)$ intertwiners into the space of $SL(2, \mathbb{C})$ intertwiners, which gives also the solution of the simplicity constraints for the intertwiner labels:

$$f : \text{Inv } \mathcal{H}_{j_1} \otimes \dots \otimes \mathcal{H}_{j_4} \longrightarrow \text{Inv } \mathcal{H}_{(n_1, \rho_1)} \otimes \dots \otimes \mathcal{H}_{(n_4, \rho_4)},$$

$$|i\rangle \longmapsto \sum_n \int d\rho (n^2 + \rho^2) f_{n\rho}^i |n, \rho\rangle \quad (199)$$

where

$$f_{n\rho}^i \equiv i^{abcd} v_{abcd}^{(n,\rho)}. \quad (200)$$

Here $v^{(n,\rho)}$ is an $SL(2, \mathbb{C})$ 4-valent intertwiner labeled by the virtual link (n, ρ) . The boundary space is once again just given by the $SU(2)$ spin-networks and the vertex amplitude has the form:

$$A(j_{ab}, i_a) = \sum_{n_a} \int d\rho_a (n_a^2 + \rho_a^2) \left(\prod_a f_{n_a \rho_a}^{i_a}(j_{ab}) \right) 15j_{SL(2,\mathbb{C})}((2j_{ab}, 2j_{ab}\gamma); (n_a, \rho_a)) . \quad (201)$$

Notice the presence of the $SL(2, \mathbb{C})$ 15j-symbol.

The final partition function for an arbitrary triangulation, both for the Euclidean and Lorentzian model, is given by gluing the vertex amplitudes with suitable face amplitudes:

$$Z = \sum_{j_f, i_e} \prod_f A_f(j_f) \prod_v A(j_f, i_e) . \quad (202)$$

An important unexpected result provided by the EPRL model comes from the calculation of the spectrum of the operator related to the area of a triangle dual to the face f , given by the formula:

$$\widehat{\text{Area}}^2 \equiv \frac{1}{2} (*\widehat{B})^{ij} (*\widehat{B})_{ij} = \frac{1}{4} \kappa^2 \gamma^2 \widehat{L}^2 . \quad (203)$$

It is *exactly* the spectrum of LQG, for both Euclidean and Lorentzian signatures:

$$\text{Area} = \kappa \gamma \sqrt{k(k+1)} . \quad (204)$$

Remarkably, imposing the simplicity constraints (178) and (186) reduces the potentially continuous spectrum to the exact discrete LQG spectrum (204). This answers, at least in the context of spin SFM, a common objection to the genuineness of the discreteness found in LQG, which is sometimes imputed to the use of $SU(2)$ (instead of the full $SO(1,3)$) group as the gauge group. Indeed $SO(3)$ is compact, while $SO(1,3)$ is non compact, and the latter is likely to yield continuous spectra. The EPRL model is an example which shows that this is not always the case, and strengthens the physical discrete picture of spacetime provided by Loop Quantum Gravity.

We close this section telling that E. Livine and S. Speziale have found an independent derivation of the EPRL vertex, based on the use of the coherent intertwiners they have introduced in [56]. With similar techniques, L. Freidel and K. Krasnov introduced another spin foam model [57] which is very similar to the EPRL one, and coincides with it for $\gamma < 1$. There is also a relation between the states of EPRL model and the *projected spin-network* states studied by E. Livine and S. Alexandrov [81, 82]. The problem of computing semiclassical quantities such as n -point functions is related to the asymptotic behavior of the vertex for large quantum numbers. In the next section we study some properties of the EPRL model investigating the semiclassical limit of its fusion coefficients [19]. We will continue the semiclassical analysis with preliminary numerical investigations and then with the calculation of the graviton propagator. The main result will be that the EPRL model gives the correct 2-point function. For different approaches to the semiclassical limit, see [83] and [84].

6 Asymptotics of LQG fusion coefficients

In the last chapter we have described the new spinfoam model Engle-Pereira-Rovelli-Livine (EPRL). Here we present a careful analysis of the asymptotics of fusion coefficients of Euclidean EPRL model. This is a preliminary step for the study of the semiclassical properties. In particular it allows to check if the new vertex has the right dependence in the intertwiners variables. The region of parameter space of interest is large spins j_{ab} (a, b label two connected nodes of a spin-network) and intertwiners i_a of the same order of magnitude of the spins.

This chapter is organized as follows: in the first section (6.1) we show a simple analytic expression for the EPRL fusion coefficients; in the second (6.2) we use this expression for the analysis of the asymptotics of the coefficients in the region of parameter space of interest, and in third part (6.3) we show that the fusion coefficients map $SO(3)$ semiclassical intertwiners into $SU(2)_L \times SU(2)_R$ semiclassical intertwiners. We conclude discussing the relevance of this result for the analysis of the semiclassical behavior of the model. In the end s we collect some useful formula involving Wigner coefficients.

6.1 Analytical expression for the fusion coefficients

The fusion coefficients provide a map from four-valent $SO(3)$ intertwiners to four-valent $SO(4)$ intertwiners. They can be defined in terms of contractions of $SU(2)$ $3j$ -symbols. In the following we use a planar diagrammatic notation for $SU(2)$ recoupling theory [85]. We represent the $SU(2)$ Wigner metric and the $SU(2)$ three-valent intertwiner respectively by an oriented line and by a node with three links oriented counter-clockwise². As we have seen before, a four-valent $SO(3)$ intertwiner $|i\rangle$ can be represented in terms of the recoupling basis as

$$|i\rangle = \sqrt{2i+1} \begin{array}{c} \begin{array}{ccc} & j_1 & \\ & \diagdown & \diagup \\ & + & \\ & \diagup & \diagdown \\ j_2 & & \end{array} \begin{array}{c} \text{---} i \text{---} \\ \text{---} + \text{---} \\ \begin{array}{ccc} & j_4 & \\ & \diagdown & \diagup \\ & + & \\ & \diagup & \diagdown \\ & & j_3 \end{array} \end{array} \end{array} \quad (205)$$

where a dashed line has been used to denote the virtual link associated to the coupling channel. Similarly a four-valent $SO(4)$ intertwiner can be represented in terms of an $SU(2)_L \times SU(2)_R$ basis as $|i_L\rangle|i_R\rangle$.

Using this diagrammatic notation, the EPRL fusion coefficients for given Immirzi parameter γ are given by

$$f_{i_L i_R}^i(j_1, j_2, j_3, j_4) = (-1)^{j_1 - j_2 + j_3 - j_4} \sqrt{(2i+1)(2i_L+1)(2i_R+1) \prod_{n=1}^4 (2j_n+1)} \quad \times \quad (206)$$

$$\times \begin{array}{c} \begin{array}{ccccc} & + & & + & \\ & \bullet & & \bullet & \\ \frac{|1-\gamma|j_4}{2} \swarrow & & & & \searrow \frac{(1+\gamma)j_3}{2} \\ + \bullet & \begin{array}{ccc} & j_4 & \\ & \diagdown & \diagup \\ & + & \\ & \diagup & \diagdown \\ & & j_3 \end{array} & + & \\ \vdots \uparrow \frac{|1-\gamma|j_3}{2} & & & & \uparrow \frac{(1+\gamma)j_4}{2} \\ i_L \uparrow & \begin{array}{ccc} & i & \\ & \text{---} & \\ & + & \\ & \text{---} & \\ & & i_R \end{array} & \cdot & \\ + \bullet & \begin{array}{ccc} & j_1 & \\ & \diagdown & \diagup \\ & + & \\ & \diagup & \diagdown \\ & & j_2 \end{array} & + & \\ \frac{|1-\gamma|j_2}{2} \swarrow & & & & \searrow \frac{(1+\gamma)j_1}{2} \\ \vdots \uparrow \frac{|1-\gamma|j_1}{2} & & & & \uparrow \frac{(1+\gamma)j_2}{2} \\ & - & & - & \end{array} \end{array}$$

²A minus sign in place of the + will be used to indicate clockwise orientation of the links.

Using the identity

$$(207)$$

where the shaded rectangles represent arbitrary closed graphs, we have that the diagram in (206) can be written as the product of two terms

$$f_{i_L i_R}^i(j_1, j_2, j_3, j_4) = \quad (208)$$

$$= (-1)^{j_1 - j_2 + j_3 - j_4} \sqrt{(2i+1)(2i_L+1)(2i_R+1)\prod_n(2j_n+1)} q_{i_L i_R}^i(j_1, j_2) q_{i_L i_R}^i(j_3, j_4) \quad (209)$$

where $q_{i_L i_R}^i$ is given by the following $9j$ -symbol

$$q_{i_L i_R}^i(j_1, j_2) = \left\{ \begin{array}{ccc} \frac{|1-\gamma|}{2} j_1 & i_L & \frac{|1-\gamma|}{2} j_2 \\ \frac{1+\gamma}{2} j_1 & i_R & \frac{1+\gamma}{2} j_2 \\ j_1 & i & j_2 \end{array} \right\}. \quad (210)$$

From the form of $q_{i_L i_R}^i$ we can read a number of properties of the fusion coefficients. First of all, the diagram in expression (210) displays a node with three links labelled i, i_L, i_R . This corresponds to a triangular inequality between the intertwiners i, i_L, i_R which is not evident from formula (206). We have that the fusion coefficients vanish outside the domain

$$|i_L - i_R| \leq i \leq i_L + i_R. \quad (211)$$

Moreover in the monochromatic case, $j_1 = j_2 = j_3 = j_4$, we have that the fusion coefficients are non-negative (as follows from (209)) and, for $i_L + i_R + i$ odd, they vanish (because the first and the third column in the $9j$ -symbol are identical).

As discussed in [57, 56], the fact that the spins labeling the links in (206) have to be half-integers imposes a quantization condition on the Immirzi parameter γ . In particular γ has to be rational and a restriction on spins may be present. Such restrictions are absent in the Lorentzian case. Now notice that for $0 \leq \gamma < 1$ we have that $\frac{1+\gamma}{2} + \frac{|1-\gamma|}{2} = 1$, while for $\gamma > 1$ we have that $\frac{1+\gamma}{2} - \frac{|1-\gamma|}{2} = 1$ (with the limiting case $\gamma = 1$ corresponding to a selfdual connection). As a result, in the first and the third column of the $9j$ -symbol in (210), the third entry is either the sum or the difference of the first two. In both cases the $9j$ -symbol admits a simple expression in terms of a product of factorials and of a $3j$ -symbol (see appendix). Using this result we have that, for $0 \leq \gamma < 1$, the coefficient $q_{i_L i_R}^i(j_1, j_2)$ can be written as

$$q_{i_L i_R}^i(j_1, j_2) = (-1)^{i_L - i_R + (j_1 - j_2)} \left(\begin{array}{ccc} i_L & i_R & i \\ \frac{|1-\gamma|(j_1 - j_2)}{2} & \frac{(1+\gamma)(j_1 - j_2)}{2} & -(j_1 - j_2) \end{array} \right) A_{i_L i_R}^i(j_1, j_2) \quad (212)$$

with $A_{i_L i_R}^i(j_1, j_2)$ given by

$$\begin{aligned}
 A_{i_L i_R}^i(j_1, j_2) &= \sqrt{\frac{(j_1 + j_2 - i)!(j_1 + j_2 + i + 1)!}{(2j_1 + 1)!(2j_2 + 1)!}} \times \\
 &\times \sqrt{\frac{(|1 - \gamma|j_1)! (|1 - \gamma|j_2)!}{\left(\frac{|1 - \gamma|j_1}{2} + \frac{|1 - \gamma|j_2}{2} - i_L\right)! \left(\frac{|1 - \gamma|j_1}{2} + \frac{|1 - \gamma|j_2}{2} + i_L + 1\right)!}} \times \\
 &\times \sqrt{\frac{((1 + \gamma)j_1)! ((1 + \gamma)j_2)!}{\left(\frac{(1 + \gamma)j_1}{2} + \frac{(1 + \gamma)j_2}{2} - i_R\right)! \left(\frac{(1 + \gamma)j_1}{2} + \frac{(1 + \gamma)j_2}{2} + i_R + 1\right)!}}.
 \end{aligned} \tag{213}$$

A similar result is available for $\gamma > 1$. The Wigner $3j$ -symbol in expression (212) displays explicitly the triangle inequality (211) among the intertwiners. Notice that the expression simplifies further in the monochromatic case as we have a $3j$ -symbol with vanishing magnetic indices.

The fact that the fusion coefficients (206) admit an analytic expression which is so simple is certainly remarkable. The algebraic expression (209),(212),(213) involves no sum over magnetic indices. On the other hand, expression (206) involves ten $3j$ -symbols (one for each node in the graph) and naively fifteen sums over magnetic indices (one for each link). In the following we will use this expression as starting point for our asymptotic analysis.

6.2 Asymptotic analysis

The new analytic formula (209),(212),(213) is well suited for studying the behavior of the EPRL fusion coefficients in different asymptotic regions of parameter space. Here we focus on the region of interest in the analysis of semiclassical correlations. This region is identified as follows: let us introduce a large spin j_0 and a large intertwiner (i.e. virtual spin in a coupling channel) i_0 ; let us also fix the ratio between i_0 and j_0 to be of order one – in particular we will take $i_0 = \frac{2}{\sqrt{3}}j_0$; then we assume that

- the spins j_1, j_2, j_3, j_4 , are restricted to be of the form $j_e = j_0 + \delta j_e$ with the fluctuation δj_e small with respect to the background value j_0 . More precisely we require that the relative fluctuation $\frac{\delta j_e}{j_0}$ is of order $o(1/\sqrt{j_0})$;
- the $SO(3)$ intertwiner i is restricted to be of the form $i = i_0 + \delta i$ with the relative fluctuation $\frac{\delta i}{i_0}$ of order $o(1/\sqrt{j_0})$;
- the intertwiners for $SU(2)_L$ and $SU(2)_R$ are studied in the region close to the background values $i_L^0 = \frac{|1 - \gamma|}{2}i_0$ and $i_R^0 = \frac{1 + \gamma}{2}i_0$. We study the dependence of the fusion coefficients on the fluctuations of these background values assuming that the relative fluctuations $\delta i_L/i_0$ and $\delta i_R/i_0$ are of order $o(1/\sqrt{j_0})$.

A detailed motivation for these assumptions is provided in section 6.3. Here we notice that, both for $0 \leq \gamma < 1$ and for $\gamma > 1$, the background value of the intertwiners i_L, i_R, i , saturate one of the two triangular inequalities (211). As a result, we have that the fusion coefficients vanish unless the

perturbations on the background satisfy the following inequality

$$\delta i \leq \delta i_L + \delta i_R \quad 0 \leq \gamma < 1 \quad (214)$$

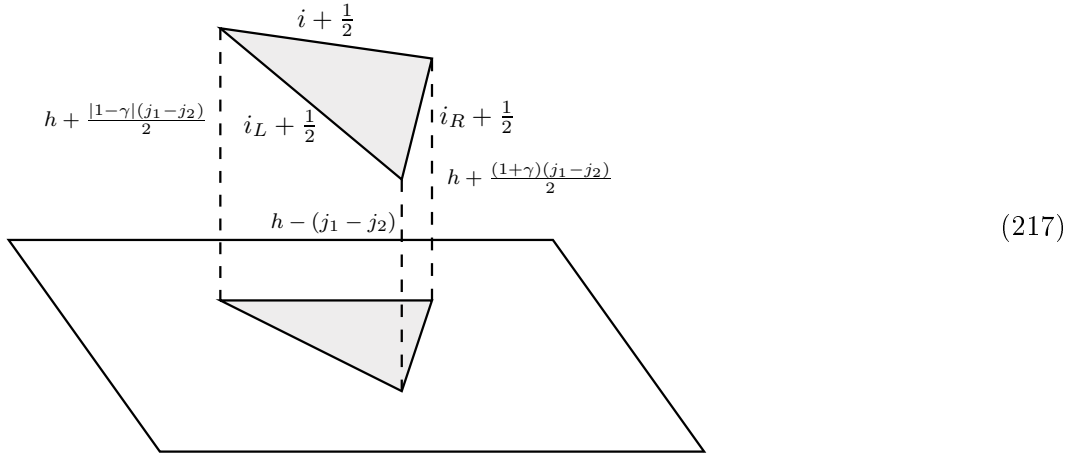
$$\delta i_R \leq \delta i + \delta i_L \quad \gamma > 1. \quad (215)$$

In order to derive the asymptotics of the EPRL fusion coefficients in this region of parameter space we need to analyze both the asymptotics of the $3j$ -symbol in (212) and of the coefficients $A_{i_L i_R}^i(j_1, j_2)$. This is done in the following two paragraphs

Asymptotics of $3j$ -symbols The behavior of the $3j$ -symbol appearing in equation (212) in the asymptotic region described above is given by Ponzano-Regge asymptotic expression (equation 2.6 in [71]; see also the last section):

$$\begin{aligned} & \left(\begin{array}{ccc} i_L & i_R & i \\ \frac{|1-\gamma|(j_1-j_2)}{2} & \frac{(1+\gamma)(j_1-j_2)}{2} & -(j_1-j_2) \end{array} \right) \sim \frac{(-1)^{i_L+i_R-i+1}}{\sqrt{2\pi A}} \times \\ & \times \cos \left((i_L + \frac{1}{2})\theta_L + (i_R + \frac{1}{2})\theta_R + (i + \frac{1}{2})\theta + \frac{|1-\gamma|(j_1-j_2)}{2}\phi_- - \frac{(1+\gamma)(j_1-j_2)}{2}\phi_+ + \frac{\pi}{4} \right). \end{aligned} \quad (216)$$

The quantities A , θ_L , θ_R , θ , ϕ_- , ϕ_+ admit a simple geometrical representation: let us consider a triangle with sides of length $i_L + \frac{1}{2}$, $i_R + \frac{1}{2}$, $i + \frac{1}{2}$ embedded in 3d Euclidean space as shown below



In the figure the height of the three vertices of the triangle with respect to a plane are given; this fixes the orientation of the triangle and forms an orthogonal prism with triangular base. The quantity A is the area of the base of the prism (shaded in picture). The quantities θ_L , θ_R , θ are dihedral angles between the faces of the prism which intersect at the sides i_L , i_R , i of the triangle. The quantities ϕ_- , ϕ_+ are dihedral angles between the faces of the prism which share the side of length $h + |1 - \gamma|(j_1 - j_2)/2$ and the side of length $h + (1 + \gamma)(j_1 - j_2)/2$, respectively. For explicit expressions we refer to the appendix.

In the monochromatic case, $j_1 = j_2$, we have that the triangle is parallel to the plane and the formula simplifies a lot; in particular we have that the area A of the base of the prism is simply given by Heron

formula in terms of i_L, i_R, i only, and the dihedral angles $\theta_L, \theta_R, \theta$ are all equal to $\pi/2$. As a result the asymptotics is given by

$$\begin{pmatrix} i_L & i_R & i \\ 0 & 0 & 0 \end{pmatrix} \sim \frac{1}{\sqrt{2\pi A}} \frac{1 + (-1)^{i_L+i_R+i}}{2} (-1)^{\frac{i_L+i_R+i}{2}}. \quad (218)$$

Notice that the sum $i_L + i_R + i$ is required to be integer and that the asymptotic expression vanishes if the sum is odd and is real if the sum is even. Now, the background configuration of i_L, i_R and i we are interested in corresponds to a triangle which is close to be degenerate to a segment. This is due to the fact that $\frac{(1-\gamma)}{2}i_0 + \frac{(1+\gamma)}{2}i_0 = i_0$ for $0 \leq \gamma < 1$, and $\frac{(\gamma+1)}{2}i_0 - \frac{(\gamma-1)}{2}i_0 = i_0$ for $\gamma > 1$. In fact the triangle is not degenerate as an offset $\frac{1}{2}$ is present in the length of its edges. As a result the area of this almost-degenerate triangle is non-zero and scales as $i_0^{3/2}$ for large i_0 . When we take into account allowed perturbations of the edge-lengths of the triangle we find

$$A = \begin{cases} \frac{1}{4}\sqrt{1-\gamma^2} i_0^{3/2} (\sqrt{1+2(\delta i_L + \delta i_R - \delta i)} + o(i_0^{-3/4})) & 0 \leq \gamma < 1 \\ \frac{1}{4}\sqrt{\gamma^2-1} i_0^{3/2} (\sqrt{1+2(\delta i + \delta i_L - \delta i_R)} + o(i_0^{-3/4})) & \gamma > 1 \end{cases}. \quad (219)$$

This formula holds both when the respective sums $\delta i_L + \delta i_R - \delta i$ and $\delta i + \delta i_L - \delta i_R$ vanish and when they are positive and at most of order $O(\sqrt{i_0})$. As a result we have that, when $\delta i_L + \delta i_R - \delta i$, or $\delta i + \delta i_L - \delta i_R$ respectively, is even the perturbative asymptotics of the square of the $3j$ -symbol is

$$\begin{pmatrix} \frac{|1-\gamma|}{2}i_0 + \delta i_L & \frac{(1+\gamma)}{2}i_0 + \delta i_R & i_0 + \delta i \\ 0 & 0 & 0 \end{pmatrix}^2 \sim \begin{cases} \frac{2}{\pi} \frac{1}{\sqrt{1-\gamma^2}} \frac{i_0^{-3/2}}{\sqrt{1+2(\delta i_L + \delta i_R - \delta i)}} \theta(\delta i_L + \delta i_R - \delta i) & 0 \leq \gamma < 1 \\ \frac{2}{\pi} \frac{1}{\sqrt{\gamma^2-1}} \frac{i_0^{-3/2}}{\sqrt{1+2(\delta i + \delta i_L - \delta i_R)}} \theta(\delta i + \delta i_L - \delta i_R) & \gamma > 1 \end{cases}. \quad (220)$$

The theta functions implement the triangular inequality on the fluctuations. In the more general case when $j_1 - j_2$ is non-zero but small with respect to the size of the triangle, we have that the fluctuation in δj_e can be treated perturbatively and, to leading order, the asymptotic expression remains unchanged.

Gaussians from factorials In this paragraph we study the asymptotics of the function $A_{i_L i_R}^i(j_1, j_2)$ which, for $0 \leq \gamma < 1$, is given by expression (213). The proof in the case $\gamma > 1$ goes the same way. In the asymptotic region of interest all the factorials in (213) have large argument, therefore Stirling's asymptotic expansion can be used:

$$j_0! = \sqrt{2\pi j_0} e^{+j_0(\log j_0 - 1)} \left(1 + \sum_{n=1}^N a_n j_0^{-n} + O(j_0^{-(N+1)})\right) \quad \text{for all } N > 0, \quad (221)$$

where a_n are coefficients which can be computed; for instance $a_1 = \frac{1}{12}$. The formula we need is a perturbative expansion of the factorial of $(1 + \xi)j_0$ when the parameter ξ is of order $o(1/\sqrt{j_0})$. We have

that

$$((1 + \xi)j_0)! = \sqrt{2\pi j_0} \exp\left(+j_0(\log j_0 - 1) + \xi j_0 \log j_0 + j_0 \sum_{k=1}^{\infty} c_k \xi^k\right) \times \quad (222)$$

$$\times \left(1 + \sum_{n=1}^N \sum_{m=1}^M a_n b_m j_0^{-n} \xi^m + O(j_0^{-(N+\frac{M}{2}+1)})\right) \quad (223)$$

where the coefficients b_m and c_k can be computed explicitly. We find that the function $A_{i_L i_R}^i(j_1, j_2)$ has the following asymptotic behavior

$$A_{\frac{i_0+\delta i}{2}+\delta i_L, \frac{(1+\gamma)i_0}{2}+\delta i_R}^{i_0+\delta i}(j_0 + \delta j_1, j_0 + \delta j_2) \sim A_0(j_0) e^{-H(\delta i_L, \delta i_R, \delta i, \delta j_1, \delta j_2)} \quad (224)$$

where $A_0(j_0)$ is the function evaluated at the background values and $H(\delta i_L, \delta i_R, \delta i, \delta j_1, \delta j_2)$ is given by

$$\begin{aligned} H(\delta i_L, \delta i_R, \delta i, \delta j_1, \delta j_2) &= \frac{1}{2}(\operatorname{arcsinh}\sqrt{3})(\delta i_L + \delta i_R - \delta i) + \quad (225) \\ &+ \frac{\sqrt{3}}{2} \frac{(\delta i_L)^2}{|1-\gamma|i_0} + \frac{\sqrt{3}}{2} \frac{(\delta i_R)^2}{(1+\gamma)i_0} - \frac{\sqrt{3}}{4} \frac{(\delta i)^2}{i_0} + \\ &- \frac{1}{2} \frac{\delta i_L + \delta i_R - \delta i}{i_0} (\delta j_1 + \delta j_2) + O\left(\frac{1}{\sqrt{j_0}}\right) \end{aligned}$$

for $0 \leq \gamma < 1$, while for $\gamma > 1$ it is given by

$$\begin{aligned} H(\delta i_L, \delta i_R, \delta i, \delta j_1, \delta j_2) &= \frac{1}{2}(\operatorname{arcsinh}\sqrt{3})(\delta i + \delta i_L - \delta i_R) + \quad (226) \\ &+ \frac{\sqrt{3}}{2} \frac{(\delta i_L)^2}{|1-\gamma|i_0} + \frac{\sqrt{3}}{2} \frac{(\delta i_R)^2}{(1+\gamma)i_0} - \frac{\sqrt{3}}{4} \frac{(\delta i)^2}{i_0} + \\ &- \frac{1}{2} \frac{\delta i + \delta i_L - \delta i_R}{i_0} (\delta j_1 + \delta j_2) + O\left(\frac{1}{\sqrt{j_0}}\right). \end{aligned}$$

Perturbative asymptotics of the fusion coefficients Collecting the previous results we find for the fusion coefficients the asymptotic formula

$$\begin{aligned} f_{\frac{i_0+\delta i}{2}+\delta i_L, \frac{(1+\gamma)i_0}{2}+\delta i_R}^{i_0+\delta i}(j_0 + \delta j_e) &\sim f_0(j_0) \frac{1}{\sqrt{1+2(\delta i_L + \delta i_R - \delta i)}} \theta(\delta i_L + \delta i_R - \delta i) \times \quad (227) \\ &\times \exp\left(-\operatorname{arcsinh}(\sqrt{3})(\delta i_L + \delta i_R - \delta i)\right) \times \\ &\times \exp\left(-\sqrt{3} \frac{(\delta i_L)^2}{|1-\gamma|i_0} - \sqrt{3} \frac{(\delta i_R)^2}{(1+\gamma)i_0} + \frac{\sqrt{3}}{2} \frac{(\delta i)^2}{i_0}\right) \times \\ &\times \exp\left(\frac{1}{2} \frac{\delta i_L + \delta i_R - \delta i}{i_0} (\delta j_1 + \delta j_2 + \delta j_3 + \delta j_4)\right) \end{aligned}$$

for $0 \leq \gamma < 1$, and

$$\begin{aligned}
 f_{\frac{1-\gamma}{2}i_0+\delta i_L, \frac{1+\gamma}{2}i_0+\delta i_R}^{i_0+\delta i}(j_0+\delta j_e) &\sim f_0(j_0) \frac{1}{\sqrt{1+2(\delta i+\delta i_L-\delta i_R)}} \theta(\delta i+\delta i_L-\delta i_R) \times \\
 &\times \exp(-\operatorname{arcsinh}(\sqrt{3})(\delta i+\delta i_L-\delta i_R)) \times \\
 &\times \exp\left(-\sqrt{3}\frac{(\delta i_L)^2}{|1-\gamma|i_0}-\sqrt{3}\frac{(\delta i_R)^2}{(1+\gamma)i_0}+\frac{\sqrt{3}}{2}\frac{(\delta i)^2}{i_0}\right) \times \\
 &\times \exp\left(\frac{1}{2}\frac{\delta i+\delta i_L-\delta i_R}{i_0}(\delta j_1+\delta j_2+\delta j_3+\delta j_4)\right)
 \end{aligned} \tag{228}$$

for $\gamma > 1$, where $f_0(j_0)$ is the value of the fusion coefficients at the background configuration. As we will show in next section, this asymptotic expression has an appealing geometrical interpretation and plays a key role in the connection between the semiclassical behavior of the spinfoam vertex and simplicial geometries.

6.3 Semiclassical behavior

To illustrate some important features of the semiclassical behavior of the fusion coefficients, we must first anticipate the principal idea of the next chapter: the propagation of boundary wave packets as a way to test the semiclassical behavior of a spinfoam model. Consider an “initial” state made by the product of four intertwiner wavepackets; this state has the geometrical interpretation of four semiclassical regular tetrahedra in the boundary of a 4-simplex of linear size of order $\sqrt{j_0}$. Then we can evolve this state (numerically) by contraction with the flipped vertex amplitude to give the “final” state, which in turn is an intertwiner wavepacket. While in [20] we considered only very small j_0 ’s, in [21] we make the same calculation for higher spins both numerically and semi-analytically, and the results are clear: the “final” state is a semiclassical regular tetrahedron with the same size as the incoming ones. This is exactly what we expect from the classical equations of motion.

The evolution is defined by

$$\sum_{i_1 \dots i_5} W(j_0, i_1, \dots, i_5) \psi(i_1, j_0) \dots \psi(i_5, j_0) \equiv \phi(i_5, j_0), \tag{229}$$

where

$$\psi(i, j_0) = C(j_0) \exp\left(-\frac{\sqrt{3}}{2}\frac{(i-i_0)^2}{i_0} + i\frac{\pi}{2}(i-i_0)\right) \tag{230}$$

is a semiclassical $SO(3)$ intertwiner (actually its components in the virtual basis $|i\rangle$), or a semiclassical tetrahedron (see section chapter 8.2) in the equilateral configuration, with $C(j_0)$ a normalization constant, and $W(j_0, i_1, \dots, i_5)$ is the vertex (195) with $\gamma = 0$ evaluated in the homogeneous spin configuration (the ten spins equal to j_0). We are also using the notation i for the imaginary unit. If we want to evaluate the sum (229) over intertwiners, for fixed j_0 , then we have to evaluate the function g defined as follows:

$$g(i_L, i_R, j_0) = \sum_i f_{i_L i_R}^i(j_0) \psi(i, j_0). \tag{231}$$

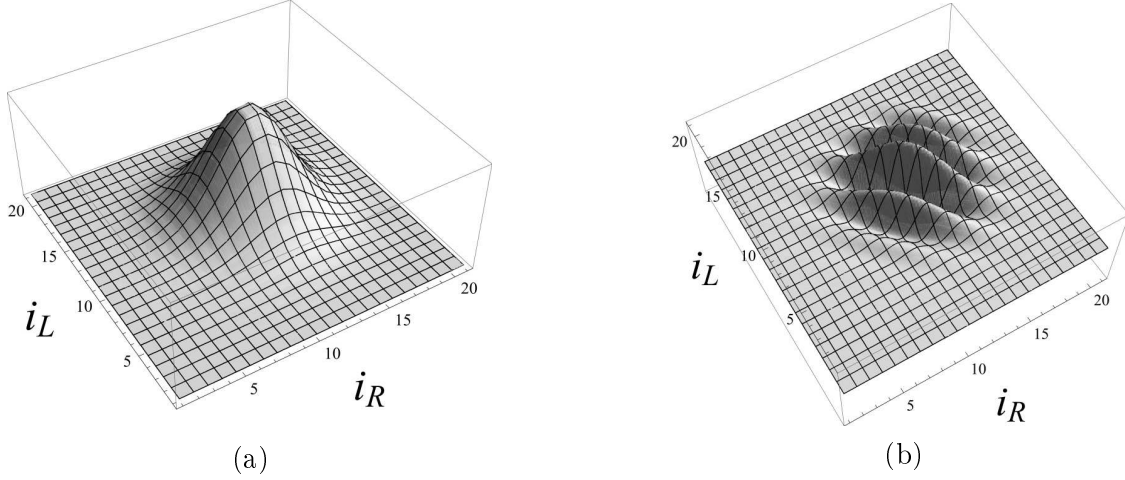


Figure 7: (a) Interpolated plot of the modulus of $g(i_L, i_R, j_0)$ for $j_0 = 20$ and $\gamma = 0$ computed using the exact formula of the fusion coefficients. (b) Top view of the imaginary part.

The values of g are the components of an $SO(4)$ intertwiner in the basis $|i_L\rangle|i_R\rangle$, where $|i_L\rangle$ is an intertwiner between four $SU(2)$ irreducible representations of spin $j_0^L \equiv \frac{1-\gamma}{2}j_0$, and $|i_R\rangle$ is an intertwiner between representations of spin $j_0^R \equiv \frac{1+\gamma}{2}j_0$.

We show that EPRL fusion coefficients map $SO(3)$ semiclassical intertwiners into $SU(2)_L \times SU(2)_R$ semiclassical intertwiners. The sum over the intertwiner i of the fusion coefficients times the semiclassical state can be computed explicitly at leading order in a stationary phase approximation, using the asymptotic formula (227)(228). The result is

$$\begin{aligned} \sum_i f_{i_L i_R}^i(j_0) \psi(i, j_0) &\approx \alpha_0 f_0(j_0) C(j_0) \times \exp\left(-\sqrt{3} \frac{(i_L - \frac{1-\gamma}{2} i_0)^2}{|1-\gamma| i_0} \pm i \frac{\pi}{2} (i_L - \frac{1-\gamma}{2} i_0)\right) \times \\ &\times \exp\left(-\sqrt{3} \frac{(i_R - \frac{1+\gamma}{2} i_0)^2}{(1+\gamma) i_0} + i \frac{\pi}{2} (i_R - \frac{1+\gamma}{2} i_0)\right) \end{aligned} \quad (232)$$

where

$$\alpha_0 = \sum_{k \in 2\mathbb{N}} \frac{e^{-\operatorname{arcsinh}(\sqrt{3})k}}{\sqrt{1+2k}} e^{\mp i \frac{\pi}{2} k} \simeq 0.97; \quad (233)$$

the plus-minus signs both in (232) and (233) refer to the two cases $\gamma < 1$ (upper sign) and $\gamma > 1$ (lower sign). The r.h.s. of (232), besides being a very simple formula for the asymptotical action of the map f on a semiclassical intertwiner, is asymptotically invariant under change of pairing of the virtual spins i_L and i_R (up to a normalization N). Recalling that the change of pairing (94) is made by means of $6j$ -symbols,

we have

$$\begin{aligned} & \sum_{i_L} \sum_{i_R} \sqrt{\dim(i_L)\dim(i_R)} (-1)^{i_L+k_L+i_R+k_R} \left\{ \begin{array}{ccc} \frac{|1-\gamma|}{2} j_0 & \frac{|1-\gamma|}{2} j_0 & i_L \\ \frac{|1-\gamma|}{2} j_0 & \frac{|1-\gamma|}{2} j_0 & k_L \end{array} \right\} \times \\ & \times \left\{ \begin{array}{ccc} \frac{1+\gamma}{2} j_0 & \frac{1+\gamma}{2} j_0 & i_R \\ \frac{1+\gamma}{2} j_0 & \frac{1+\gamma}{2} j_0 & k_R \end{array} \right\} g(i_L, i_R) \approx N(j_0) g(k_L, k_R, j_0). \end{aligned} \quad (234)$$

This result holds because each of the two exponentials in (232) is of the form

$$\exp\left(-\frac{\sqrt{3}}{2} \frac{(k-k_0)^2}{k_0} \pm i\frac{\pi}{2}(k-k_0)\right), \quad (235)$$

which is a semiclassical equilateral tetrahedron (section 8.2) with area quantum numbers k_0 ; it follows that g is (asymptotically) an $SO(4)$ semiclassical intertwiner. The formula (232) can be checked against plots of the exact formula for large j_0 's; a particular case is provided in fig.7.

In addition, we can ask whether the inverse map f^{-1} has the same semiclassical property. Remarkably, the answer is positive: f^{-1} maps semiclassical $SO(4)$ intertwiners into semiclassical $SO(3)$ intertwiners. The calculation, not reported here, involves error functions (because of the presence of the theta function) which have to be expanded to leading order in $1/j_0$.

A final remark on our choice for the asymptotic region is needed. The goal we have in mind is to apply the asymptotic formula for the fusion coefficients to the calculation of observables like the semiclassical correlations for two local geometric operators $\hat{\mathcal{O}}_1, \hat{\mathcal{O}}_2$

$$\langle \hat{\mathcal{O}}_1 \hat{\mathcal{O}}_2 \rangle_q = \frac{\sum_{j_{ab} i_a} W(j_{ab}, i_a) \hat{\mathcal{O}}_1 \hat{\mathcal{O}}_2 \Psi_q(j_{ab}, i_a)}{\sum_{j_{ab} i_a} W(j_{ab}, i_a) \Psi_q(j_{ab}, i_a)} \quad (236)$$

in the semiclassical regime (at the single-vertex level). If the classical (intrinsic and the extrinsic) geometry q over which the boundary state is peaked is the geometry of the boundary of a regular 4-simplex, then the sums in (236) are dominated by spins of the form $j_{ab} = j_0 + \delta j_{ab}$ and intertwiners of the form $i_a = i_0 + \delta i_a$, with $i_0 = 2j_0/\sqrt{3}$, where the fluctuations must be such that the relative fluctuations $\delta j/j_0, \delta i/j_0$ go to zero in the limit $j_0 \rightarrow \infty$. More precisely, the fluctuations are usually chosen to be at most of order $O(\sqrt{j_0})$. This is exactly the region we study here. As to the region in the (i_L, i_R) parameter space, the choice of the background values $\frac{|1-\gamma|}{2} i_0, \frac{1+\gamma}{2} i_0$ and the order of their fluctuations is made *a posteriori* both by numerical investigation and by the form of the asymptotic expansion. It is evident that the previous considerations hold in particular for the function g analyzed in this section.

6.4 The case $\gamma = 1$

When $\gamma = 1$ we have that $j_L \equiv \frac{|1-\gamma|}{2} j = 0$ and we can read from the graph (206) that the fusion coefficients vanish unless $i_L = 0$. Furthermore it is easy to see that for $\gamma = 1$ the fusion coefficients vanish also when

i_R is different from i . This can be seen, for instance, applying the identity

$$\begin{array}{c} \text{---} \\ | \\ | \\ | \\ \text{---} \end{array} \begin{array}{c} i \\ | \\ | \\ | \\ i_R \end{array} = \frac{1}{\dim i} \delta_{i, i_R} \begin{array}{c} \text{---} \\ \curvearrowright \\ i \\ \curvearrowleft \\ i_R \\ \text{---} \end{array} \quad (237)$$

to the graph (206) with $i_L = 0$. As a result, we have simply

$$f_{i_L i_R}^i(j_1, j_2, j_3, j_4) = \delta_{i_L, 0} \delta_{i_R, i} \quad (238)$$

and the asymptotic analysis is trivial. The previous equation can be also considered as a normalization check; in fact, with the definition (206) for the fusion coefficients, the EPRL vertex amplitude (424) reduces for $\gamma = 1$ to the usual $SO(3)$ BF vertex amplitude. Now one can argue that the case $\gamma = 1$ should correspond to self-dual (quantum) gravity and not to the topological $SO(3)$ BF theory. However notice that $\gamma = 1$ is a singular value for the Barbero-Immirzi parameter in the derivation of EPRL Euclidean vertex amplitude from the classical theory [15].

6.5 Summary of semiclassical properties of fusion coefficients

We provided and a simple analytic asymptotic formula for the fusion coefficients; thanks to this formula, we found the asymptotical action of the fusion coefficients on a semiclassical intertwiner (see chapter 8). We resume briefly some properties, focusing on the case $\gamma = 0$.

The action of f_{i_L, i_R}^i (viewed as a map between intertwiner spaces) on a semiclassical intertwiner is given by

$$g(i_L, i_R) \equiv \sum_i f_{i_L, i_R}^i \psi(i). \quad (239)$$

We showed that, for large j_0 's

$$g(i_L, i_R) \simeq C \exp\left(-\frac{3}{2j_0}(i_L - \frac{i_0}{2})^2 - \frac{3}{2j_0}(i_R - \frac{i_0}{2})^2 + i\frac{\pi}{2}(i_L + i_R)\right), \quad (240)$$

where C is an irrelevant normalization factor not depending on i_L and i_R at leading order in $1/j_0$ powers. Hence, asymptotically, the function g factorizes into left and right parts; we indicate them, with abuse of notation, $g(i_L)$ and $g(i_R)$. The values of $g(i_L, i_R)$ are the components of an $SO(4) \simeq SU(2) \times SU(2)$ intertwiner in the basis $|i_L, i_R\rangle$, which we call $SO(4)$ semiclassical intertwiner. Also the converse holds: the asymptotical action of the fusion coefficients on an $SO(4)$ semiclassical intertwiner is an $SO(3)$ semiclassical intertwiner, i.e.

$$\sum_{i_L, i_R} f_{i_L, i_R}^i g(i_L, i_R) \simeq \psi(i). \quad (241)$$

6.6 Properties of $9j$ -symbols and asymptotics of $3j$ -symbol

The $9j$ -symbol with two columns with third entry given by the sum of the first two can be written as

$$\left\{ \begin{array}{ccc} a & f & c \\ b & g & d \\ a+b & h & c+d \end{array} \right\} = (-1)^{f-g+a+b-(c+d)} \left(\begin{array}{ccc} f & g & h \\ a-c & b-d & -(a+b-(c+d)) \end{array} \right) \times \quad (242)$$

$$\times \sqrt{\frac{(2a)!(2b)!(2c)!(2d)!(a+b+c+d-h)!(a+b+c+d+h+1)!}{(2a+2b+1)!(2c+2d+1)!(a+c-f)!(a+c+f+1)!(b+d-g)!(b+d+g+1)!}}.$$

An analogous formula for the $9j$ -symbol with two columns with third entry given by the difference of the first two can be obtained from the formula above noting that

$$\left\{ \begin{array}{ccc} a & f & c \\ b & g & d \\ b-a & h & d-c \end{array} \right\} = \left\{ \begin{array}{ccc} b-a & h & d-c \\ a & f & c \\ b & g & d \end{array} \right\}, \quad (243)$$

so we are in the previous case.

The $3j$ -symbol with vanishing magnetic numbers has the simple expression

$$\left(\begin{array}{ccc} a & b & c \\ 0 & 0 & 0 \end{array} \right) = (-1)^{a-b} \pi^{1/4} \frac{2^{\frac{a+b-c-1}{2}}}{\left(\frac{c-a-b-1}{2}\right)! \sqrt{(a+b-c)!}} \sqrt{\frac{\left(\frac{c+a-b-1}{2}\right)! \left(\frac{c-a+b-1}{2}\right)! \left(\frac{a+b+c}{2}\right)!}{\left(\frac{c+a-b}{2}\right)! \left(\frac{c-a+b}{2}\right)! \left(\frac{a+b+c+1}{2}\right)!}}. \quad (244)$$

These formula can be derived from [85, 86].

The asymptotic formula of $3j$ -symbols for large spins a, b, c and admitted magnetic numbers, i.e. $m_a + m_b + m_c = 0$, given by G. Ponzano and T. Regge in [71] is

$$\left(\begin{array}{ccc} a & b & c \\ m_a & m_b & m_c \end{array} \right) \sim \frac{(-1)^{a+b-c+1}}{\sqrt{2\pi A}} \cos \left(\left(a + \frac{1}{2}\right)\theta_a + \left(b + \frac{1}{2}\right)\theta_b + \left(c + \frac{1}{2}\right)\theta_c + m_a\phi_a - m_b\phi_b + \frac{\pi}{4} \right) \quad (245)$$

with

$$\theta_a = \frac{\arccos \left(2\left(a + \frac{1}{2}\right)^2 m_c + m_a \left(\left(c + \frac{1}{2}\right)^2 + \left(a + \frac{1}{2}\right)^2 - \left(b + \frac{1}{2}\right)^2 \right) \right)}{\sqrt{\left(\left(a + \frac{1}{2}\right)^2 - m_a^2 \right) \left(4\left(c + \frac{1}{2}\right)^2 \left(a + \frac{1}{2}\right)^2 - \left(\left(c + \frac{1}{2}\right)^2 + \left(a + \frac{1}{2}\right)^2 - \left(b + \frac{1}{2}\right)^2 \right)^2}} \quad (246)$$

$$\phi_a = \arccos \left(\frac{1}{2} \frac{\left(a + \frac{1}{2}\right)^2 - \left(b + \frac{1}{2}\right)^2 - \left(c + \frac{1}{2}\right)^2 - 2m_b m_c}{\sqrt{\left(\left(b + \frac{1}{2}\right)^2 - m_b^2 \right) \left(\left(c + \frac{1}{2}\right)^2 - m_c^2 \right)}} \right) \quad (247)$$

$$A = \sqrt{-\frac{1}{16} \det \begin{pmatrix} 0 & \left(a + \frac{1}{2}\right)^2 - m_a^2 & \left(b + \frac{1}{2}\right)^2 - m_b^2 & 1 \\ \left(a + \frac{1}{2}\right)^2 - m_a^2 & 0 & \left(c + \frac{1}{2}\right)^2 - m_c^2 & 1 \\ \left(b + \frac{1}{2}\right)^2 - m_b^2 & \left(c + \frac{1}{2}\right)^2 - m_c^2 & 0 & 1 \\ 1 & 1 & 1 & 0 \end{pmatrix}} \quad (248)$$

and $\theta_b, \theta_c, \phi_b$ are obtained by cyclic permutations of (a, b, c) .

7 Numerical investigations on the semiclassical limit

In this chapter we introduce a new technique to test the spinfoam dynamics, which is complementary to the calculation of n -point functions. This technique, presented for the first time in [20], and improved in [21], is the propagation of semiclassical wavepackets: as in ordinary Quantum Mechanics, the theory has the correct semiclassical limit only if semiclassical wavepackets follow the trajectory predicted by classical equations of motion.

In [20], the wave-packet propagation in the intertwiner sector of EPR model was studied numerically. In brief, we considered the most simple solution of discretized Einstein equations given by a single flat 4-simplex with boundary constituted by five regular tetrahedra. In the dual LQG picture this boundary is represented by a pentagonal 4-valent spin-network, labeled by ten spins and five intertwiners; in order to have a semiclassical state one has to construct some (infinite) linear combination of spin-networks of this kind. It is well known (see [87] and chapter 8) that we can take a superposition of intertwiners in the virtual spin basis with a Gaussian weight, in order to be catch the classical geometry of a tetrahedron: since in a quantum tetrahedron the angles do not commute, one has to consider semiclassical superpositions of angle eigenstates in order to peak *all* angles on the right classical value. We chose an initial state formed by four coherent intertwiners at four nodes, and made the drastic approximation of taking the ten spins fixed to be equal to some j_0 . Then we calculated numerically its evolution, here called 4-to-1 evolution, that is its contraction with the EPR spin foam vertex amplitude. Classical Einstein equations impose the final state to be a coherent intertwiner with the same geometrical properties (mean and phase). We found good indications but, due to the very low j_0 's used in the numerical simulation, we were not in a good semiclassical regime.

In the second paper [21] we found the general behavior of the evolution at high j_0 's. In fact we will see that the propagation is perfectly “rigid”: four gaussian wave-packets evolve into one gaussian wave-packet with the same parameters, except for a flip in the phase. The phase of the evolved phase, and in particular its flipping, are the right ones which yield the correct physical expectation values. This is why the evolution of intertwiner wave-packets can check if a vertex amplitude has the correct dependence on the intertwiner variables. We have made our analysis in two independent ways: the first is semi-analytical and based on a numerical result about the $15j$ -symbol, viewed as a propagation kernel, and the asymptotic properties of the fusion coefficients (chapter 6); the second is purely numerical. The first has the advantage of giving a nice picture of the dynamics in terms of wave-packets evolving separately in the left and right sectors of $SO(4)$. We also explore the possibility of propagating three coherent intertwiners into two (we will refer to it as the 3-to-2 evolution), finding similar results. Then we present the results from another point of view, namely as physical expectation values, finding that these are asymptotically the classical ones. Though we use the drastic approximation of fixing all spins, these results were the first clear indication that the EPRL model possesses good semiclassical properties.

7.1 *Wave-packets propagation*

Suppose you are explicitly given the propagation kernel $W_t(x, y)$ of a one-dimensional nonrelativistic quantum system defined by a Hamiltonian operator H

$$W_t(x, y) = \langle x | e^{-\frac{i}{\hbar} H t} | y \rangle \quad (249)$$

and you want to study whether the classical ($\hbar \rightarrow 0$) limit of this quantum theory yields a certain given classical evolution. One of the (many) ways of doing so is to propagate a wave-packet $\psi_{x,p}(x)$ with $W_t(x, y)$. Suppose that in the time interval t the classical theory evolves the initial position and momentum x_i, p_i to the final values x_f, p_f . Then you can consider a semiclassical wave-packet $\psi_{x_i, p_i}(y)$ centered on the initial values x_i, p_i , compute its evolution under the kernel

$$\phi(x) \equiv \int dy W_t(x, y) \psi_{x_i, p_i}(y) \quad (250)$$

and ask whether or not this state is a semiclassical wave-packet centered on the correct final values x_f, p_f . Here, we consider the possibility of using this method for exploring the semiclassical limit of the dynamics of nonperturbative quantum gravity.

We are interested in investigating the intertwiner dependence of the EPR vertex. The derivation of the vertex amplitude presented in [88] indicates that the process described by one vertex can be seen as the dynamics of a single cell in a Regge triangulation of General Relativity. This is a fortunate situation, because it allows us to give a simple and direct geometrical interpretation to the dynamical variables entering the vertex amplitude, and a simple formulation of the dynamical equations.

We consider the boundary of a Regge cell that is formed by five tetrahedra joined along all their faces, thus forming a closed space with the topology of a 3-sphere. Recall that the ten spins j_{nm} ($n, m = 1, \dots, 5$) are the quantum numbers of the areas A_{nm} that separates the tetrahedra n and m , and the five intertwiners i_n are the quantum numbers associated to the angles between the triangles (mp) and (qr) in the tetrahedron n (see section 8.2). These quantities determine entirely the intrinsic and extrinsic classical geometry of the boundary surface. Each tetrahedron has six such angles, of which only two are independent (at given values of the areas); but the corresponding quantum operators do not commute [87] and a basis of the Hilbert space on which they act can be obtained by diagonalizing just a single arbitrary one among these angles. Therefore the intrinsic geometry of the boundary of a classical Regge cell is determined by twenty numbers, but the the corresponding quantum numbers are only fifteen: the fifteen quantities j_{nm}, i_n . These are the fifteen arguments of the vertex. When using the intertwiners labeled by virtual spins i_n , we have of course to specify to which pairing we are referring.

The equations of motion of any dynamical system can be expressed as constraints on the set formed by the initial, final and (if it is the case) boundary variables. For instance, in the case of the evolution of a free particle in the time interval t , the equations of motion can be expressed as constraints on the set (x_i, p_i, x_f, p_f) . These constraints are of course $m(x_f - x_i)/t = p_i = p_f$ (for the general logic of this approach to dynamics, see [7]). In General Relativity, the Einstein equations can be seen as constraints on a boundary 3-surface. These, in fact, can be viewed as the ensemble of the initial, boundary and final data for a process happening inside the boundary 3-sphere. Such constraints are a bit difficult to write explicitly, but one solution is easy: the one that corresponds to flat space and to the boundary of a *regular* 4-simplex. This is given by all equal areas $A_{nm} = j_0$, all equal angles $i_n = i_0$, and equal extrinsic curvature angles $\theta_{nm} = \theta$. Elementary geometry gives

$$i_0 = \frac{2}{\sqrt{3}} j_0, \quad \cos \theta = -\frac{1}{4}. \quad (251)$$

It follows immediately from these considerations that a boundary wave-packet centered on these values must be correctly propagated by the vertex amplitude, if the vertex amplitude is to give the Einstein equations in the classical limit.

The simplest wave packet we may consider is a factored Gaussian wave-packet

$$\Psi(j_{nm}, i_n) = \prod_{nm} \tilde{\psi}(j_{nm}) \prod_n \psi(i_n) \quad (252)$$

where

$$\tilde{\psi}(j_{nm}) = e^{-\frac{1}{\tau}(j_{nm}-j_0)^2 + i\theta j_{nm}} \quad (253)$$

and

$$\psi(i) = N \sqrt{\dim(i)} e^{-\frac{3}{4j_0}(i-i_0)^2 + i\frac{\pi}{2}i}. \quad (254)$$

In other words, the state considered has a Gaussian weight over the spins, with phase θ given by the extrinsic curvature angle and by a “coherent tetrahedron” state (see [87] and section 8.2) for each tetrahedron. Let us write the wave packet (252) as an “initial state” times a “final state” by viewing the process represented by the spacetime region described by the Regge cell as a process evolving four tetrahedra into one. That is, let us write this state in the form

$$\Psi(j_{nm}, i_n) = \psi_{\text{init}}(j_{nm}, i'_n) \psi(i_5) \quad (255)$$

where $i'_n = (i_1, \dots, i_4)$. Then we can test the classical limit of the vertex amplitude by computing the evolution of the four “incoming” tetrahedra generated by the vertex amplitude

$$\phi(i) = \sum_{j_{nm}, i'_n} W(j_{nm}, i'_n, i) \psi_{\text{init}}(j_{nm}, i'_n) \quad (256)$$

where i is i_5 , and comparing $\phi(i)$ with $\psi(i)$. For large j_0 , the evolution should evolve the “initial” boundary state $\psi_i(j_{nm}, i'_n)$ into a final state $\phi(i)$ which is still a wave-packet centered on the same classical tetrahedron as the state $\psi(i)$ given in (254). That is, $\phi(i)$ must be a state “similar” to $\psi(i)$, plus perhaps quantum corrections representing the quantum spread of the wave packet.

We have tested this hypothesis numerically, under a drastic approximation: replacing the Gaussian dependence on the spins with a state concentrated on $j_{nm} = j_0$. That is, we have tested the hypothesis in the $\tau \rightarrow \infty$ limit. Explicitly, we considered the boundary state

$$\Psi(j_{nm}, i_n) \propto \prod_{n=1}^{10} \delta_{j_n, j_0} \prod_{m=1}^5 \psi(i_m). \quad (257)$$

We want to compare the evolved state

$$\phi(i) = \sum_{i_1 \dots i_4} W(i_1, \dots, i_4, i) \prod_{n=1}^4 \psi(i_n) \quad (258)$$

with the coherent tetrahedron state (254), where

$$W(i_n) \equiv W(j_{nm}, i_n)|_{j_{nm}=j_0}. \quad (259)$$

If the function $\phi(i)$ turns out to be sufficiently close to the coherent tetrahedron state $\psi(i)$, we can say that the EPR vertex amplitude appears to evolve four coherent tetrahedra into one coherent tetrahedron,

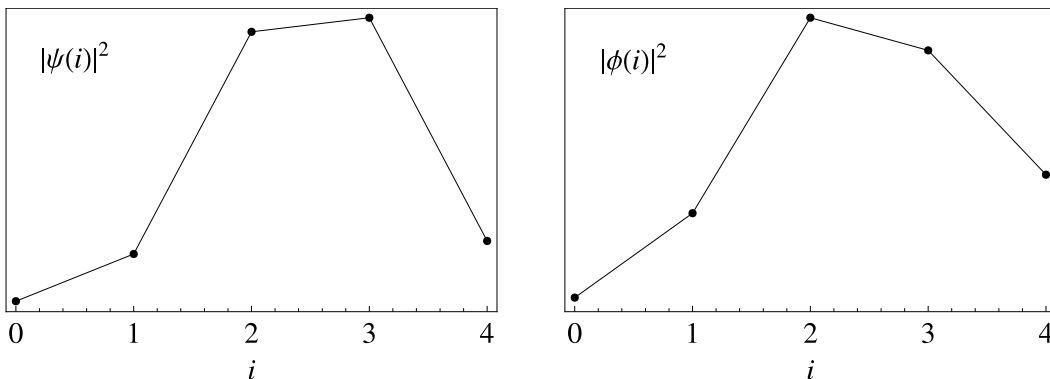


Figure 8: $j_0=2$. Modulus square of the amplitude. Left: coherent tetrahedron ($i_{\text{mean}} \pm \sigma/2 = 2.54 \pm 0.39$). Right: Evolved state ($i_{\text{mean}} \pm \sigma/2 = 2.54 \pm 0.46$). CPU time with a 1.8 Ghz processor: few seconds (old code), $\sim 10^{-1}$ s (new code)

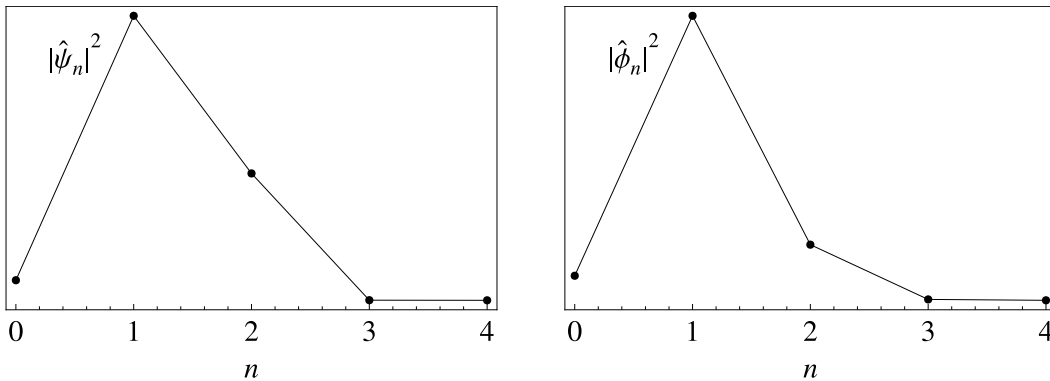


Figure 9: $j_0=2$. Modulus square of the (discrete) Fourier transform of the amplitude. Left: coherent tetrahedron ($n_{\text{mean}} \pm \sigma/2 = 1.25 \pm 0.27$). Right: Evolved state ($n_{\text{mean}} \pm \sigma/2 = 1.15 \pm 0.31$).

consistently with the geometry of a classical 4-simplex. In the first paper [20] we have compared the two functions $\psi(i)$ (coherent tetrahedron) and $\phi(i)$ (evolved state) for the cases $j_0 = 2$ and $j_0 = 4$. The numerical results are shown in the figures below. The overall relative amplitude of $\psi(i)$ and $\phi(i)$ is freely adjusted by fixing the normalization constant N and therefore is not significant. The quantity i_{mean} is the mean value of i . It gives the position of the wave-packet. The quantity $\sigma/2$ is the corresponding variance. It gives the (half) width of the wave packet. In Fig.8 and Fig.10 we compare the modulus square of the wave function (for the two values of j_0). In Fig.9 and Fig.11 we compare the modulus square of the discrete Fourier transform of the wave function: n stands for the n^{th} multiple of the fundamental frequency $2\pi/j_0$.

The agreement between the evolved state and the coherent tetrahedron state is quite good. Besides the overall shape of the state, notice the concordance of the mean values and the widths of the wave packet. Considering the small value of j_0 , which is far from the large scale limit, and the $\tau \rightarrow \infty$ limit we have taken, we find this quite surprising.

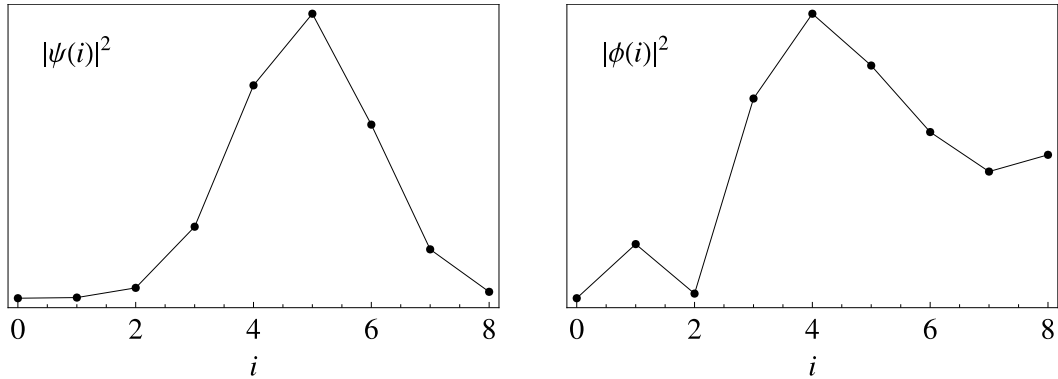


Figure 10: $j_0 = 4$. Modulus square of the amplitude. Left: coherent tetrahedron ($i_{\text{mean}} \pm \sigma/2 = 4.88 \pm 0.56$). Right: Evolved state ($i_{\text{mean}} \pm \sigma/2 = 4.85 \pm 0.96$). CPU time with a 1.8 Ghz processor: 6 h (old code), few seconds (new code)

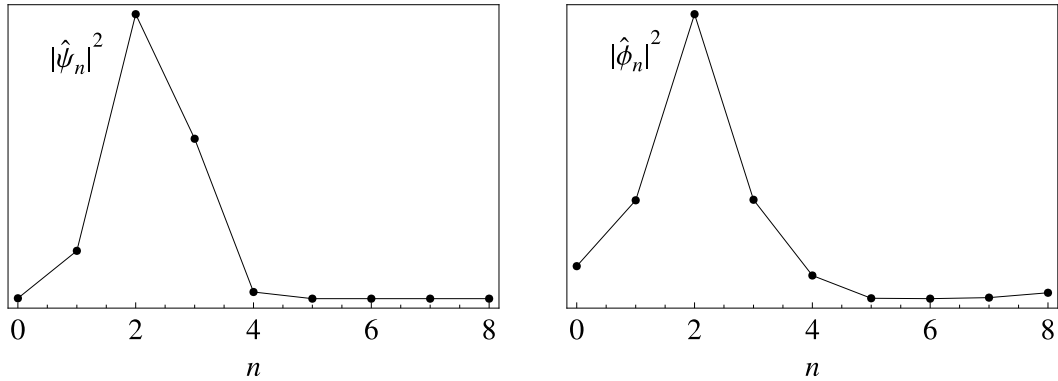


Figure 11: $j_0 = 4$. Modulus square of the (discrete) Fourier transform of the amplitude. Left: coherent tetrahedron ($n_{\text{mean}} \pm \sigma/2 = 2.25 \pm 0.32$). Right: Evolved state ($n_{\text{mean}} \pm \sigma/2 = 2.08 \pm 0.59$).

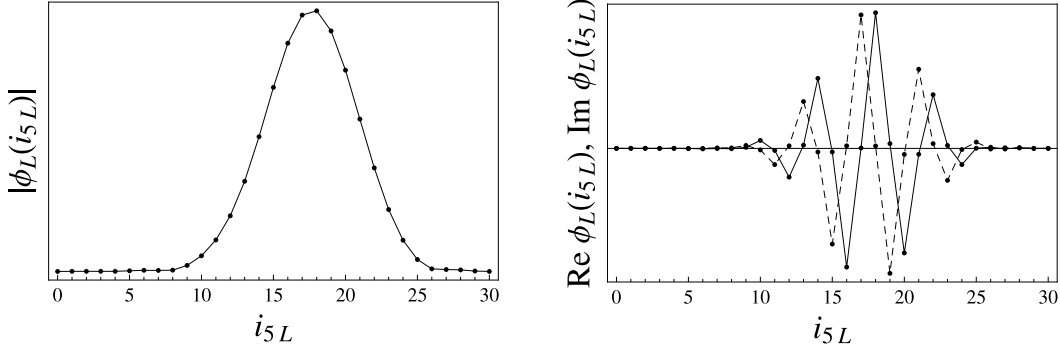


Figure 12: On the left: modulus of the evolved state for the 4-to-1 propagation performed by one $15j$ ($j_0 = 30$). On the right: its real and imaginary (dashed) part. CPU time with a 1.8 Ghz processor: few seconds

7.2 The semi-analytic approach

The property (240) gives a new picture of the dynamics in the semiclassical regime. The EPR vertex is given by (we omit normalization factors, which are not essential in this semiclassical analysis):

$$W(i_1 \dots i_5) \equiv \sum_{\{i_{nL}\}\{i_{nR}\}} 15j(i_{1L}, \dots, i_{5L}) 15j(i_{1R}, \dots, i_{5R}) \prod_{n=1}^5 f_{i_{nL}, i_{nR}}^{i_n}. \quad (260)$$

Four of the fusion coefficients are contracted in (258) with the four initial packets (making the sum over $i_1 \dots i_4$). By (240), for large j_0 's this contraction gives four $SO(4)$ semiclassical intertwiners, so the evolved state (258) becomes

$$\begin{aligned} \phi(i_5) \simeq \sum_{i_{5L}, i_{5R}} & \left[\sum_{i_{1L} \dots i_{4L}} 15j(i_{1L}, \dots, i_{5L}) g(i_{1L}) \dots g(i_{4L}) \right] \times \\ & \times \left[\sum_{i_{1R} \dots i_{4R}} 15j(i_{1R}, \dots, i_{5R}) g(i_{1R}) \dots g(i_{4R}) \right] f_{i_{5L}, i_{5R}}^{i_5}. \end{aligned} \quad (261)$$

We can see in the last expression the action of two $15j$'s separately on the left and right part (the expressions in square brackets). Those actions are interpreted as independent 4-to-1-evolutions in the left and right sectors, namely the evolution of the left and right part of four $SO(4)$ semiclassical intertwiners, where the propagation kernel is the $15j$ -symbol. By numerical investigations (Fig. 12), it turns out that the final state of the right (left) partial evolution is the right (left) part of an $SO(4)$ semiclassical intertwiner, with the phase flipped as compared to the incoming packets. For example, for the left part:

$$\phi_L(i_{5L}) \equiv \sum_{i_{1L} \dots i_{4L}} 15j_N(i_{1L} \dots i_{5L}) g(i_{1L}) \dots g(i_{4L}) \simeq \overline{g(i_{5L})}. \quad (262)$$

Then (261) becomes

$$\phi(i_5) \simeq \sum_{i_{5L}, i_{5R}} \overline{g(i_{5L})} \overline{g(i_{5R})} f_{i_{5L}, i_{5R}}^{i_5}. \quad (263)$$

The last expression is the contraction between the a single fusion coefficient and an $SO(4)$ semiclassical intertwiner. By (241), this gives an $SO(3)$ semiclassical intertwiner:

$$\phi(i_5) \simeq \overline{\psi(i_5)}. \quad (264)$$

While in [20] we expected only a conservation of mean values, and possibly a spread of wave-packets, the present argument shows that the gaussian shape is conserved, together with its mean value and width, while the phase is flipped, because of the complex conjugation in (264). Similarly, the 3-to-2 evolution is the contraction between the EPR vertex and three initial semiclassical intertwiners. Numerical results about this type of evolution are discussed in section 7.4.

7.3 Physical expectation values

Another perspective is to interpret the results about wave-packet propagation as expectation values of geometric observables associated to the intertwiners degrees of freedom. By construction, the boundary state (257) is peaked *kinematically* on a semiclassical geometry. This should be also true in a *dynamical* sense, that is as a physical expectation value. Consider the physical expectation value of an intertwiner on this boundary state, defined as:

$$\langle i_1 \rangle \equiv \frac{\sum_{j_{nm} i_n} W(j_{nm}, i_n) i_1 \Psi(j_{nm}, i_n)}{\sum_{j_{nm} i_n} W(j_{nm}, i_n) \Psi(j_{nm}, i_n)}. \quad (265)$$

We expect this quantity to be equal to i_0 for large j_0 's, if the dynamics has the correct semiclassical limit. Analogously, we can consider the expectation value of two intertwiners:

$$\langle i_1 i_2 \rangle \equiv \frac{\sum_{j_{nm} i_n} W(j_{nm}, i_n) i_1 i_2 \Psi(j_{nm}, i_n)}{\sum_{j_{nm} i_n} W(j_{nm}, i_n) \Psi(j_{nm}, i_n)}; \quad (266)$$

the last expression should be asymptotically equal to i_0^2 . The results about wave-packet propagation permit to extract the previous physical expectation values. In fact, (265) can be viewed as the contraction between the evolved state and a semiclassical boundary intertwiner with one insertion, so

$$\langle i_1 \rangle = \frac{\sum_{i_1} \phi(i_1) i_1 \psi(i_1)}{\sum_{i_1} \phi(i_1) \psi(i_1)} \simeq \frac{\sum_{i_1} \overline{\psi(i_1)} i_1 \psi(i_1)}{\sum_{i_1} \overline{\psi(i_1)} \psi(i_1)} = i_0, \quad (267)$$

where we used (264), and evaluated the sum with a simple Gaussian integration; what we have found is that dynamical and kinematical means coincide in the asymptotic regime. We stress that the result holds because of the peakedness properties of the evolved state and because of the flip in the phase: the phase of the evolved state has to be opposite and cancel with the phase of the initial state, otherwise the sum would be suppressed through the mechanism of rapid oscillations. The same qualitative properties (peakedness and phase flip) hold for the 3-to-2 propagation (see numerical results in the next section), and the expectation value of $i_1 i_2$ turns out to be the correct one: i_0^2 .

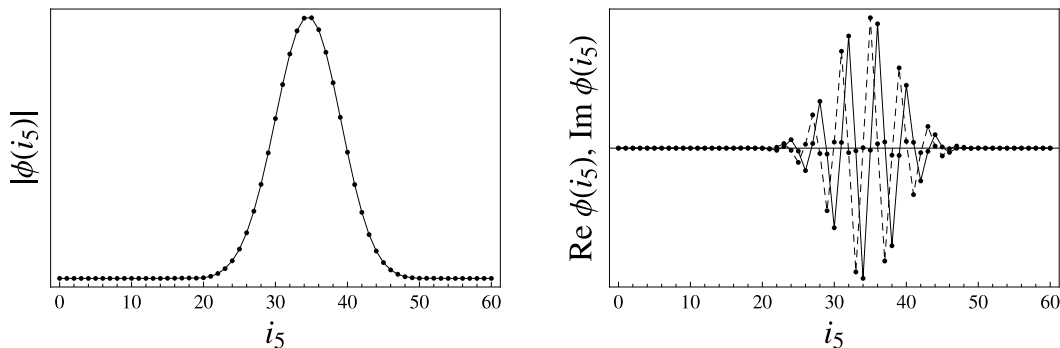


Figure 13: On the left: modulus of the evolved state for the 4-to-1 propagation performed by the flipped vertex ($j_0 = 30$). On the right: its real and imaginary (dashed) part. CPU time with a 1.8 Ghz processor: ~ 10 minutes

7.4 Improved numerical analysis

We wrote an improved, efficient numerical algorithm in the C++ programming language. This algorithm performs the 4-to-1 and 3-to-2 evolutions, and compute the physical expectation values (265)(266). It evaluates very big, nested sums serially (similar algorithms were used in [89, 90]). The results are shown in the figures. In Fig.13 the result of the 4-to-1 evolution for $j_0 = 30$ is reported. From the plot on the left (the modulus) we can see that the evolved state is a Gaussian peaked on i_0 with the same width of the “incoming” Gaussians. On the right the real and imaginary parts are plotted, and it is clearly visible that the frequency of oscillation is $-\pi/2$, which is exactly the phase opposite to the one of initial packets. In Fig.15 are shown the results of the 3-to-2 propagation (moduli), from $j_0 = 10$ to $j_0 = 32$ for even j_0 's. Compared with the 4-to-1 case, here the Gaussian shape seems not to be conserved, but the state is nevertheless peaked on i_0 and presents a $-\pi/2$ phase in both variables; going to higher spins (we explored up to $j_0 = 56$), the result seems to converge slowly to Gaussian as well. Non-Gaussianity has to be imputed to quantum effects. Small deviations from Gaussianity are present also in the 4-to-1-evolution, though less pronounced. Both in the 4-to-1 and 3-to-2 evolution, non-Gaussianity gives rise to deviations of physical expectation values from the classical behavior, in the quantum regime. Deviations are well visible in the plots in Fig.14.

In conclusion, the physical expectation values (Fig.14) are in complete agreement with the expected ones. The small deviations from the semiclassical values gradually disappear as j_0 increases.

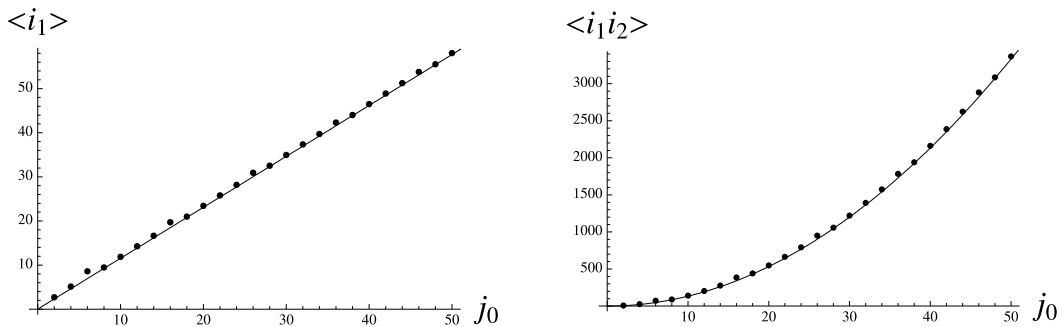


Figure 14: On the left: physical expectation value of i_1 . On the right: physical expectation value of $i_1 i_2$. The solid line is the expected behavior.

8 Semiclassical states for quantum gravity

The concept of *semiclassical states* is a key ingredient in the semiclassical analysis of LQG. Semiclassical states are kinematical states peaked on a prescribed intrinsic and extrinsic geometry of space. The simplest semiclassical geometry one can consider is the one associated to a single node of a spin-network with given spin labels. The node is labeled by an intertwiner, i.e. an invariant tensor in the tensor product of the representations meeting at the node. However a generic intertwiner does not admit a semiclassical interpretation because expectation values of non-commuting geometric operators acting on the node do not give the correct classical result in the large spin limit. For example, the 4-valent intertwiners defined with the virtual spin do not have the right semiclassical behavior; one has to take a superposition of them with a specific weight in order to construct semiclassical intertwiners. The Rovelli-Speziale quantum tetrahedron described in section 8.2 is an example of semiclassical geometry; there the weight in the linear superposition of virtual links is taken as a Gaussian with phase. The Rovelli-Speziale quantum tetrahedron is actually equivalent to the Livine-Speziale coherent intertwiner with valence 4 (introduced section 8.1); more precisely, the former constitutes the asymptotic expansion of the latter for large spins. Coherent intertwiners, introduced for general valence in the next section, are defined on a robust mathematical setting as the geometric quantization of the classical phase space associated to the degrees of freedom of a tetrahedron. But from the point of view of LQG they are only a first step. The missing step is to define in the most physically motivated way semiclassical states associated to a spin-network graph; we expect them to be a superposition over spins of spin-network states, as we shall argue in a moment.

In the recent graviton propagator calculations [91, 92, 93, 79, 94, 95, 96], semiclassical states associated to a spin-network graph Γ have been already considered. The states used in the definition of semiclassical n -point functions (see chapter 10) are labeled by a spin j_e^0 and an angle ξ_e per link e of the graph, and for each node a set of unit vectors \vec{n} , one for each link at that node. Such variables are suggested by the simplicial interpretation of these states: the graph Γ is in fact assumed to be dual to a simplicial decomposition of the spatial manifold, the vectors \vec{n} are associated to unit-normals to faces of tetrahedra, and the spin j_e^0 is the average of the area of a face. Moreover, the simplicial extrinsic curvature is an angle associated to faces shared by tetrahedra and is identified with the label ξ_e . Therefore, these states are labeled by an intrinsic and extrinsic simplicial 3-geometry. They are obtained via a superposition over spins of spin-networks having nodes labeled by Livine-Speziale coherent intertwiners [56, 97, 98]. The

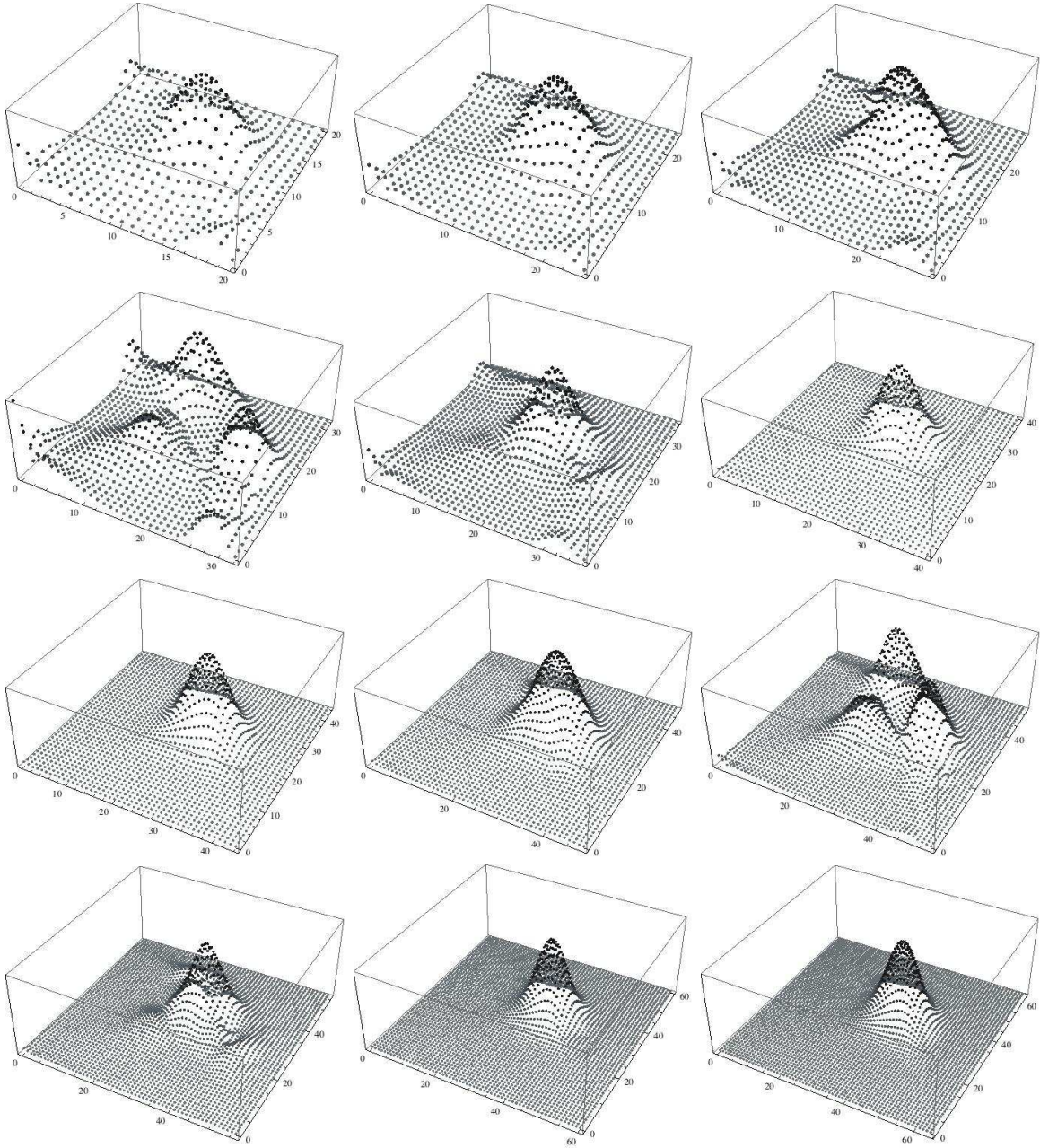


Figure 15: Modulus of the evolved state for the 3-to-2 intertwiner propagation, from $j_0 = 10$ to $j_0 = 32$ with step 2.

coefficients c_j of the superposition over spins are given by a Gaussian times a phase as originally proposed by Rovelli in [91]

$$c_j(j_0, \xi) = \exp\left(-\frac{(j-j_0)^2}{2\sigma_0}\right) \exp(-i\xi j). \quad (268)$$

Such proposal is motivated by the need of having a state peaked both on the area *and* on the extrinsic angle. The dispersion is chosen to be given by $\sigma_0 \approx (j_0)^k$ (with $0 < k < 2$) so that, in the large j_0 limit, both variables have vanishing relative dispersions (as explained in [92]). Moreover, a recent result of Freidel and Speziale strengthens the status of these classical labels [99, 100]: they show that the phase space associated to a graph in LQG can actually be described in terms of the labels $(j_e^0, \xi_e, \vec{n}_e, \vec{n}'_e)$ associated to links of the graph. The states have good semiclassical properties and a clear geometrical interpretation, finding a better top-down derivation of the coefficients (268) is strongly desirable. This is one of the objectives of this thesis.

On the other hand, within the canonical framework, Thiemann and collaborators have strongly advocated the use of complexifier coherent states [101, 102, 103, 104, 105, 106, 107, 108, 109, 110]. Such states are labeled by a graph Γ and by an assignment of a $SL(2, \mathbb{C})$ group element to each of its links. The state is obtained from the gauge-invariant projection of a product over links of modified³ heat-kernels for the complexification of $SU(2)$. Their peakedness properties have been studied in detail [102, 108]. However the geometric interpretation of the $SL(2, \mathbb{C})$ labels and the relation with semiclassical states used in Spin Foams has largely remained unexplored. Exploring these aspects is the other objective of this paper.

Surprisingly, the two goals discussed above turn out to be strictly related. In this chapter we present a proposal of *coherent spin-network states*: the proposal is to consider the gauge invariant projection of a product over links of Hall's heat-kernels for the cotangent bundle of $SU(2)$ [111, 112]. The labels of the state are the ones used in Spin Foams: two normals, a spin and an angle for each link of the graph. This set of labels can be written as an element of $SL(2, \mathbb{C})$ per link of the graph. Therefore, these states coincide with Thiemann's coherent states with the area operator chosen as complexifier, the $SL(2, \mathbb{C})$ labels written in terms of the phase space variables $(j_e^0, \xi_e, \vec{n}_e, \vec{n}'_e)$ and the heat-kernel time given as a function of j_e^0 .

We show that, for large j_e^0 , coherent spin-networks reduce to the semiclassical states used in the spin-foam framework. In particular we find that they reproduce a superposition over spins of spin-networks with nodes labeled by Livine-Speziale coherent intertwiners and coefficients c_j given by a Gaussian times a phase as originally proposed by Rovelli. This provides a clear interpretation of the geometry these states are peaked on. The relation between coherent spin-networks and the semiclassical states used in SFMs is also briefly discussed at the beginning of section 10.1.

8.1 Livine-Speziale coherent intertwiners

In ordinary Quantum Mechanics, $SU(2)$ coherent states are defined as the states that minimize the dispersion

$$\Delta J^2 \equiv \langle \vec{J}^2 \rangle - \langle \vec{J} \rangle^2 \quad (269)$$

³In particular, the modified heat-kernels reduce to ordinary Hall's heat-kernels for the complexification of $SU(2)$ when the complexifier is chosen to be the area operator.

of the angular momentum operator \vec{J} , acting as a generator of rotations on the representation space $\mathcal{H}_j \simeq \mathbb{C}^{2j+1}$ of the spin j representation of $SU(2)$. On the usual basis $|j, m\rangle$ formed by simultaneous eigenstates of J^2 and J_3 we have

$$\langle j, m | \vec{J}^2 | j, m \rangle - \langle j, m | \vec{J} | j, m \rangle^2 = j(j+1) - m^2, \quad (270)$$

so the maximal and minimal weight vectors $|j, \pm j\rangle$ are coherent states. Starting from $|j, j\rangle$, the whole set of coherent states is constructed through the group action

$$|j, g\rangle \equiv g|j, j\rangle \quad g \in SU(2). \quad (271)$$

One can take a subset of them labeled by unit vectors on the sphere S^2 :

$$|j, \hat{n}\rangle = g(\hat{n})|j, j\rangle, \quad (272)$$

where \hat{n} is a unit vector defining a direction on the sphere S^2 and $g(\hat{n})$ a $SU(2)$ group element rotating the direction $\hat{z} \equiv (0, 0, 1)$ into the direction \hat{n} . In other words, a coherent states is a state satisfying

$$\vec{J} \cdot \hat{n} |j, \hat{n}\rangle = j |j, \hat{n}\rangle. \quad (273)$$

For each \hat{n} there is a $U(1)$ family of coherent states that satisfy (273), and they are related one another by a phase factor. The choice of this arbitrary phase is equivalent to a section of the Hopf fiber bundle $s : S^2 \simeq SU(2)/U(1) \rightarrow SU(2)$. Explicitly, denoting $\hat{n} = (\sin \theta \cos \phi, \sin \theta \sin \phi, \cos \theta)$, a possible section is

$$g(\hat{n}) \equiv \exp\{i \hat{m} \cdot \vec{\sigma}\}, \quad (274)$$

where $\hat{m} \equiv (\sin \phi, -\cos \phi, 0)$ is a unit vector orthogonal both to \hat{z} and \hat{n} . A coherent state can be expanded in the usual basis as

$$|j, \hat{n}\rangle = \sum_{m=-j}^j a_m(\hat{n}) |j, m\rangle, \quad (275)$$

where

$$a_m(\hat{n}) = \sqrt{\frac{(2j)!}{(j-m)!(j+m)!}} \frac{\zeta^{j-m}}{(1+|\zeta|^2)^j}, \quad \zeta = \tan \frac{\theta}{2} e^{-i\phi}. \quad (276)$$

Coherent states are normalized but not orthogonal, and their scalar product is

$$\langle j, \hat{n}_1 | j, \hat{n}_2 \rangle = \left(\frac{1 + \hat{n}_1 \cdot \hat{n}_2}{2} \right)^j e^{ijA(z, \hat{n}_1, \hat{n}_2)}, \quad (277)$$

where A is the area of the geodesic triangle on the sphere S^2 with vertices \hat{z} , \hat{n}_1 and \hat{n}_2 . Furthermore they provide an overcomplete basis for the Hilbert space \mathcal{H}_j of the spin j irreducible representation of $SU(2)$, and the resolution of the identity can be written as $\mathbb{1}_j = d_j \int d^2 \hat{n} |j, \hat{n}\rangle \langle j, \hat{n}|$, with $d^2 \hat{n}$ the normalized Lebesgue measure on the sphere S^2 .

The Livine-Speziale coherent intertwiners are naturally defined taking the tensor product of V coherent states (V stands for valence of the node) and projecting onto the gauge-invariant subspace:

$$|\underline{j}, \underline{\hat{n}}\rangle_0 \equiv \int dh \otimes_{i=1}^V h |j_i, \hat{n}_i\rangle = \sum_{i_1 \dots i_{V-3}} c_{i_1 \dots i_{V-3}}(j_i, \hat{n}_i) |j_1 \dots j_V, i_1 \dots i_{V-3}\rangle. \quad (278)$$

Here the projection is implemented by group averaging. They are labeled by V spins \underline{j} and V unit vectors $\underline{\hat{n}}$. The explicit coefficients entering (278) can be found using (275) to decompose $|\underline{j}, \underline{\hat{n}}\rangle_0$ into the conventional basis of $\mathcal{H}_0 = \text{Inv} \otimes_{i=1}^V \mathcal{H}_{j_i}$. To each node of valence V of a spin-network we can associate V areas and $2(V-3)$ angles between them. Alternatively, one can use the normal vectors \hat{n}_i normalized to the areas, constrained to *close*, namely to satisfy $\sum_i j_i \hat{n}_i = 0$. The conventional recoupling basis used in LQG gives quantum numbers for V areas but only $V-3$ angles, because one associates $SU(2)$ generators \vec{J}_i with each face, and only $V-3$ of the possible scalar products $\vec{J}_i \cdot \vec{J}_k$ commute among each other. Thus half the classical angles are missing. The states $|\underline{j}, \underline{\hat{n}}\rangle_0$ instead carry enough information to describe a classical geometry associated to the node. In fact we interpret the vectors $j_i \hat{n}_i$ as normal vectors to triangles, normalized to the areas j_i of the triangles.

8.2 Coherent tetrahedron

The case of 4-valent coherent intertwiners is of particular importance for LQG and especially for Spin Foam Models. In fact it is the lowest valence carrying a non-zero volume and most SFMs are build over a simplicial triangulation, so that the boundary state space has only 4-valent nodes, dual to tetrahedra. A 4-valent coherent intertwiner with normals satisfying the closure condition can be interpreted as a semiclassical tetrahedron. In fact expectation values of geometric operators associated to a node give the correct classical quantities in the semiclassical regime. This regime is identified with the large spin (large areas) asymptotics. In the following we give some details.

Define $\vec{n} = j\hat{n}$ as the normals normalized to the area. In terms of them, the volume (squared) of the tetrahedron is given by the simple relation:

$$V^2 = -\frac{1}{36} \vec{n}_1 \cdot \vec{n}_2 \times \vec{n}_3. \quad (279)$$

The geometric quantization of these degrees of freedom is based on the identification of generators \vec{J}_i of $SU(2)$ as quantum operators corresponding to the \vec{n}_i [113]. As mentioned, this construction gives directly the same quantum geometry that one finds via a much longer path by quantising the phase space of General Relativity, that is via Loop Quantum Gravity. The squared lengths $|\vec{n}_i|^2$ are the $SU(2)$ Casimir operators $C^2(j)$, as in LQG. A quantum tetrahedron with fixed areas lives in the tensor product $\otimes_{i=1}^4 \mathcal{H}_{j_i}$. The closure constraint reads:

$$\sum_{i=1}^4 \vec{J}_i = 0, \quad (280)$$

and imposes that the state of the quantum tetrahedron is invariant under global rotations. The state space of the quantum tetrahedron with given areas is thus the Hilbert space of intertwiners

$$I_{j_1 \dots j_4} = \text{Inv} \otimes_{i=1}^4 \mathcal{H}_{j_i}. \quad (281)$$

The operators $\vec{J}_i \cdot \vec{J}_j$ are well defined on this space, and so is the operator

$$U = -\epsilon_{abc} J_1^a J_2^b J_3^c. \quad (282)$$

Its absolute value $|U|$ can immediately be identified with the quantization of the classical squared volume $36V^2$, by analogy with (279), again in agreement with standard LQG results (equation 119).

To find the angle operators, let us introduce the quantities $\vec{J}_{ij} := \vec{J}_i + \vec{J}_j$. Their geometrical interpretation can be found applying the same arguments as above to $\vec{n}_i + \vec{n}_j$. It turns out that $\sqrt{J_{ij}^2}$ is proportional to the area A_{ij} of the internal parallelogram, whose vertices are given by the midpoints of the segments belonging to either the triangle i or the triangle j but not to both (see [113]), $A_{ij} \equiv \frac{1}{4\sqrt{2}} \sqrt{J_{ij}^2}$. Given these quantities, the angle operators θ_{ij} can be recovered from

$$J_i J_j \cos \theta_{ij} = \vec{J}_i \cdot \vec{J}_j = \frac{1}{2}(J_{ij}^2 - J_i^2 - J_j^2). \quad (283)$$

We conclude that the quantum geometry of a tetrahedron is encoded in the operators J_i^2, J_{ij}^2 and U , acting on $I_{j_1 \dots j_4}$. It is a fact that out of the six independent classical variables parametrizing a tetrahedron, only five commute in the quantum theory. Indeed while we have $[J_k^2, J_i \cdot J_j] = 0$, it is easy to see that:

$$[J_1 \cdot J_2, J_1 \cdot J_3] = \frac{1}{4} [J_{12}^2, J_{13}^2] = i \epsilon_{abc} J_1^a J_2^b J_3^c = -iU \neq 0. \quad (284)$$

A complete set of commuting operators, in the sense of Dirac, is given by the operators J_i^2, J_{12}^2 . In other words, a basis for $I_{j_1 \dots j_4}$ is provided by the eigenvectors of any one of the operators J_{ij}^2 . We write the corresponding eigenbasis as $|j\rangle_{ij}$. These are the virtual links introduced in section 3.2 with a graphical notation; here we are introducing them via a geometric quantization of the classical tetrahedron. For instance, the basis $|j\rangle_{12}$ diagonalises the four triangle areas and the dihedral angle θ_{12} (or, equivalently, the area A_{12} of one internal parallelogram). As we already said, the relation between different basis is easily obtained from $SU(2)$ recoupling theory: the matrix describing the change of basis in the space of intertwiners is given by the usual Wigner $6j$ -symbol,

$$W_{jk} := {}_{12}\langle j|k\rangle_{13} = (-1)^{\sum_i j_i} \sqrt{\dim(j) \dim(k)} \left\{ \begin{array}{ccc} j_1 & j_2 & j \\ j_3 & j_4 & k \end{array} \right\}, \quad (285)$$

so that

$$|k\rangle_{13} = \sum_j W_{jk} |j\rangle_{12}. \quad (286)$$

Notice that from the orthogonality relation of the $6j$ -symbol,

$$\sum_i \dim(i) \left\{ \begin{array}{ccc} j_1 & j_2 & i \\ j_3 & j_4 & j \end{array} \right\} \left\{ \begin{array}{ccc} j_1 & j_2 & i \\ j_3 & j_4 & k \end{array} \right\} = \frac{\delta_{jk}}{\dim(j)}, \quad (287)$$

we have

$$\sum_i W_{ij} W_{ik} = \delta_{jk}. \quad (288)$$

The states $|j\rangle_{12}$ are eigenvectors of the five commuting geometrical operators J_i^2, J_{12}^2 , thus the average value of the operator corresponding to the sixth classical observable, say J_{13}^2 , is on these states maximally

spread. This means that a basis state has undetermined classical geometry or, in other words, is not an eigenstate of the geometry. We are then led to consider superpositions of states to be able to study the semiclassical limit of the geometry. Suitable superpositions could be constructed for instance requiring that they minimise the uncertainty relations between non-commuting observables, such as

$$\Delta^2 J_{12}^2 \Delta^2 J_{13}^2 \geq \frac{1}{4} |\langle [J_{12}^2, J_{13}^2] \rangle|^2 \equiv 4 |\langle U \rangle|^2. \quad (289)$$

States minimising the uncertainty above are usually called coherent states. Coherent intertwiners seem not to verify exactly (289), but they are such that all relative uncertainties $\langle \Delta^2 J_{ij} \rangle / \langle J_{ij}^2 \rangle$, or equivalently $\langle \Delta \theta_{ij} \rangle / \langle \theta_{ij} \rangle$, vanish in the large scale limit. The limit is defined by taking the limit when all spins involved go uniformly to infinity, namely $j_i = \lambda k_i$ with $\lambda \rightarrow \infty$. Notice that this is a different requirement than minimising (289), but the two are likely to be intimately related. Because of these good semiclassical properties we can associate to a coherent intertwiner the geometrical interpretation of a semiclassical tetrahedron; an analogous interpretation should be also valid nodes of higher valence. In the next section we introduce coherent states which are associated not to a single node, but to the entire graph; we are forced to use them if we consider the full phase space of General Relativity.

8.3 *Bianchi-Magliaro-Perini coherent spin-networks*

In this section we discuss a proposal of coherent states for Loop Quantum Gravity, an original contribution appeared in reference [114]. These states are labeled by a point in the phase space of General Relativity as captured by a spin-network graph. They are defined as the gauge invariant projection of a product over links of Hall's heat-kernels [115] for the cotangent bundle of $SU(2)$. The labels of the state are written in terms of two unit-vectors, a spin and an angle for each link of the graph. The heat-kernel time is chosen to be a function of the spin. These labels are the ones used in the Spin Foam setting and admit a clear geometric interpretation. Moreover, the set of labels per link can be written as an element of $SL(2, \mathbb{C})$. Therefore, these states coincide with Thiemann's coherent states with the area operator as complexifier. We study the properties of semiclassicality of these states and show that, for large spins, they reproduce a superposition over spins of spin-networks with nodes labeled by Livine-Speziale coherent intertwiners. Moreover, the weight associated to spins on links turns out to be given by a Gaussian times a phase as originally proposed by Rovelli.

The Hilbert space of LQG decomposes into sectors isomorphic to $\mathcal{K}_\Gamma = L^2(SU(2)^L / SU(2)^N, d\mu^L)$ associated to an embedded graph Γ having L links and N nodes. States $\Psi(h_1, \dots, h_L)$ in \mathcal{K}_Γ capture a finite number of degrees of General Relativity: the ones associated to the classical phase space $T^*SU(2)^L$ of holonomies of the Ashtekar-Barbero connection along links of the graph and fluxes through surfaces dual to links of the graph. Here we consider states belonging to \mathcal{K}_Γ and labeled by a point in phase space. Notice that the cotangent bundle $T^*SU(2)$ is diffeomorphic⁴ to the group $SL(2, \mathbb{C})$, the universal covering of the Lorentz group $SO(1, 3)$. This fact is largely exploited in the following: the states we consider are in fact labeled by an element of $SL(2, \mathbb{C})$ per link of the graph.

⁴In fact, since $SU(2)$ is a Lie group, its tangent bundle is trivial: $T^*SU(2) \simeq SU(2) \times su(2)^* \simeq SU(2) \times su(2)$; then observe that every element in $SL(2, \mathbb{C})$ is of the form $x \exp(iy)$ with $x \in SU(2)$ and $y \in su(2)$. Moreover, the complex structure of $SL(2, \mathbb{C})$ and the symplectic structure of $T^*SU(2)$ fit together so as to form a Kähler manifold.

Let us consider the heat kernel $K_t(h, h_0)$ on $SU(2)$. Being an L^2 function over $SU(2)$, it has the following Peter-Weyl expansion

$$K_t(h, h_0) = \sum_j (2j+1) e^{-j(j+1)t} \chi^{(j)}(h h_0^{-1}). \quad (290)$$

It is easy to show that, as a function of h , it is peaked on the conjugacy class of h_0 . Moreover, when seen as an LQG state associated to a loop γ , $\Psi_\gamma(h) = K_t(h, h_0)$, it is peaked on small areas (that is small j). There is a rather simple variant of $K_t(h, h_0)$ that allows to peak on a prescribed spin j_0 : it is given by the complexified heat kernel, i.e. by $K_t(h, H_0)$ with the group element H_0 belonging to the complexification of $SU(2)$:

$$SU(2)^\mathbb{C} \simeq SL(2, \mathbb{C}). \quad (291)$$

This complexified Heat kernel is the unique analytic continuation of the $SU(2)$ heat kernel. These objects are the building blocks of Thiemann's complexifier coherent states. To simplify the notation, in the following we assume that Γ is a complete graph so that, if $a, b, \dots = 1, \dots, N$ label nodes of the graph, then links are labeled by couples ab . For instance, the holonomy associated to an oriented link is h_{ab} and its inverse is $h_{ab}^{-1} = h_{ba}$. The generalization to arbitrary graphs is immediate.

Coherent spin-networks are defined as follows: we consider the gauge-invariant projection of a product over links of heat kernels,

$$\Psi_{\Gamma, H_{ab}}(h_{ab}) = \int \left(\prod_a dg_a \right) \prod_{ab} K_{t_{ab}}(h_{ab}, g_a H_{ab} g_b^{-1}). \quad (292)$$

These states were first considered in [101]. Here the positive numbers t_{ab} are fixed in terms of the labels H_{ab} as explained later on. Now, notice that every element H_{ab} of $SL(2, \mathbb{C})$ can be written in terms of two unit-vectors in \mathbb{R}^3 , a positive real number and an angle, that is: exactly the labels used in the semiclassical states adopted in spin foams (see chapter 9), the ones that in a simplicial setting correspond to 'twisted geometries' [100]. Let us see how.

An element H_{ab} of $SL(2, \mathbb{C})$ can be written in terms of a positive real number η_{ab} and two *unrelated* $SU(2)$ group elements g_{ab} and g_{ba} as⁵ [116]

$$H_{ab} = g_{ab} e^{\eta_{ab} \tau_3} g_{ba}^{-1}. \quad (293)$$

In turn, a $SU(2)$ group element can be uniquely written in terms of an angle $\tilde{\phi}$ and a unit-vector \vec{n} . Let us define \vec{n} via its inclination and azimuth

$$\vec{n} = (\sin \theta \cos \phi, \sin \theta \sin \phi, \cos \theta), \quad (294)$$

and introduce the associated group element $n \in SU(2)$ defined as

$$n = e^{-i\tilde{\phi}\tau_3} e^{-i\theta\tau_2}. \quad (295)$$

⁵In the following $\tau_i = \frac{\sigma_i}{2}$ with σ_i hermitian Pauli matrices.

Then the $SU(2)$ group element g is given by $g = n e^{+i\tilde{\phi}\tau_3}$. Using such parametrization in (293) we finally find

$$H_{ab} = n_{ab} e^{-iz_{ab}\tau_3} n_{ba}^{-1}. \quad (296)$$

with $z_{ab} = \xi_{ab} + i\eta_{ab}$ and $\xi_{ab} = \tilde{\phi}_{ba} - \tilde{\phi}_{ab}$. Therefore, for each link we have as labels the set $(\vec{n}_{ab}, \vec{n}_{ba}, \xi_{ab}, \eta_{ab})$. These variables admit the following classical interpretation: a link connects two nodes living inside two adjacent chunks of space; the interface between them is a surface dual to the link; let us choose a frame in each of the two chunks; the variable \vec{n}_{ab} can be interpreted as the (unit-)flux of the electric field E^i in the chunk a through the surface; similarly \vec{n}_{ba} can be viewed as the flux in b through this surface. In general, the two vectors are different as we have not chosen the same frame. There is a rotation R such that $R\vec{n}_{ab} = -\vec{n}_{ba}$. The product $R e^{-i\xi\vec{n}_{ab}\cdot\vec{\tau}} \in SU(2)$ can be understood as the holonomy of the Ashtekar-Barbero connection, $A^i = \Gamma^i + \gamma K^i$. Finally, the positive parameter η_{ab} can be related to the area of the surface, i.e. to the spin j_{ab} .

In order to test and strengthen our geometric interpretation of the $SL(2, \mathbb{C})$ labels, in the following we study the asymptotics of coherent spin-networks for large parameter η_{ab} . This allows to test the proposal against candidate semiclassical states that have been studied previously. The state (292) can be expanded on the spin-network⁶ basis $\Psi_{\Gamma, j_{ab}, i_a}(h_{ab})$. Its components f_{j_{ab}, i_a} ,

$$\Psi_{\Gamma, H_{ab}}(h_{ab}) = \sum_{j_{ab}} \sum_{i_a} f_{j_{ab}, i_a} \Psi_{\Gamma, j_{ab}, i_a}(h_{ab}) \quad (297)$$

are given by⁷

$$f_{j_{ab}, i_a} = \left(\prod_{ab} (2j_{ab} + 1) e^{-j_{ab}(j_{ab}+1)t_{ab}} D^{(j_{ab})}(H_{ab}) \right) \cdot \left(\prod_a v_{i_a} \right), \quad (298)$$

where from now on H_{ab} is given by (296). Notice that here the sum over spins runs over half-integers *including zero*. Thus, strictly speaking, a coherent spin-network does not live on a single graph Γ but on a superposition of all the subgraphs of Γ .

Here we are interested in its asymptotics for $\eta_{ab} \gg 1$. First of all, notice that, in the limit $\eta_{ab} \rightarrow +\infty$, we have the following asymptotic behavior

$$D^{(j_{ab})}(e^{-iz_{ab}\tau_3})^m_{m'} = \delta_{m'}^m e^{-imz_{ab}} = \delta_{m'}^m e^{+\eta_{ab}j_{ab}} \left(\delta_{m, j_{ab}} e^{-i\xi_{ab}j_{ab}} + O(e^{-\eta_{ab}}) \right). \quad (299)$$

Therefore, introducing the projector

$$P_+ = |j_{ab}, +j_{ab}\rangle \langle j_{ab}, +j_{ab}| \in \mathcal{H}_{j_{ab}}^* \otimes \mathcal{H}_{j_{ab}} \quad (300)$$

onto the highest magnetic number, we can write (299) as

$$D^{(j_{ab})}(e^{-iz_{ab}\tau_3}) \sim e^{-i\xi_{ab}j_{ab}} e^{+\eta_{ab}j_{ab}} P_+. \quad (301)$$

⁶Here spin-network states can be viewed as functions of holonomies, as opposed to functions of distributional connections because we have fixed a graph.

⁷The notation \cdot in (298) stands for a contraction of dual spaces. To be more explicit we recall that, if $V^{(j)}$ is the vector space where the representation j of $SU(2)$ acts, then the tensor product of representations $D^{(j_e)}(h_e)$ lives in $\otimes_e (V^{(j_e)*} \otimes V^{(j_e)})$ while the tensor product of intertwiners lives precisely in the dual of this space.

Recall that the coherent intertwiners $\Phi_a(\vec{n}_{ab})$ introduced by Livine and Speziale [56] have components on a orthonormal basis v_{i_a} in intertwiner space, $\Phi_a(\vec{n}_{ab})^{m_1 \dots m_r} = \sum_{i_a} \Phi_{i_a}(\vec{n}_{ab}) v_{i_a}^{m_1 \dots m_r}$, given by

$$\Phi_{i_a}(\vec{n}_{ab}) = v_{i_a} \cdot \left(\bigotimes_b |j_{ab}, \vec{n}_{ab}\rangle \right) \quad (302)$$

where $|j_{ab}, \vec{n}_{ab}\rangle = n_{ab} |j_{ab}, +j_{ab}\rangle$. Moreover, notice that

$$-j(j+1)t + j\eta = -\left(j - \frac{\eta-t}{2t}\right)^2 t + \frac{(\eta-t)^2}{4t}. \quad (303)$$

Therefore, up to an overall normalization of the state, we find the following asymptotics for our states:

$$f_{j_{ab}, i_a} \approx \left(\prod_{ab} \exp\left(-\frac{(j_{ab} - j_{ab}^0)^2}{2\sigma_{ab}^0}\right) e^{-i\xi_{ab} j_{ab}} \right) \left(\prod_a \Phi_{i_a}(n_{ab}) \right) \quad (304)$$

with

$$(2j_{ab}^0 + 1) \equiv \frac{\eta_{ab}}{t_{ab}} \quad \text{and} \quad \sigma_{ab}^0 \equiv \frac{1}{2t_{ab}}. \quad (305)$$

Finally, introducing spin-networks with nodes labeled by coherent intertwiners as in [96],

$$\Psi_{\Gamma, j_{ab}, \Phi_a(\vec{n}_{ab})}(h_{ab}) = \sum_{i_a} \left(\prod_a \Phi_{i_a}(\vec{n}_{ab}) \right) \Psi_{\Gamma, j_{ab}, i_a}(h_{ab}), \quad (306)$$

we find that the coherent spin-networks, for large η_{ab} , are given by the following superposition

$$\Psi_{\Gamma, H_{ab}}(h_{ab}) \approx \sum_{j_{ab}} \left(\prod_{ab} \exp\left(-\frac{(j_{ab} - j_{ab}^0)^2}{2\sigma_{ab}^0}\right) e^{-i\xi_{ab} j_{ab}} \right) \Psi_{\Gamma, j_{ab}, \Phi_a(\vec{n}_{ab})}(h_{ab}). \quad (307)$$

Unexpectedly, these are exactly the states considered in the definition of semiclassical correlation functions (chapter 9). There, the graph Γ is assumed to be the one dual to the boundary triangulation of a 4-simplex, the quantities j_{ab}^0 and \vec{n}_{ab} are areas and normals of faces of tetrahedra chosen so to reproduce the intrinsic geometry of the boundary of a *regular Euclidean 4-simplex*. Moreover, the parameters ξ_{ab} are chosen so to reproduce its extrinsic curvature. The analysis of the correlation function of metric operators confirms that the appropriate value is $\xi_{ab} = \gamma K_{ab} = \gamma \arccos(-1/4)$. This result confirms the geometric interpretation of our variables and extends the validity of the semiclassical states used in [96] well beyond the simplicial setting: coherent spin-networks are defined in full LQG.

In order to better test the interpretation of our variables, we consider a rather simple example: the coherent loop. This example allows us to discuss the importance of the appropriate choice of heat-kernel time t_{ab} in (292). When the graph is given by a loop γ , the dependence of the state on the normals \vec{n} in (292) drops out and the state is simply labeled by ξ and η . For large η , we find

$$\Psi_{\gamma, \xi + i\eta}(h) = \sum_j \exp\left(-\frac{(j - j_0)^2}{2\sigma_0}\right) e^{-i\xi j} \chi^{(j)}(h) \quad (308)$$

with j_0 and σ_0 given in terms of η and t by (305). Now we compute the expectation value of the area operator \mathcal{A} for a surface that is punctured once by the loop. As well known (equation 114), we have

$$\widehat{\mathcal{A}} \Psi_{\gamma, \xi + i\eta}(h) = \gamma L_P^2 \sum_j \exp\left(-\frac{(j - j_0)^2}{2\sigma_0}\right) e^{-i\xi j} \sqrt{j(j+1)} \chi^{(j)}(h). \quad (309)$$

In the limit of large η and large j_0 , the expectation value of the area operator is easily computed

$$\langle \mathcal{A} \rangle = \frac{(\Psi_{\gamma, \xi + i\eta}, \widehat{\mathcal{A}} \Psi_{\gamma, \xi + i\eta})}{(\Psi_{\gamma, \xi + i\eta}, \Psi_{\gamma, \xi + i\eta})} = \gamma L_P^2 \sqrt{j_0(j_0 + 1)} \quad (310)$$

and confirms the interpretation of η as the quantity that prescribes the expectation value of the area. Now we consider the other observable acting on the Hilbert space \mathcal{K}_γ : the Wilson loop operator W_γ . Recall that it acts on basis vectors as

$$\widehat{W}_\gamma \chi^{(j)}(h) \equiv \chi^{(\frac{1}{2})}(h) \chi^{(j)}(h) = \chi^{(j+\frac{1}{2})}(h) + \chi^{(j-\frac{1}{2})}(h). \quad (311)$$

As a result, we find

$$\langle W_\gamma \rangle = 2 \cos(\xi/2) e^{-\frac{t}{8}}. \quad (312)$$

Therefore, in the limit $t \rightarrow 0$ compatible with η and j_0 large, the parameter ξ identifies the conjugacy class of the group element h_0 where the Ashtekar-Barbero connection is peaked on. According to the Aharonov-Bohm picture of LQG [117], the angle ξ is thus the expectation value of the flux of the magnetic field through a line defect encircled by the loop γ . Similarly, we can compute the dispersions of the area operator and of the Wilson loop. We find

$$\Delta \mathcal{A} \equiv \sqrt{\langle \mathcal{A}^2 \rangle - \langle \mathcal{A} \rangle^2} = \frac{1}{2} \gamma L_P^2 \sqrt{2\sigma_0}, \quad (313)$$

and

$$\Delta W_\gamma \equiv \sqrt{\langle W_\gamma^2 \rangle - \langle W_\gamma \rangle^2} = \sqrt{(\sin(\xi/2))^2} \frac{1}{\sqrt{2\sigma_0}}. \quad (314)$$

Now notice that, due to the relation (305), the limit “large η and large j_0 ” can be attained only if we assume that t scales with j_0 as

$$t \sim (j_0)^k \quad \text{with } k > -1. \quad (315)$$

Moreover, as the area and the Wilson loop are non-commuting operators, we cannot make both their dispersions vanish at the same time. Small heat-kernel time means that the state is sharply peaked on the holonomy, while large heat-kernel time means that the state is sharply peaked on the spin. A good requirement of semiclassicality is that the relative dispersions of both operators vanish in the large j_0 limit. Using the results derived above, we find the following behavior for relative dispersions:

$$\frac{\Delta \mathcal{A}}{\langle \mathcal{A} \rangle} \sim (j_0)^{-\frac{k+2}{2}} \quad \text{and} \quad \frac{\Delta W_\gamma}{\langle W_\gamma \rangle} \sim (j_0)^{\frac{k}{2}}. \quad (316)$$

The first requires $k > -2$ and the second $k < 0$. Taking into account the three bounds (315)-(316) we find that the coherent loop behaves semiclassically when the heat-kernel time scales as $(j_0)^k$ with $-1 < k < 0$. For instance, the choice $t = 1/\sqrt{j_0}$ guarantees the semiclassicality of the state.

8.4 Resolution of the identity and holomorphic representation

In the previous section we focused on the properties of semiclassicality of coherent spin-networks: peakedness on a classical configuration with small dispersions. In this section we discuss their *coherence* properties: for a given choice of parameters t_{ab} , coherent spin-networks provide a holomorphic representation for Loop Quantum Gravity. This result was obtained long ago by Ashtekar, Lewandowski, Marolf, Mourão and Thiemann [112] and is based on the Segal-Bargmann transform for compact Lie groups introduced by Hall [111]. Here we report their result in the formalism of this paper and comment on its relevance for the analysis of the semiclassical behavior of Loop Quantum Gravity.

Let us consider the $SL(2, \mathbb{C})$ heat-kernel⁸ $F_t(H)$ and introduce a function $\Omega_t(H)$ on $SL(2, \mathbb{C})$ given by

$$\Omega_t(H) = \int_{SU(2)} F_t(Hg) dg. \quad (317)$$

This function is just the heat-kernel on $SL(2, \mathbb{C})/SU(2)$, regarded as a $SU(2)$ -invariant function on $SL(2, \mathbb{C})$. A key result of Hall [111] is that the delta function on $SU(2)$ can be written in terms of the following $SL(2, \mathbb{C})$ integral

$$\delta(h, h') = \int_{SL(2, \mathbb{C})} K_t(hH^{-1}) \overline{K_t(h'H^{-1})} \Omega_{2t}(H) dH, \quad (318)$$

where dH is the Haar measure on $SL(2, \mathbb{C})$. This expression admits a straightforward generalization in terms of coherent spin-networks.

We recall that, in the holonomy representation, the identity operator $\mathbf{1}_\Gamma$ on the Hilbert space \mathcal{K}_Γ is given by the distribution $\delta_\Gamma(h_{ab}, h'_{ab})$ on $SU(2)^L/SU(2)^N$. It can be written in terms of the spin-network basis as

$$\begin{aligned} \delta_\Gamma(h_{ab}, h'_{ab}) &= \int \left(\prod_a dg_a \right) \left(\prod_a dg'_a \right) \prod_{ab} \delta(g_a^{-1} h_{ab} g_b, g'_a{}^{-1} h'_{ab} g'_b) \\ &= \sum_{j_{ab} i_a} \Psi_{\Gamma, j_{ab}, i_a}(h_{ab}) \overline{\Psi_{\Gamma, j_{ab}, i_a}(h'_{ab})}. \end{aligned} \quad (319)$$

The resolution of the identity for coherent spin-networks is given by

$$\delta_\Gamma(h_{ab}, h'_{ab}) = \int_{SL(2, \mathbb{C})^L} \Psi_{\Gamma, H_{ab}}(h_{ab}) \overline{\Psi_{\Gamma, H_{ab}}(h'_{ab})} \left(\prod_{ab} \Omega_{2t_{ab}}(H_{ab}) dH_{ab} \right) \quad (320)$$

with the measure on $SL(2, \mathbb{C})^L$ that factors in a product of measures per link given by the $SU(2)$ -averaged heat-kernel for $SL(2, \mathbb{C})$ at time $2t$, times the Haar measure dH_{ab} . Expression (320) for the resolution of the identity can be easily proved using formula (318), the definition of coherent spin-networks (292) and expression (319) for $\delta_\Gamma(h_{ab}, h'_{ab})$.

As shown in [112], coherent spin-networks provide a Segal-Bargmann transform for Loop Quantum Gravity. In fact, given a state $\Psi_{\Gamma, f}(h_{ab})$, its scalar product with a coherent spin-network $\Psi_{\Gamma, H_{ab}}(h_{ab})$

⁸The $SL(2, \mathbb{C})$ heat-kernel $F_t(H, H_0)$ is not to be confused with the analytic continuation to $SL(2, \mathbb{C})$ of the $SU(2)$ heat-kernel $K_t(h, h_0)$.

defines a function $\Phi_{\Gamma,f}(H_{ab})$ that is holomorphic in H_{ab} ,

$$\Phi_{\Gamma,f}(H_{ab}) = \int_{SU(2)^L} \Psi_{\Gamma,H_{ab}}(h_{ab}) \overline{\Psi_{\Gamma,f}(h_{ab})} \prod_{ab} dh_{ab}, \quad (321)$$

and belongs to the Hilbert space $\mathcal{HL}^2(SL(2, \mathbb{C})^L, (\Omega_{2t} dH)^L)$ of holomorphic functions normalizable with respect to the measure $(\Omega_{2t} dH)^L$. Moreover, from expression (320) follows that the transform preserves the scalar product,

$$\int_{SU(2)^L} \Psi_{\Gamma,f_1}(h_{ab}) \overline{\Psi_{\Gamma,f_2}(h_{ab})} \prod_{ab} dh_{ab} = \int_{SL(2, \mathbb{C})^L} \Phi_{\Gamma,f_1}(H_{ab}) \overline{\Phi_{\Gamma,f_2}(H_{ab})} \left(\prod_{ab} \Omega_{2t_{ab}}(H_{ab}) dH_{ab} \right).$$

What is now available is a representation for Loop Quantum Gravity where states are functions of classical variables H_{ab} that admit a clear geometric interpretation in terms of areas, extrinsic angles and normals, $(\eta_{ab}, \xi_{ab}, \vec{n}_{ab})$, the variables generally used in the Spin Foam setting.

In the following we present the proof of formula (318). The representation of the delta function of $SU(2)$ in terms of an integral on $SL(2, \mathbb{C})$, formula (318), is a key ingredient in the proof of the resolution of the identity provided by coherent spin-networks. To make the paper self-contained, in this appendix we report an elementary proof of formula (318). The proof is by direct computation and is similar to the derivation of [102] (section 4.4). A more general proof for compact Lie groups can be found in [111] (section 7).

Let us use the polar decomposition

$$H = g e^{\vec{p} \cdot \frac{\vec{\sigma}}{2}} \quad (322)$$

to parametrize an element H of $SL(2, \mathbb{C})$ in terms of an element g of $SU(2)$ and a vector \vec{p} in \mathbb{R}^3 . In these variables, the Haar measure dH on $SL(2, \mathbb{C})$ factors into a $SU(2)$ term and a \mathbb{R}^3 term

$$dH = \frac{(\sinh |\vec{p}|)^2}{|\vec{p}|^2} d^3 \vec{p} dg, \quad (323)$$

where dg is the Haar measure on $SU(2)$ and $d^3 \vec{p}$ is the Lebesgue measure on \mathbb{R}^3 .

The $SU(2)$ -averaged heat kernel on $SL(2, \mathbb{C})$ coincides with the heat kernel on the hyperboloid $H^3 = SL(2, \mathbb{C})/SU(2)$. Its explicit form in terms of the variables (322) can be found in [?] and is given by

$$\Omega_t(g e^{\vec{p} \cdot \frac{\vec{\sigma}}{2}}) = \frac{1}{(\pi t)^{3/2}} e^{-t/4} \frac{|\vec{p}|}{\sinh |\vec{p}|} e^{-|\vec{p}|^2/t}. \quad (324)$$

Therefore, the measure in the resolution of the identity (318) is given by

$$\Omega_{2t}(H_{ab}) dH_{ab} = \rho_t(|\vec{p}|) d^3 \vec{p} dg \quad (325)$$

where

$$\rho_t(|\vec{p}|) = \frac{1}{(2\pi t)^{3/2}} e^{-t/2} \frac{\sinh |\vec{p}|}{|\vec{p}|} e^{-\frac{|\vec{p}|^2}{2t}}. \quad (326)$$

Now we want to compute the integral that appears on the rhs of (318). Using the Peter-Weyl expansion of the heat-kernel we find

$$\int_{SL(2, \mathbb{C})} K_t(hH^{-1}) \overline{K_t(h'H^{-1})} \Omega_{2t}(H) dH = \sum_{j,j'} (2j+1)(2j'+1) e^{-j(j+1)t} e^{-j'(j'+1)t} f_{j,j'}(h, h'), \quad (327)$$

where the coefficients in the sum are given by

$$f_{j,j'}(h, h') = \int_{SL(2, \mathbb{C})} \chi^{(j)}(hH^{-1}) \overline{\chi^{(j')}(h'H^{-1})} \Omega_{2t}(H) dH . \quad (328)$$

This quantity can be computed in two steps: (i) first we integrate over the subgroup $SU(2)$ and obtain

$$f_{j,j'}(h, h') = \frac{\delta^{j,j'}}{2j+1} \text{Tr}(D^j(hh'^{-1})A) \quad (329)$$

where A is a $(2j+1) \times (2j+1)$ matrix. Then, (ii) we compute the matrix A . It is given by the following integral over \mathbb{R}^3

$$A = \int_{\mathbb{R}^3} D^{(j)}(e^{-\vec{p} \cdot \frac{\vec{\sigma}}{2}}) \rho_t(|\vec{p}|) d^3\vec{p} . \quad (330)$$

Notice that the matrix A commutes with the irreducible representation j of $SU(2)$. Therefore it has to be a multiple of the identity

$$A = \frac{c}{2j+1} \mathbf{1} \quad (331)$$

with the constant c given by the trace of the matrix. Such constant can be computed explicitly performing the integral and is given by

$$c = \text{Tr}A = 4\pi \int_0^\infty \frac{\sinh((2j+1)p)}{\sinh(p)} \rho_t(p) dp = (2j+1) e^{+j(j+1)2t} . \quad (332)$$

Therefore the integral (328) is simply given by

$$f_{j,j'}(h, h') = \delta^{j,j'} e^{+j(j+1)2t} \chi^{(j)}(hh'^{-1}) . \quad (333)$$

Inserting this result into the rhs of expression (327) we find the Peter-Weyl expansion of the delta-function,

$$\delta(h, h') = \sum_j (2j+1) \chi^{(j)}(hh'^{-1}) . \quad (334)$$

This proves expression (318).

9 Graviton propagator in Loop Quantum Gravity

In this short chapter we discuss a possible definition of the n -point functions for nonperturbative quantum gravity, and shall reserve the next chapter to the effective implementation of the formal definition in Spin Foam Models. The goal is to compare them with the standard n -point functions of perturbative quantum gravity. Agreement at large distance can be taken as evidence that the nonperturbative quantum theory has the correct low energy limit, while the differences at short distance reflect the improved ultraviolet behavior of the nonperturbative theory. The difficulty is that general covariance makes conventional n -point functions ill-defined in the absence of a background. A strategy for addressing this problem has been suggested in [118]; the idea is to study the boundary amplitude, namely the functional integral over a finite spacetime region, seen as a function of the boundary value of the gravitational field [17]. In conventional quantum field theory, this boundary amplitude is well-defined [119, 120] and codes the physical information of the theory; so does in quantum gravity, but in a fully background-independent manner [121].

A generally covariant definition of n -point functions can be based on the idea that the distance between physical points (arguments of the n -point function) is determined by the state of the gravitational field on the boundary of the spacetime region considered. This strategy was first implemented by C. Rovelli in the letter [91], where some components of the graviton propagator were computed to the first order in the Group Field Theory expansion parameter λ . The calculation of the so-called diagonal components to second order in λ is performed in [91] (for an implementation of these ideas in 3 dimensions, see [122, 123]). Only a few components of the boundary state contribute to the leading order in λ , namely the ones supported on the dual graph, boundary of a single 4-simplex. This reduces the calculation to a generalization of the “nutshell” 3d model studied in [124]. The boundary amplitude which defines n -point functions can be read as the creation, interaction and annihilation of “atoms of space”, in the sense in which Feynman diagrams in conventional Quantum Field theory can be viewed as creation, interaction and annihilation of particles. Using a natural Gaussian weight for of the boundary state, peaked on the intrinsic *as well as* the extrinsic geometry of a Euclidean 3-sphere, we can compute the graviton propagator. In the Euclidean EPRL Spin Foam Model, this agrees with the conventional Euclidean graviton propagator, in the limit of vanishing Barbero-Immirzi parameter. In the first part of this section we show how to define n -point functions for generally covariant field theories, in the context of the general boundary formulation.

In order to explain the concept of boundary amplitude, we first illustrate a very simple example: the harmonic oscillator. Then we sketch the philosophy behind the general boundary formulation for field theories, in particular for quantum gravity. We conclude showing a formal expression for quantum gravity n -point functions, well suited for an implementations in SFMs.

In the section we present the main ingredients for the graviton propagator definition and the results skipping the calculations. In the third section we stress the problem of the gauge choice for the comparison with the standard linearized theory and how in principle the problem is solved by the compatibility between radial and harmonic gauge. The Feynman rules of perturbative quantum gravity are mostly known in harmonic gauge, but the calculation we present in Loop Quantum Gravity is made in a sort of radial gauge (the field insertions have vanishing radial components). We show [125] that radial and harmonic gauges are compatible, and it is possible to compare the full tensorial structure of the LQG propagator with the standard propagator.

9.1 n -point functions in generally covariant field theories

In standard perturbative quantum gravity the metric is split in a flat background metric η plus a perturbation: $g_{\mu\nu}(x) = \eta_{\mu\nu} + h_{\mu\nu}(x)$; the background is classical, and only the perturbation is considered a dynamical quantum field. The 2-point function is defined as the vacuum expectation value

$$G_{\mu\nu\rho\sigma}(x, y) = \langle 0 | h_{\mu\nu}(x) h_{\rho\sigma}(y) | 0 \rangle . \quad (335)$$

If a candidate fully nonperturbative theory, diffeomorphism invariance implies that the propagator does not depend on the points x, y , namely it must be constant. This problem can only be solved if we change our perspective. It is physically more motivated to define n -point functions associated to a finite region of spacetime, since any real measurement process is done in a finite amount of time, and in a finite region of space. The theory which deals with finite region measurements is a generalization of Quantum Field Theory called Genal Boundary QFT [17]. Of course, for flat time slices separated far away, the theory reduces to the ordinary one found in text-books. We now cast the quantum mechanics of an harmonic oscillator in the form of a general boundary theory, and define the associated 2-point function. This will give an intuitive feeling of general boundary formalism.

The 2-point function, or propagator, for the quantum harmonic oscillator propagator is the “vacuum” expectation value of two position operators:

$$G_0(t_1, t_2) = \langle 0 | \hat{x}(t_1) \hat{x}(t_2) | 0 \rangle = \langle 0 | \hat{x} e^{-iH(t_1-t_2)} \hat{x} | 0 \rangle , \quad (336)$$

where the “vacuum” state is the eigenstate of the Hamiltonian with minimal energy, the ground state. In the Schrödinger representation $L^2(\mathbb{R}, dx)$, the 2-point function is a Lebesgue integral over positions:

$$G_0(t_1, t_2) = \int dx_1 dx_2 \overline{\psi_0(x_1)} x_1 W(x_1, x_2; t_1, t_2) x_2 \psi_0(x_2) , \quad (337)$$

where $\psi_0 = \langle x | 0 \rangle$ is the wave function of ground state. The integral kernel W is called propagation kernel and it codes the full dynamics of the system. In the more formal functional representation, the 2-point function reads

$$G_0(t_1, t_2) = \int Dx x(t_1) x(t_2) e^{i \int L dt} . \quad (338)$$

The Schrödinger representation is recovered by breaking the functional integral into five spacetime regions: the two regions external to the initial and final time, the two regions (planes) at initial and final time and the region in between. The external integration gives back the ground state, the internal integration gives back the propagation kernel W and the integration on the time slices t_1 and t_2 is just the integration appearing in the Schrödinger representation. Now we introduce the relativistic form of the 2-point function. By *relativistic* here we mean “general relativistic” in the sense that we want to eliminate as much as possible the preferred role of time, which is present in any non relativistic theory. This idea is well illustrated in [7].

Let us glue the initial and final background configuration $\overline{\psi}_0$ and ψ_0 in single composite state, the tensor product of the two. Call it “boundary state” Ψ_0 , an element in $\mathcal{H}^* \otimes \mathcal{H}$. \mathcal{H} the Hilbert space of configurations at fixed time. Then H^* and H have to be interpreted as the spaces of initial and final data, respectively. We use the notation $H_{t_1}^* \otimes H_{t_2}$. Then we define the relativistic position operators $\hat{x}_1 = \hat{x} \otimes \mathbb{1}$ and $\hat{x}_2 = \mathbb{1} \otimes \hat{x}$, which act separately on the two Hilbert spaces. The propagation kernel W

can be interpreted as linear functional (a “bra”) on $H_{t_1}^* \otimes H_{t_2}$. With the previous definitions, the 2-point function assumes the compact form

$$G_0(t_1, t_2) = \langle W_{t_1 t_2} | \hat{x}_1 \hat{x}_2 | \Psi_0 \rangle . \quad (339)$$

The physical interpretation is the following: Ψ_0 represents the joint configuration at initial and final time with no excitations present; W codes the dynamics and \hat{x}_1, \hat{x}_2 create two excitations at initial and final time. The state $\hat{x}_1 \hat{x}_2 | \Psi_0 \rangle$ is the excited boundary configuration detected in the experiment. In this new language, we can consider the following normalization condition:

$$\langle 0 | e^{iH(t_1-t_2)} | 0 \rangle = \langle W_{t_1 t_2} | \Psi_0 \rangle = 1 . \quad (340)$$

Its physical meaning is the following. When (340) holds, then the final state is exactly the time evolution of the initial state; in other words, the joint “boundary state” satisfies the quantum dynamics. In the jargon of quantum gravity, this normalization condition is called Wheeler-deWitt equation.

More in general, we can consider a joint coherent state peaked on the doubled phase space point (q_1, p_1, q_2, p_2) :

$$\Psi_{q_1, p_1, q_2, p_2}(x_1, x_2) \equiv \overline{\psi_{q_1, p_1}(x_1)} \psi_{q_2, p_2}(x_2) . \quad (341)$$

The main object we consider is then the *semiclassical 2-point function* constructed this way:

$$G_{q_1, p_1, q_2, p_2}(t_1, t_2) = \langle W_{t_1, t_2} | \Psi_{q_1, p_1, q_2, p_2} \rangle . \quad (342)$$

The associated Wheeler-deWitt equation is:

$$\langle W_{t_1 t_2} | \Psi_{q_1, p_1, q_2, p_2} \rangle = 1 . \quad (343)$$

We choose the couple position/momentum q_1, p_1 to be the classical evolution of q_2, p_2 . For the harmonic oscillator, since the coherent states are Gaussian wave-packets and the dynamics does not destroy the coherence properties (in fact the evolution is rigid) the Wheeler-deWitt equation is satisfied exactly. We call the quadruplet (q_1, q_2, p_1, p_2) a physical boundary configuration, denoted \mathbf{q} . The 2-point function for a physical boundary configuration is the quantum amplitude for a quantum excitation to propagate over a classical trajectory starting with initial condition (q_2, p_2) .

In quantum field theory we can do the very same step. As before, we define the 2-point function, e.g. for a scalar field theory:

$$G_{\mathbf{q}}(x, y) = \int D\phi_1 D\phi_2 \overline{\psi_{q_1, p_1}(\phi_1)} \phi_1(x) W(\phi_1, \phi_2; t_1, t_2) \psi_{q_2, p_2}(\phi_2) \phi_2(y) . \quad (344)$$

Here x, y are points on two space-like hyperplanes in Minkowski space, and \mathbf{q} is the joint boundary configuration (it comprehends both the scalar field ϕ and its conjugate momentum Π). It is well-known that in the Schrödinger representation of the free theory the vacuum state is a functional with Gaussian dependence on the scalar field, just like the “vacuum” state of harmonic oscillator is a Gaussian. The propagation kernel W comes from the functional integration restricted to the spacetime region between two time slices

$$W(\phi_1, \phi_2; t_1, t_2) = \int_{\phi|_{t_1}=\phi_1}^{\phi|_{t_2}=\phi_2} D\varphi e^{i \int_{t_1}^{t_2} dt \int d^3\vec{x} \mathcal{L}[\varphi]} . \quad (345)$$

Now it is the time for the crucial step: instead of time slices, which is a rather particular and unphysical choice, we define the 2-point function for a general 3-dimensional boundary Σ of a *finite* spacetime region R in the following way:

$$G_{\mathbf{q}}(x, y) = \int D\phi \phi(x)\phi(y) W(\phi, \Sigma)\Psi(\phi). \quad (346)$$

In this expression x and y are points on the boundary Σ ; W is, as before, the result of the functional integration restricted to the interior of the region considered:

$$W(\phi; \Sigma) = \int_{\partial\varphi=\phi} D\varphi e^{i\int_R d^4x \mathcal{L}[\varphi]}. \quad (347)$$

This definition is suitable for generally covariant field theories, like nonperturbative quantum gravity. In ordinary quantum field theories it is the condition we put on the fields at infinity in the path integral that determine the boundary state, but this is an operation that becomes ill defined in a generally covariant context; in the absence of a background structure it does not even make sense generally to speak about fields at infinity. Expression (346) gives instead a good definition of 2-point function: the ill-defined functional integration in the external region is encoded in the well-defined boundary state. The dependence on the boundary state determines the non-trivial behavior of the 2-point function under diffeomorphisms:

$$G_{\mathbf{q}}(x, y) = G_{\mathbf{q}'}(x', y'). \quad (348)$$

We stress again the physical meaning of this general boundary formalism. The 2-point function (346) defines an amplitude associated to a joint set of measurements performed on the 3-dimensional boundary: we detect the mean geometry \mathbf{q} with two excitations in x and y (possibly at different times). Suppose now we are describing the physical world and so include the gravitational field among the other fields in our general boundary field theory. In nonrelativistic physics we have to know the spacetime location of detectors and then we perform measures on the fields (except the gravitational field). On the other hand, in relativistic physics we perform measures on the fields, *including* the gravitational field, and this is sufficient to determine also the geometry of the apparatus. Conversely, measuring the geometry of the apparatus is a measurement of the gravitational field on the boundary.

Notice that, because of the Feynman path integral, the geometry in the interior is free to fluctuate quantum-mechanically. The point is that the propagation kernel W can be interpreted as a sum over geometries. It is this radical point of view which is usually adopted, and concretely implemented in the context of Spin Foam Models. The calculation of graviton propagator in the new SFMs in chapter 9 is an application of the general boundary formalism in quantum gravity.

9.2 Compatibility between of radial, Lorenz and harmonic gauges

A technical point in the calculation of n-point functions in quantum gravity is the choice of the gauge. Which gauge shall we use in order to make a comparison between the LQG and the standard graviton propagator? The LQG propagator is defined in a generalized temporal gauge: $h_{\mu\nu}$ has vanishing components along the normals to the boundary 3-sphere. This gauge is called radial, or Fock-Schwinger gauge [126, 127, 128]. Perturbative quantum gravity is mostly known in harmonic gauge. We show that in linearize General Relativity there exists a gauge in which the linearized gravitational field is radial *and*

harmonic [125]. We present this original result, and an analogous original result for Maxwell electromagnetic theory.

The radial gauge, or Fock-Schwinger gauge is defined by

$$x^\mu A_\mu(x) = 0 \quad (349)$$

in Maxwell theory, and by

$$x^\mu h_{\mu\nu}(x) = 0 \quad (350)$$

in linearized General Relativity. Here x^μ are Lorentzian (or Euclidean) spacetime coordinates in $d + 1$ spacetime dimensions, where $\mu=0, 1, \dots, d$; $A_\mu(x)$ is the electromagnetic potential. The radial gauge has been considered with various motivations. For instance, radial-gauge perturbation theory was studied in [129, 128, 130, 131], where an expression for the propagator and Feynman rules in this gauge were derived. A number of papers implicitly use this gauge in the context of nonperturbative Euclidean Loop Quantum Gravity [7, 91, 92, 123, 93]. Here, indeed, consider a spherical region in spacetime, and identify the degrees of freedom on the 3d boundary Σ of this region with the degrees of freedom described by Hamiltonian Loop Quantum Gravity. The last is defined in a “temporal” gauge where the field components in the direction *normal to the boundary surface* Σ are gauge fixed. Since the direction normal to a sphere is radial, this procedure is equivalent to imposing the radial gauge (350) in the linearization around flat spacetime.

The radial gauge is usually viewed as an *alternative* to the commonly used Lorenz and harmonic gauges, defined respectively by

$$\partial_\mu A^\mu = 0 \quad (351)$$

in Maxwell theory and by

$$\partial_\mu h^\mu{}_\nu - \frac{1}{2} \partial_\nu h^\mu{}_\mu = 0 \quad (352)$$

in linearized General Relativity. Here we observe, instead, that the radial gauge is *compatible* with the Lorenz and the harmonic gauges. That is, if A_μ and $h_{\mu\nu}$ solve the Maxwell and the linearized Einstein equations, then they can be gauge-transformed to fields A'_μ and $h'_{\mu\nu}$ satisfying (349,350) *and* (351,352). This is analogous to the well known fact (see for instance [28]) that the Lorenz and the harmonic gauges can be imposed simultaneously with the temporal gauge

$$A_0 = 0, \quad (353a)$$

$$h_{0\mu} = 0. \quad (353b)$$

We find convenient, below, to utilize the language of tensor calculus. To avoid confusion, let us point out that this does not mean that we work on a curved spacetime. We are only concerned here with Maxwell theory on flat space and with linearized General Relativity also on flat space. Tensor calculus is used below only as a tool for dealing in compact form with expressions in the hyperspherical coordinates that simplify the analysis of the radial gauge.

Maxwell theory is discussed in the first paragraph, gravity in the second. We work in an arbitrary number of dimensions, and we cover the Euclidean and the Lorentzian signatures at the same time. That is, we can take either $(\eta_{\mu\nu}) = \text{diag}[1, 1, 1, 1, \dots]$ or $(\eta_{\mu\nu}) = \text{diag}[1, -1, -1, -1, \dots]$. The analysis is local in spacetime and disregards singular points such as the origin.

9.2.1 Maxwell theory

In this paragraph we show the compatibility between Lorenz and radial gauge in electromagnetism. Maxwell vacuum equations are

$$\partial_\nu F^{\nu\mu} = 0, \quad (354)$$

where $F_{\mu\nu} = \partial_\mu A_\nu - \partial_\nu A_\mu$. That is

$$\square A_\mu - \partial_\mu \partial_\nu A^\nu = 0, \quad (355)$$

where $\square = \eta^{\mu\nu} \partial_\mu \partial_\nu$. This equation is of course invariant under the gauge transformation

$$A_\mu \rightarrow A'_\mu = A_\mu + \partial_\mu \lambda. \quad (356)$$

Temporal and Lorenz gauge We begin by recalling how one can derive the well-know result that the Lorenz and *temporal* gauges are compatible. This is a demonstration that can be found in most elementary books on electromagnetism; we recall it here in a form that we shall reproduce below for the radial gauge.

Let us write $(x^\mu) = (x^0, x^i) = (t, \vec{x})$, where $i = 1, \dots, d$. Let A_μ satisfy the Maxwell equations (355). We now show that there is a gauge equivalent field A'_μ satisfying the temporal as well as the Lorenz gauge conditions. That is, there exist a scalar function λ such that A'_μ defined in (356) satisfies (353a) and (351). The equation (353a) for A'_μ defined in (356) gives $A_0 + \partial_0 \lambda = 0$, with the general solution

$$\lambda(t, \vec{x}) = - \int_{t_0}^t A_0(\tau, \vec{x}) d\tau + \tilde{\lambda}(\vec{x}), \quad (357)$$

where $\tilde{\lambda}(\vec{x})$ is an integration “constant”, which is an arbitrary function on the surface Σ defined by $t = t_0$. Can $\tilde{\lambda}(\vec{x})$ (which is a function of d variables) be chosen in such a way that the Lorenz gauge condition (which is a function of $d + 1$ variables) is satisfied? To show that this is the case, let us first fix $\tilde{\lambda}(\vec{x})$ in such a way that the Lorenz gauge condition is satisfied *on* Σ . Inserting A'_μ in (351) and using (353a) we have

$$\partial_\mu A'^\mu = \partial_i A'^i = \partial_i A^i + \Delta \lambda = 0, \quad (358)$$

where $\Delta = \partial_i \partial^i$ is the Laplace operator⁹ on Σ . The restriction of this equation to Σ gives the Poisson equation

$$\Delta \tilde{\lambda}(\vec{x}) = -\partial_i A^i(t_0, \vec{x}), \quad (359)$$

which determines $\tilde{\lambda}(\vec{x})$. With $\tilde{\lambda}(\vec{x})$ satisfying this equation, A'_μ satisfies the temporal gauge condition everywhere and the Lorenz gauge condition on Σ . However, this implies immediately that A'_μ satisfies the Lorenz gauge condition everywhere as well, thanks to the Maxwell equations. In fact, the time component of (355) reads

$$\square A'_0 - \partial_0 \partial_\nu A'^\nu = -\partial_0(\partial_\nu A'^\nu) = 0. \quad (360)$$

That is: for a field in the temporal gauge, the Maxwell equations imply that if the Lorenz gauge is satisfied on Σ then it is satisfied everywhere.

⁹Minus the Laplace operator in the Lorentzian case.

Radial and Lorenz gauge We now show that the *radial* and Lorenz gauge are compatible, following steps similar to the ones above. We want to show that there exists a function λ such that A'_μ defined in (356) satisfies (349) and (351), assuming that A_μ satisfies the Maxwell equations.

Due to the symmetry of the problem, it is convenient to use polar coordinates. We write these as $(x^a) = (x^r, x^i) = (r, \vec{x})$, where $r = \sqrt{|\eta_{\mu\nu}x^\mu x^\nu|}$ is the $(d+1)$ -dimensional radius and $\vec{x} = (x^i)$ are three angular coordinates. In these coordinates the metric tensor $\eta_{\mu\nu}$ takes the simple form

$$ds^2 = \gamma_{ab}(r, \vec{x}) dx^a dx^b = dr^2 + r^2 \xi_{ij}(\vec{x}) dx^i dx^j, \quad (361)$$

where $\xi_{ij}(\vec{x})$ is independent from r and is the metric of a 3-sphere of unit radius in the Euclidean case, and the metric of an hyperboloid of unit radius in the Lorentzian case. It is easy to see that in these coordinates, the radial gauge condition (349) takes the simple form

$$A'_r = 0. \quad (362)$$

Inserting the definition of A'_μ gives

$$\partial_r \lambda = -A_r, \quad (363)$$

with the general solution

$$\lambda(r, \vec{x}) = - \int_{r_0}^r A_r(\rho, \vec{x}) d\rho + \tilde{\lambda}(\vec{x}), \quad (364)$$

where the integration constant $\tilde{\lambda}$ is now a function on the surface Σ defined by $r = r_0$. The surface Σ is a d -sphere in the Euclidean case and a d -dimensional hyperboloid in the Lorentzian case. As in the previous section, we fix $\tilde{\lambda}(\vec{x})$ by requiring the Lorenz condition to be satisfied on Σ . It is convenient to use general covariant tensor calculus in order to simplify the expressions in polar coordinates. In arbitrary coordinates, the Lorenz condition reads

$$\nabla_a A'^a = \frac{1}{\sqrt{\gamma}} \partial_a (\sqrt{\gamma} A'^a) = 0, \quad (365)$$

where ∇_a is the covariant derivative, $A_b = A^a g_{ab}$, and γ is the determinant of γ_{ab} . This determinant has the form $\gamma = r^{2d} \xi$, where ξ is the determinant of ξ_{ij} . When the radial gauge is satisfied, (365) reduces to

$$\partial_i (\sqrt{\xi} A'^i) = 0. \quad (366)$$

Let us now require that A'_μ satisfies this equation on Σ . Using (356), this requirement fixes $\tilde{\lambda}$ to be the solution of a Poisson equation on Σ , that is

$$\Delta \tilde{\lambda} = - \frac{1}{\sqrt{\xi}} \partial_i (\sqrt{\xi} A^i), \quad (367)$$

where the Laplace operator is $\Delta = \nabla_i \xi^{ij} \nabla_j$. In arbitrary coordinates, Maxwell equations read

$$\nabla_a F^{ab} = \frac{1}{\sqrt{\gamma}} \partial_a (\sqrt{\gamma} F^{ab}) = 0, \quad (368)$$

where

$$F^{ab} = \nabla^a A^b - \nabla^b A^a. \quad (369)$$

Consider the radial ($b = r$) component of (368); since $A'_r = 0$, using the form (361) of the metric, we have

$$\begin{aligned} \frac{1}{\sqrt{\gamma}} \partial_a (\sqrt{\gamma} F^{ar}) &= \frac{1}{\sqrt{\gamma}} \partial_a (\sqrt{\gamma} \gamma^{ab} F_{br}) = \frac{1}{\sqrt{\gamma}} \partial_a (\sqrt{\gamma} \gamma^{ab} (\partial_b A'_r - \partial_r A'_b)) = \\ &= -\frac{1}{\sqrt{\xi}} \partial_i \left(\sqrt{\xi} \frac{\xi^{ij}}{r^2} \partial_r A'_j \right) = -\frac{1}{r^2 \sqrt{\xi}} \partial_r \partial_i (\sqrt{\xi} \xi^{ij} A'_j) = 0, \end{aligned} \quad (370)$$

which shows that the Lorenz gauge condition (366) is satisfied everywhere if it is satisfied on Σ . This shows that we can find a function λ such that both the radial and the Lorenz gauge are satisfied everywhere.

9.2.2 Linearized General Relativity

We now consider the compatibility between the radial gauge and the harmonic traceless gauge (also known as transverse traceless gauge [28]) in linearized General Relativity. Einstein equations in vacuum are given by the vanishing of the Ricci tensor. If $|h_{\mu\nu}(x)| \ll 1$, and we linearize these equations in $h_{\mu\nu}$, we obtain the linearized Einstein equations

$$\partial_\mu \partial_\nu h^\alpha{}_\alpha + \partial_\alpha \partial^\alpha h_{\mu\nu} - \partial_\mu \partial^\alpha h_{\alpha\nu} - \partial_\nu \partial^\alpha h_{\alpha\mu} = 0. \quad (371)$$

Under infinitesimal coordinate transformations,

$$h_{\mu\nu} \rightarrow h'_{\mu\nu} = h_{\mu\nu} + \frac{1}{2} (\partial_\mu \lambda_\nu + \partial_\nu \lambda_\mu), \quad (372)$$

where the factor 1/2 is inserted for convenience. These are gauge transformations of the linearized theory. The harmonic gauge is defined by the condition

$$\nabla^\nu \nabla_\nu x^\mu = 0, \quad (373)$$

where ∇_ν is the covariant partial derivative¹⁰; in the linearized theory (373) reduces to

$$\partial_\nu h^{\nu\mu} - \frac{1}{2} \partial^\mu h^\nu{}_\nu = 0, \quad (374)$$

and in this gauge the Einstein equations (371) read simply

$$\square h_{\mu\nu} = 0. \quad (375)$$

¹⁰Notice that (373) means the covariant Laplacian of $d+1$ scalars ($d+1$ coordinates), not the covariant Laplacian of a $(d+1)$ -vector.

Temporal and harmonic gauge As we did for Maxwell theory, we begin by recalling how the compatibility between *temporal* and harmonic gauge can be proved. Start by searching a gauge parameter λ_μ that takes $h_{\mu\nu}$ to the temporal gauge $h'_{0\nu} = 0$. Equation (353b) gives

$$h_{0\mu} + \frac{1}{2}(\partial_0\lambda_\mu + \partial_\mu\lambda_0) = 0 \quad (376)$$

with the general solution

$$\lambda_0(t, \vec{x}) = - \int_{t_0}^t h_{00}(\tau, \vec{x}) d\tau + \tilde{\lambda}_0(\vec{x}) , \quad (377)$$

$$\lambda_i(t, \vec{x}) = - \int_{t_0}^t \left(2h_{0i}(\tau, \vec{x}) + \partial_i\lambda_0(\tau, \vec{x}) \right) d\tau + \tilde{\lambda}_i(\vec{x}) , \quad (378)$$

where the integration constants $\tilde{\lambda}_\mu(\vec{x})$ are functions on the 3d surface Σ defined by $t = t_0$. Next, we fix $\tilde{\lambda}_i$ by imposing the harmonic gauge condition (374) on Σ . Since we are in temporal gauge, this gives

$$\Delta\tilde{\lambda}_j = -2\partial_i h^i_j + \partial_j h^i_i , \quad (379)$$

which can be clearly solved on Σ . The time-time component of Einstein equations becomes

$$\partial_t^2 h^i_i = 0 , \quad (380)$$

whose only well behaved solution is $h^i_i = 0$; so in the temporal gauge the invariant trace of $h'_{\mu\nu}$ vanishes:

$$h'^\mu_\mu = \eta^{\mu\nu} h'_{\mu\nu} = 0 , \quad (381)$$

and the harmonic condition (374) takes the simpler form

$$\partial_\nu h^{\nu\mu} = 0 , \quad (382)$$

similar to the Lorenz gauge. Now the (t, i) components of Einstein equations read

$$\partial_t \partial_j h'^j_i = 0 , \quad (383)$$

which gives $\partial_j h'^j_i = 0$ everywhere, once imposed on Σ .

Radial and harmonic gauge Let us finally come to the compatibility between the *radial* and harmonic gauges. We return to the polar coordinates used in the Maxwell case. In these coordinates, the radial gauge condition (350) reads

$$h'_{rr} = h'_{ri} = 0 . \quad (384)$$

Inserting the gauge transformation (372) gives

$$\partial_r \lambda_r = -h_{rr} , \quad (385)$$

$$\partial_r \lambda_i + \partial_i \lambda_r - \frac{2}{r} \lambda_i = -2h_{ri} , \quad (386)$$

with the general solution

$$\lambda_r(r, \vec{x}) = - \int_{r_0}^r h_{rr}(\rho, \vec{x}) d\rho + \tilde{\lambda}_r(\vec{x}) , \quad (387)$$

$$\lambda_i(r, \vec{x}) = -r^2 \int_{r_0}^r \frac{2h_{ri}(\rho, \vec{x}) + \partial_i \lambda_r(\rho, \vec{x})}{\rho^2} d\rho + r^2 \tilde{\lambda}_i(\vec{x}) , \quad (388)$$

where $\tilde{\lambda}_r, \tilde{\lambda}_i$ are functions on the surface Σ given by $r = r_0$. We can then fix $\tilde{\lambda}_i$ by imposing the harmonic condition on Σ precisely as before. In the polar coordinates (361), we have easily the following rules for the Christoffel symbols:

$$\Gamma^a_{rr} = 0 , \quad \Gamma^i_{jr} = \frac{1}{r} \delta^i_j , \quad \Gamma^r_{ra} = 0 . \quad (389)$$

We note also that Γ^i_{jk} is independent of r . Consider the (r, r) component of Einstein equations:

$$\nabla_r \nabla_r h'^a_a + \nabla_a \nabla^a h'_{rr} - \nabla_r \nabla^a h_{ar} - \nabla_r \nabla^a h'_{ar} = 0 . \quad (390)$$

Taking into account (361) and (389), it is verified after a little algebra that the previous equation becomes

$$\partial_r^2 h'^a_a + \frac{2}{r} \partial_r h'^a_a = 0 , \quad (391)$$

which is a differential equation for the trace h'^a_a . Its only solution well-behaved at the origin and at infinity is $h'^a_a = 0$. Using this, the (r, i) components of Einstein equations read:

$$\nabla_a \nabla^a h'_{ri} - \nabla_r \nabla^a h'_{ai} - \nabla_i \nabla^a h'_{ar} = -\partial_r \nabla_a h'^a_i = 0 , \quad (392)$$

and the harmonic condition is simply

$$\nabla_a h'^{ab} = 0 . \quad (393)$$

Equation (392) shows immediately that the $b=i$ components of the gauge condition (393) hold everywhere if they hold on Σ . The vanishing of the $b=r$ component of (393) follows immediately since, using (389), we have

$$\nabla_a h'^a_r = -\frac{1}{r} h'^a_a = 0 . \quad (394)$$

Therefore the harmonic gauge condition, the radial gauge condition and the vanishing of the trace are all consistent with one another.

10 LQG propagator from the new spin foams

This chapter is the reproduction of the original work of reference [96]. We compute metric correlations in Loop Quantum Gravity and compare them with the scaling and the tensorial structure of the graviton propagator in perturbative Quantum Gravity [132, 133, 134]. The strategy is the one introduced in [91] and developed in [92, 93, 135, 136, 79, 94, 95, 137]. In particular, we use the boundary amplitude formalism [7, 17, 138, 121]. The dynamics is implemented in terms of (the group field theory expansion of) the new spin foam models introduced by Engle, Pereira, Rovelli and Livine (EPRL model) [15] and by Freidel and Krasnov (FK model) [57]. We restrict attention to Euclidean signature and Immirzi parameter smaller than one: $0 < \gamma < 1$. In this case the two models coincide.

Previous attempts to derive the graviton propagator from LQG adopted the Barrett-Crane spin foam vertex [139] as model for the dynamics [91, 92, 93, 135, 136, 79, 94, 95, 137] (see also [122, 123, 140] for investigations in the three-dimensional case). The analysis of [79, 94] shows that the Barrett-Crane model fails to give the correct scaling behavior for off-diagonal components of the graviton propagator. The problem can be traced back to a missing coherent cancellation of phases between the intertwiner wave function of the semiclassical boundary state and the intertwiner dependence of the model. The attempt to correct this problem was part of the motivation for the lively search of *new* spin foam models with non-trivial intertwiner dependence [141, 88, 15, 57, 56]. The intertwiner dynamics of the new models was investigated numerically in [142, 143, 144, 145], and presented here in chapter 7. The analysis of the large spin asymptotics of the vertex amplitude of the new models was performed in [146, 84, 97, 147] in the Euclidean setting and in [148] in the Lorentzian. In [95], the obstacle that prevented the Barrett-Crane model from yielding the correct behaviour of the propagator was shown to be absent for the new models: the new spin foams feature the correct dependence on intertwiners to allow a coherent cancellation of phases with the boundary semiclassical state. Here we restart from scratching the calculation and derive the graviton propagator from the new Spin Foam Models.

In this introduction we briefly describe the quantity we want to compute. We consider a manifold \mathcal{R} with the topology of a 4-ball. Its boundary is a 3-manifold Σ with the topology of a 3-sphere S^3 . We associate to Σ a boundary Hilbert space of states: the LQG Hilbert space \mathcal{H}_Σ spanned by (abstract) spin-networks. We call $|\Psi\rangle$ a generic state in \mathcal{H}_Σ . A spin foam model for the region \mathcal{R} provides a map from the boundary Hilbert space to \mathbb{C} . We call this map $\langle W|$ (see section 9.1). It provides a sum over the bulk geometries with a weight that defines our model for quantum gravity. The dynamical expectation value of an operator \mathcal{O} on the state $|\Psi\rangle$ is defined via the following expression¹¹

$$\langle \mathcal{O} \rangle = \frac{\langle W | \mathcal{O} | \Psi \rangle}{\langle W | \Psi \rangle}. \quad (396)$$

The operator \mathcal{O} can be a geometric operator as the area, the volume or the length [149, 150, 151, 152,

¹¹This expression corresponds to the standard definition in (perturbative) quantum field theory where the *vacuum* expectation value of a product of local observables is defined as

$$\langle O(x_1) \cdots O(x_n) \rangle_0 = \frac{\int D[\varphi] O(x_1) \cdots O(x_n) e^{iS[\varphi]}}{\int D[\varphi] e^{iS[\varphi]}} \equiv \frac{\int D[\phi] W[\phi] O(x_1) \cdots O(x_n) \Psi_0[\phi]}{\int D[\phi] W[\phi] \Psi_0[\phi]}. \quad (395)$$

The vacuum state $\Psi_0[\phi]$ codes the boundary conditions at infinity.

153, 154, 155]. The geometric operator we are interested in here is the (density-two inverse-) metric operator $q^{ab}(x) = \delta^{ij} E_i^a(x) E_j^b(x)$. We focus on the *connected* two-point correlation function $G^{abcd}(x, y)$ on a semiclassical boundary state $|\Psi_0\rangle$. It is defined as

$$G^{abcd}(x, y) = \langle q^{ab}(x) q^{cd}(y) \rangle - \langle q^{ab}(x) \rangle \langle q^{cd}(y) \rangle. \quad (397)$$

The boundary state $|\Psi_0\rangle$ is semiclassical in the following sense: it is peaked on a given configuration of the intrinsic and the extrinsic geometry of the boundary manifold Σ . In terms of Ashtekar-Barbero variables these boundary data correspond to a couple (E_0, A_0) . The boundary data are chosen so that there is a solution of Einstein equations in the bulk which induces them on the boundary. A spin foam model has good semiclassical properties if the dominant contribution to the amplitude $\langle W|\Psi_0\rangle$ comes from the bulk configurations close to the classical 4-geometries compatible with the boundary data (E_0, A_0) . By *classical* we mean that they satisfy Einstein equations.

The classical bulk configuration we focus on is flat space. The boundary configuration that we consider is the following: we decompose the boundary manifold S^3 in five tetrahedral regions with the same connectivity as the boundary of a 4-simplex; then we choose the intrinsic and the extrinsic geometry to be the ones proper of the boundary of a Euclidean 4-simplex. By construction, these boundary data are compatible with flat space being a classical solution in the bulk.

For our choice of boundary configuration, the dominant contribution to the amplitude $\langle W|\Psi_0\rangle$ is required to come from bulk configurations close to flat space. The connected two-point correlation function $G^{abcd}(x, y)$ probes the fluctuations of the geometry around the classical configuration given by flat space. As a result it can be compared to the graviton propagator computed in perturbative quantum gravity.

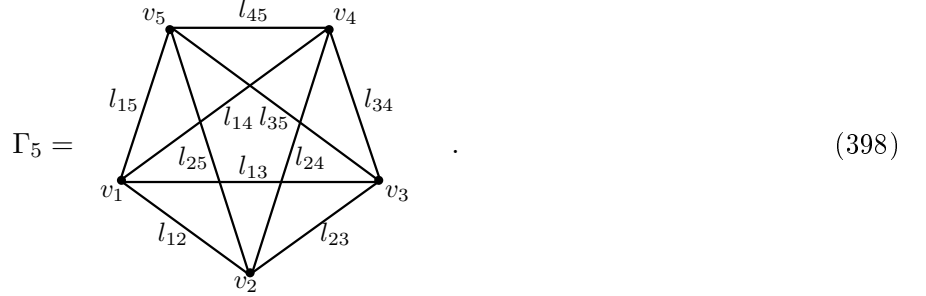
The plan of this chapter is the following: in section 10.1 we introduce the metric operator and construct a semiclassical boundary state; in section 10.2 we recall the form of the new spin foam models; in section 10.3 we define the LQG propagator and provide an integral formula for it at the lowest order in a vertex expansion; in section 10.6 we compute its large spin asymptotics; in section 10.11 we discuss expectation values of metric operators; in section 10.12 we present our main result: the scaling and the tensorial structure of the LQG propagator at the leading order of our expansion; in section 10.13 we attempt a comparison with the graviton propagator of perturbative quantum gravity.

10.1 *Semiclassical boundary state and the metric operator*

Semiclassical boundary states are a key ingredient in the definition of boundary amplitudes. Here we describe in detail the construction of a boundary state peaked on the intrinsic and the extrinsic geometry of the boundary of a Euclidean 4-simplex. The construction is new: it uses the coherent intertwiners of Livine and Speziale [56] (see also [97]) together with a superposition over spins as done in [91, 92]. It can be considered as an improvement of the boundary state used in [79, 94, 95] where Rovelli-Speziale gaussian states [87] for intertwiners were used. Remarkably, the semiclassical states we use can be derived from the mathematical construction of coherent states for the natural phase space associated to the $SU(2)$ gauge group (this derivation is discussed in chapter 8). More precisely, and in order to not confuse the notation, here we call “coherent spin-networks” the states with *fixed* spins, with nodes labeled by Livine-Speziale coherent intertwiners, and take a superposition over spins in order to construct the desired semiclassical geometry. In chapter 8 instead we call coherent spin-networks the coherent states derived in a more systematic way from the analysis of the phase space of General Relativity. The superposition over spins

used here and the coherent spin-networks introduced in chapter 8 do not coincide exactly, but only in the large spin limit.

We consider a simplicial decomposition Δ_5 of S^3 . The decomposition Δ_5 is homeomorphic to the boundary of a 4-simplex: it consists of five cells t_a which meet at ten faces f_{ab} ($a, b = 1, \dots, 5$ and $a < b$). Then we consider the sector of the Hilbert space \mathcal{H}_Σ spanned by spin-network states with graph Γ_5 dual to the decomposition Δ_5 ,



Γ_5 is a complete graph with five nodes. We call v_a its nodes and l_{ab} ($a < b$) its ten links. Spin-network states supported on this graph are labelled by ten spins j_{ab} ($a < b$) and five intertwiners i_a . We denote them by $|\Gamma_5, j_{ab}, i_a\rangle$ and call \mathcal{H}_{Γ_5} the Hilbert space they span. On \mathcal{H}_{Γ_5} we can introduce a *metric operator* smearing the electric field on surfaces dual to links, i.e. considering scalar products of fluxes. We focus on the node n and consider a surface f_{na} which cuts the link from the node n to the node a . The flux operator through the surface f_{na} , parallel transported in the node n , is denoted¹² $(E_n^a)_i$. It has the following three non-trivial properties:

(i) the flux operators $(E_n^a)_i$ and $(E_a^n)_i$ are related by a $SU(2)$ parallel transport g_{an} from the node a to the node n together with a change of sign which takes into account the different orientation of the face f_{an} ,

$$(E_n^a)_i = -(R_{an})_i^j (E_a^n)_j, \quad (399)$$

where R_{an} is the rotation which corresponds to the group element g_{an} associated to the link l_{an} , i.e. $R_{an} = D^{(1)}(g_{ab})$;

(ii) the commutator of two flux operators for the same face f_{na} is¹³

$$[(E_n^a)_i, (E_n^a)_j] = i\gamma\epsilon_{ij}^k (E_n^a)_k; \quad (400)$$

(iii) a spin-network state is annihilated by the sum of the flux operators over the faces bounding a node

$$\sum_{c \neq n} (E_n^c)_i |\Gamma_5, j_{ab}, i_a\rangle = 0. \quad (401)$$

This last property follows from the $SU(2)$ gauge invariance of the spin-network node.

Using the flux operator we can introduce the density-two inverse-metric operator at the node n , projected in the directions normal to the faces f_{na} and f_{nb} . It is defined as $E_n^a \cdot E_n^b = \delta^{ij} (E_n^a)_i (E_n^b)_j$. Its diagonal components $E_n^a \cdot E_n^a$ measure the area square of the face f_{na} ,

$$E_n^a \cdot E_n^a |\Gamma_5, j_{ab}, i_a\rangle = \left(\gamma \sqrt{j_{na}(j_{na} + 1)} \right)^2 |\Gamma_5, j_{ab}, i_a\rangle. \quad (402)$$

¹²Throughout the chapter $i, j, k \dots = 1, 2, 3$ are indices for vectors in \mathbb{R}^3 .

¹³Throughout the chapter we put $c = \hbar = G_{\text{Newton}} = 1$.

Spin-network states are eigenstates of the diagonal components of the metric operator. On the other hand, the off-diagonal components $E_n^a \cdot E_n^b$ with $a \neq b$ measure the dihedral angle between the faces f_{na} and f_{nb} (weighted with their areas). It reproduces the angle operator [153]. Using the recoupling basis for intertwiner space, we have that in general the off-diagonal components of the metric operator have non-trivial matrix elements

$$E_n^a \cdot E_n^b |\Gamma_5, j_{ab}, i_a\rangle = \sum_{i'_c} (E_n^a \cdot E_n^b)_{i_c}^{i'_c} |\Gamma_5, j_{ab}, i'_a\rangle. \quad (403)$$

We refer to [79, 94] and to section 8.2 for a detailed discussion. In particular, from property (ii), we have that some off-diagonal components of the metric operator at a node do not commute [152]

$$[E_n^a \cdot E_n^b, E_n^a \cdot E_n^c] \neq 0. \quad (404)$$

From this non-commutativity an Heisenberg inequality for dispersions of metric operators follows. Here we are interested in states which are peaked on a given value of *all* the off-diagonal components of the metric operator and which have dispersion of the order of Heisenberg's bound. Such states can be introduced using the technique of coherent intertwiners ([56, 97] and section 8.1). We recall the definition in order to introduce the notation used in this chapter. A coherent intertwiner between the representations j_1, \dots, j_4 is defined as¹⁴

$$\Phi^{m_1 \dots m_4}(\vec{n}_1, \dots, \vec{n}_4) = \frac{1}{\sqrt{\Omega(\vec{n}_1, \dots, \vec{n}_4)}} \int_{SU(2)} dh \prod_{a=1}^4 \langle j_a, m_a | D^{(j_a)}(h) | j_a, \vec{n}_a \rangle \quad (405)$$

and is labelled by four unit vectors $\vec{n}_1, \dots, \vec{n}_4$ satisfying the closure condition

$$j_1 \vec{n}_1 + \dots + j_4 \vec{n}_4 = 0. \quad (406)$$

The function $\Omega(\vec{n}_1, \dots, \vec{n}_4)$ provides normalization to one of the intertwiner. The function $\Phi^{m_1 \dots m_4}$ is invariant under rotations of the four vectors $\vec{n}_1, \dots, \vec{n}_4$. In the following we always assume that this invariance has been fixed with a given choice of orientation¹⁵.

Nodes of the spin-network can be labelled with coherent intertwiners. In fact such states provide an overcomplete basis of \mathcal{H}_{Γ_5} . Calling $v_i^{m_1 \dots m_4}$ the standard recoupling basis for intertwiners, we can define the coefficients

$$\Phi_i(\vec{n}_1, \dots, \vec{n}_4) = v_i^{m_1 \dots m_4} \Phi_{m_1 \dots m_4}(\vec{n}_1, \dots, \vec{n}_4). \quad (407)$$

We define a *coherent spin-network* $|\Gamma_5, j_{ab}, \Phi_a\rangle$ as the state labelled by ten spins j_{ab} and 4×5 normals \vec{n}_{ab} and given by the superposition

$$|\Gamma_5, j_{ab}, \Phi_a(\vec{n})\rangle = \sum_{i_1 \dots i_5} \left(\prod_{a=1}^5 \Phi_{i_a}(\vec{n}_{ab}) \right) |\Gamma_5, j_{ab}, i_a\rangle. \quad (408)$$

¹⁴There is a phase ambiguity in the definition of the coherent intertwiner. Such ambiguity becomes observable when a superposition over spins is considered.

¹⁵For instance we can fix this redundancy assuming that the sum $j_1 \vec{n}_1 + j_2 \vec{n}_2$ is in the positive z direction while the vector $\vec{n}_1 \times \vec{n}_2$ in the positive y direction. Once chosen this orientation, the four unit-vectors $\vec{n}_1, \dots, \vec{n}_4$ (which satisfying the closure condition) depend only on two parameters. These two parameters can be chosen to be the dihedral angle $\cos \theta_{12} = \vec{n}_1 \cdot \vec{n}_2$ and the twisting angle $\tan \phi_{(12)(34)} = \frac{(\vec{n}_1 \times \vec{n}_2) \cdot (\vec{n}_3 \times \vec{n}_4)}{|\vec{n}_1 \times \vec{n}_2| |\vec{n}_3 \times \vec{n}_4|}$.

The expectation value of the metric operator on a coherent spin-network is simply

$$\langle \Gamma_5, j_{ab}, \Phi_a | E_c^a \cdot E_c^b | \Gamma_5, j_{ab}, \Phi_a \rangle \simeq \gamma^2 j_{ca} j_{cb} \vec{n}_{ca} \cdot \vec{n}_{cb} \quad (409)$$

in the large spin limit. As a result we can choose the normals \vec{n}_{ab} so that the coherent spin-network state is peaked on a given intrinsic geometry of Σ .

Normals in different tetrahedra cannot be chosen independently if we want to peak on a Regge geometry [156]. The relation between normals is provided by the requirement that they are computed from the lengths of the edges of the triangulation Δ_5 . In fact, a state with generic normals (satisfying the closure condition (406)) is peaked on a discontinuous geometry. This fact can be seen in the following way: let us consider an edge of the triangulation Δ_5 ; this edge is shared by three tetrahedra; for each tetrahedron we can compute the expectation value of the length operator for an edge in its boundary [155]; however in general the expectation value of the length of an edge seen from different tetrahedra will not be the same; this fact shows that the geometry is *discontinuous*. The requirement that the semiclassical state is peaked on a Regge geometry amounts to a number of relations between the labels \vec{n}_{ab} . In the case of the boundary of a Euclidean 4-simplex (excluding the ‘rectangular’ cases discussed in [157]), the normals turn out to be completely fixed once we give the areas of the ten triangles or equivalently the ten spins j_{ab} ,

$$\vec{n}_{ab} = \vec{n}_{ab}(j_{cd}) . \quad (410)$$

This assignment of normals guarantees that the geometry we are peaking on is Regge-like. In particular, in this chapter we are interested in the case of a 4-simplex which is approximately regular. In this case the spins labelling the links are of the form $j_{ab} = j_0 + \delta j_{ab}$ with $\frac{\delta j_{ab}}{j_0} \ll 1$ and a perturbative expression for the normals solving the continuity condition is available:

$$\vec{n}_{ab}(j_0 + \delta j) = \vec{n}_{ab}(j_0) + \sum_{cd} v^{(ab)(cd)} \delta j_{cd} . \quad (411)$$

The coefficients $v^{(ab)(cd)}$ can be computed in terms of the derivative of the normals \vec{n}_{ab} (for a given choice of orientation, see footnote 15) with respect to the ten edge lengths, using the Jacobian of the transformation from the ten areas to the ten edge lengths of the 4-simplex.

In the following we are interested in superpositions over spins of coherent spin-networks. As coherent intertwiners are defined only up to a spin-dependent arbitrary phase, a choice is in order. We make the canonical choice of phases described in [147]. We briefly recall it here. Consider a non-degenerate Euclidean 4-simplex; two tetrahedra t_a and t_b are glued at the triangle $f_{ab} \equiv f_{ba}$. Now, two congruent triangles f_{ab} and f_{ba} in \mathbb{R}^3 can be made to coincide via a unique rotation $R_{ab} \in SO(3)$ which, together with a translation, takes one outward-pointing normal to minus the other one,

$$R_{ab} \vec{n}_{ab} = -\vec{n}_{ba} . \quad (412)$$

The canonical choice of phase for the spin coherent states $|j_{ab}, \vec{n}_{ab}\rangle$ and $|j_{ab}, \vec{n}_{ba}\rangle$ entering the coherent intertwiners Φ_a and Φ_b is given by lifting the rotation R_{ab} to a $SU(2)$ transformation g_{ab} and requiring that

$$|j_{ab}, \vec{n}_{ba}\rangle = D^{(j_{ab})}(g_{ab}) J |j_{ab}, \vec{n}_{ab}\rangle \quad (413)$$

where $J : \mathcal{H}_j \rightarrow \mathcal{H}_j$ is the standard antilinear map for $SU(2)$ representations defined by

$$\langle \epsilon | (|\alpha\rangle \otimes J|\beta\rangle) = \langle \beta | \alpha \rangle \quad \text{with} \quad |\alpha\rangle, |\beta\rangle \in \mathcal{H}_j \quad (414)$$

and $\langle \epsilon |$ is the unique intertwiner in $\mathcal{H}_j \otimes \mathcal{H}_j$. In the following we will always work with coherent spin-networks $|\Gamma_5, j_{ab}, \Phi_a(\vec{n}(j))\rangle$ satisfying the continuity condition, and with the canonical choice for the arbitrary phases of coherent states. From now on we use the shorter notation $|j, \Phi(\vec{n})\rangle$.

Coherent spin-networks are eigenstates of the diagonal components of the metric operator, namely the area operator for the triangles of Δ_5 . The extrinsic curvature to the manifold Σ measures the amount of change of the 4-normal to Σ , parallel transporting it along Σ . In a piecewise-flat context, the extrinsic curvature has support on triangles, that is it is zero everywhere except that on triangles. For a triangle f_{ab} , the extrinsic curvature K_{ab} is given by the angle between the 4-normals N_a^μ and N_b^μ to two tetrahedra t_a and t_b sharing the face f_{ab} . As the extrinsic curvature is the momentum conjugate to the intrinsic geometry, we have that a semiclassical state cannot be an eigenstate of the area as it would not be peaked on a given extrinsic curvature. In order to define a state peaked both on intrinsic and extrinsic geometry, we consider a superposition of coherent spin-networks,

$$|\Psi_0\rangle = \sum_{j_{ab}} \psi_{j_0, \phi_0}(j) |j, \Phi(\vec{n})\rangle, \quad (415)$$

with coefficients $\psi_{j_0, \phi_0}(j)$ given by a gaussian times a phase,

$$\psi_{j_0, \phi_0}(j) = \frac{1}{N} \exp\left(-\sum_{ab, cd} \alpha^{(ab)(cd)} \frac{j_{ab} - j_{0ab}}{\sqrt{j_{0ab}}} \frac{j_{cd} - j_{0cd}}{\sqrt{j_{0cd}}}\right) \exp\left(-i \sum_{ab} \phi_0^{ab} (j_{ab} - j_{0ab})\right). \quad (416)$$

As we are interested in a boundary configuration peaked on the geometry of a regular 4-simplex, we choose all the background spins to be equal, $j_{0ab} \equiv j_0$. Later we will consider an asymptotic expansion for large j_0 . The phases ϕ_0^{ab} are also chosen to be equal. The extrinsic curvature at the face f_{ab} in a regular 4-simplex is $K_{ab} = \arccos N_a \cdot N_b = \arccos(-\frac{1}{4})$. In Ashtekar-Barbero variables (E_0, A_0) we have

$$\phi_0 \equiv \phi_0^{ab} = \gamma K_{ab} = \gamma \arccos(-1/4). \quad (417)$$

The 10×10 matrix $\alpha^{(ab)(cd)}$ is assumed to be complex with positive definite real part. Moreover we require that it has the symmetries of a regular 4-simplex. We introduce the matrices $P_k^{(ab)(cd)}$ with $k = 0, 1, 2$ defined as

$$P_0^{(ab)(cd)} = 1 \quad \text{if } (ab) = (cd) \quad \text{and zero otherwise,} \quad (418)$$

$$P_1^{(ab)(cd)} = 1 \quad \text{if } \{a = c, b \neq d\} \text{ or a permutation of it} \quad \text{and zero otherwise,} \quad (419)$$

$$P_2^{(ab)(cd)} = 1 \quad \text{if } (ab) \neq (cd) \quad \text{and zero otherwise.} \quad (420)$$

Their meaning is simple: a couple (ab) identifies a link of the graph Γ_5 ; two links can be either coincident, or touching at a node, or disjoint. The matrices $P_k^{(ab)(cd)}$ correspond to these three different cases. Using the basis $P_k^{(ab)(cd)}$ we can write the matrix $\alpha^{(ab)(cd)}$ as

$$\alpha^{(ab)(cd)} = \sum_{k=0}^2 \alpha_k P_k^{(ab)(cd)}. \quad (421)$$

As a result our ansatz for a semiclassical boundary state $|\Psi_0\rangle$ is labelled by a (large) half-integer j_0 and has only three complex free parameters, the numbers α_k .

10.2 The new spin foam dynamics

The dynamics is implemented in terms of a spin foam functional $\langle W |$. Here we are interested in its components on the Hilbert space spanned by spin-networks with graph Γ_5 . The sum over 2-complexes can be implemented in terms of a formal perturbative expansion in the parameter λ of a Group Field Theory [158]:

$$\langle W | \Gamma_5, j_{ab}, i_a \rangle = \sum_{\sigma} \lambda^{N_{\sigma}} W(\sigma) \quad (422)$$

The sum is over spinfoams (colored 2-complexes) whose boundary is the spin-network (Γ_5, j_{ab}, i_a) , $W(\sigma)$ is the spinfoam amplitude

$$W(\sigma) = \prod_{f \subset \sigma} W_f \prod_{v \subset \sigma} W_v \quad (423)$$

where W_v and W_f are the vertex and face amplitude respectively. The quantity N_{σ} in (422) is the number of vertices in the spin foam σ , therefore the formal expansion in λ is in fact a *vertex expansion*.

The spin foam models we consider here are the EPRL [15] and FK [57] models. We restrict attention to $0 < \gamma < 1$; in this case the two models coincide. The vertex amplitude is given by

$$W_v(j_{ab}, i_a) = \sum_{i_a^+ i_a^-} \{15j\}(j_{ab}^+, i_a^+) \{15j\}(j_{ab}^-, i_a^-) \prod_a f_{i_a^+ i_a^-}^{i_a}(j_{ab}) \quad (424)$$

where the unbalanced spins j^+, j^- are

$$j_{ab}^{\pm} = \gamma^{\pm} j_{ab}, \quad \gamma^{\pm} = \frac{1 \pm \gamma}{2}. \quad (425)$$

This relation puts restrictions¹⁶ on the value of γ and of j_{ab} . The fusion coefficients $f_{i_a^+ i_a^-}^{i_a}(j_{ab})$ are defined in [15] (see also [159]) and built out of the intertwiner $v_i^{m_1 \dots m_4}$ in $\mathcal{H}_{j_1} \otimes \dots \otimes \mathcal{H}_{j_4}$ and the intertwiners $v_{i_{\pm}}^{m_1^{\pm} \dots m_4^{\pm}}$ in $\mathcal{H}_{j_1^{\pm}} \otimes \dots \otimes \mathcal{H}_{j_4^{\pm}}$. Defining a map $Y : \mathcal{H}_j \rightarrow \mathcal{H}_{j^+} \otimes \mathcal{H}_{j^-}$ with matrix elements $Y_{m^+ m^-}^m = \langle j^+, m^+; j^-, m^- | Y | j, m \rangle$ given by Clebsh-Gordan coefficients, we have that the fusion coefficients $f_{i_a^+ i_a^-}^{i_a}$ are given by

$$f_{i_a^+ i_a^-}^{i_a} = Y_{m_1 m_1^+ m_1^-} \dots Y_{m_4 m_4^+ m_4^-} v_i^{m_1 \dots m_4} v_{i_+}^{m_1^+ \dots m_4^+} v_{i_-}^{m_1^- \dots m_4^-}. \quad (426)$$

Indices are raised and lowered with the Wigner metric.

Throughout this chapter we will restrict attention to the lowest order in the vertex expansion. To this order, the boundary amplitude of a spin-network state with graph Γ_5 is given by

$$\langle W | \Gamma_5, j_{ab}, i_a \rangle = \mu(j_{ab}) W_v(j_{ab}, i_a), \quad (427)$$

i.e. it involves a single spin foam vertex.

The function μ is defined as $\mu(j) = \prod_{ab} W_{f_{ab}}(j)$. A natural choice for the face amplitude is $W_f(j^+, j^-) = (2j^+ + 1)(2j^- + 1) = (1 - \gamma^2)j^2 + 2j + 1$. Other choices can be considered. We assume that $\mu(\lambda j_{ab})$ scales as λ^p for some p for large λ . We will show in the following that, at the leading order in large j_0 , the LQG propagator (397) is in fact independent from the choice of face amplitude, namely from the function $\mu(j)$.

¹⁶Formula (424) is well-defined only for j^{\pm} half-integer. As a result, for a fixed value of γ , there are restrictions on the boundary spin j . For instance, if we choose $\gamma = 1/n$ with n integer, then we have that j has to be integer and $j \geq n$, i.e. $j \in \{n, n+1, n+2, \dots\}$.

10.3 LQG propagator: integral formula

In this section we define the LQG propagator and then provide an integral formula for it. The dynamical expectation value of an operator \mathcal{O} on the state $|\Psi_0\rangle$ is defined via the following expression

$$\langle \mathcal{O} \rangle = \frac{\langle W | \mathcal{O} | \Psi_0 \rangle}{\langle W | \Psi_0 \rangle}. \quad (428)$$

The geometric operator we are interested in is the metric operator $E_n^a \cdot E_n^b$ discussed in section 10.1. We focus on the *connected* two-point correlation function G_{nm}^{abcd} on a semiclassical boundary state $|\Psi_0\rangle$. It is defined as

$$G_{nm}^{abcd} = \langle E_n^a \cdot E_n^b E_m^c \cdot E_m^d \rangle - \langle E_n^a \cdot E_n^b \rangle \langle E_m^c \cdot E_m^d \rangle. \quad (429)$$

We are interested in computing this quantity using the boundary state $|\Psi_0\rangle$ introduced in section 10.1 and the spin foam dynamics (424). This is what we call the *LQG propagator*. As the boundary state is a superposition of coherent spin-networks, the LQG propagator involves terms of the form $\langle W | \mathcal{O} | j, \Phi(\vec{n}) \rangle$. Its explicit formula is

$$G_{nm}^{abcd} = \frac{\sum_j \psi(j) \langle W | E_n^a \cdot E_n^b E_m^c \cdot E_m^d | j, \Phi(\vec{n}) \rangle}{\sum_j \psi(j) \langle W | j, \Phi(\vec{n}) \rangle} - \frac{\sum_j \psi(j) \langle W | E_n^a \cdot E_n^b | j, \Phi(\vec{n}) \rangle}{\sum_j \psi(j) \langle W | j, \Phi(\vec{n}) \rangle} \frac{\sum_j \psi(j) \langle W | E_m^c \cdot E_m^d | j, \Phi(\vec{n}) \rangle}{\sum_j \psi(j) \langle W | j, \Phi(\vec{n}) \rangle} \quad (430)$$

In the following two subsections we recall the integral formula for the amplitude of a coherent spin-network $\langle W | j, \Phi(\vec{n}) \rangle$ and derive analogous integral expressions for the amplitude with metric operator insertions $\langle W | E_n^a \cdot E_n^b | j, \Phi(\vec{n}) \rangle$ and $\langle W | E_n^a \cdot E_n^b E_m^c \cdot E_m^d | j, \Phi(\vec{n}) \rangle$.

10.4 Integral formula for the amplitude of a coherent spin-network

The boundary amplitude of a coherent spin-network $|j, \Phi(\vec{n})\rangle$ admits an integral representation [97, 146, 147]. Here we go through its derivation as we will use a similar technique in next section.

The boundary amplitude $\langle W | j, \Phi(\vec{n}) \rangle$ can be written as an integral over five copies of $SU(2) \times SU(2)$ (with respect to the Haar measure):

$$\langle W | j_{ab}, \Phi_a(\vec{n}) \rangle = \sum_{i_a} \left(\prod_a \Phi_{i_a}(\vec{n}) \right) \langle W | j_{ab}, i_a \rangle = \mu(j) \int \prod_{a=1}^5 dg_a^+ dg_a^- \prod_{ab} P^{ab}(g^+, g^-). \quad (431)$$

The function $P^{ab}(g^+, g^-)$ is given by

$$P^{ab}(g^+, g^-) = \langle j_{ab}, -\vec{n}_{ba} | Y^\dagger D^{(j_{ab}^+)}((g_a^+)^{-1} g_b^+) \otimes D^{(j_{ab}^-)}((g_a^-)^{-1} g_b^-) Y | j_{ab}, \vec{n}_{ab} \rangle. \quad (432)$$

where the map Y is defined in section 10.2. Using the factorization property of spin coherent states,

$$Y | j, \vec{n} \rangle = | j^+, \vec{n} \rangle \otimes | j^-, \vec{n} \rangle, \quad (433)$$

we have that the function $P^{ab}(g^+, g^-)$ factorizes as

$$P^{ab}(g^+, g^-) = P^{ab+}(g^+) P^{ab-}(g^-) \quad (434)$$

with

$$P^{ab\pm} = \langle j_{ab}, -\vec{n}_{ba} | D^{(j_{ab}^\pm)} ((g_a^\pm)^{-1} g_b^\pm) | j_{ab}, \vec{n}_{ab} \rangle = \left(\langle \frac{1}{2}, -\vec{n}_{ba} | (g_a^\pm)^{-1} g_b^\pm | \frac{1}{2}, \vec{n}_{ab} \rangle \right)^{2j_{ab}^\pm}. \quad (435)$$

In the last equality we have used (again) the factorization property of spin coherent states to exponentiate the spin j_{ab}^\pm . In the following we will drop the $1/2$ in $|\frac{1}{2}, \vec{n}_{ab}\rangle$ and write always $|\vec{n}_{ab}\rangle$ for the coherent state in the fundamental representation.

The final expression we get is

$$\langle W | j, \Phi(\vec{n}) \rangle = \mu(j) \int \prod_{a=1}^5 dg_a^+ dg_a^- e^S \quad (436)$$

where the ‘‘action’’ S is given by the sum $S = S^+ + S^-$, with

$$S^\pm = \sum_{ab} 2j_{ab}^\pm \log \langle -\vec{n}_{ab} | (g_a^\pm)^{-1} g_b^\pm | \vec{n}_{ba} \rangle. \quad (437)$$

10.5 LQG operators as group integral insertions

In this section we use a similar technique to derive integral expressions for the expectation value of metric operators. In particular we show that

$$\langle W | E_n^a \cdot E_n^b | j_{ab}, \Phi_a(\vec{n}) \rangle = \mu(j) \int \prod_{a=1}^5 dg_a^+ dg_a^- q_n^{ab}(g^+, g^-) e^S \quad (438)$$

and that

$$\langle W | E_n^a \cdot E_n^b E_m^c \cdot E_m^d | j_{ab}, \Phi_a(\vec{n}) \rangle = \mu(j) \int \prod_{a=1}^5 dg_a^+ dg_a^- q_n^{ab}(g^+, g^-) q_m^{cd}(g^+, g^-) e^S \quad (439)$$

where we assume¹⁷ $n \neq m$ and $a, b, c, d \neq n, m$. The expression for the insertions $q_n^{ab}(g^+, g^-)$ in the integral is derived below.

We start focusing on $\langle E_n^a \cdot E_n^b \rangle$ in the case $a \neq b$. The metric field $(E_n^b)_i$ acts on a state $|j_{ab}, m_{ab}\rangle$ as γ times the generator J_i of $SU(2)$. As a result we can introduce a quantity Q_i^{ab} defined as

$$Q_i^{ab}(g^+, g^-) = \langle j_{ab}, -\vec{n}_{ba} | Y^\dagger D^{(j_{ab}^+)} ((g_a^+)^{-1} g_b^+) \otimes D^{(j_{ab}^-)} ((g_a^-)^{-1} g_b^-) Y (E_n^b)_i | j_{ab}, \vec{n}_{ab} \rangle, \quad (440)$$

so that

$$\langle W | E^{na} \cdot E^{nb} | j, \Phi(\vec{n}) \rangle = \int \prod_{a=1}^5 dg_a^+ dg_a^- \delta^{ij} Q_i^{na} Q_j^{nb} \prod'_{cd} P^{cd}(g^+, g^-). \quad (441)$$

The product \prod' is over couples (cd) different from $(na), (nb)$. Thanks to the invariance properties of the map Y , we have that

$$Y J_i^{ab} | j_{ab}, m_{ab} \rangle = (J_i^{ab+} + J_i^{ab-}) Y | j_{ab}, m_{ab} \rangle. \quad (442)$$

¹⁷Similar formulae can be found also in the remaining cases but are not needed for the calculation of the LQG propagator.

Thus Q_i^{ab} can be written as

$$Q_i^{ab} = Q_i^{ab+} P^{ab-} + P^{ab+} Q_i^{ab-} \quad (443)$$

with

$$Q_i^{ab\pm} = \gamma \langle j_{ab}^\pm, -\vec{n}_{ba} | D^{(j_{ab}^\pm)} ((g_a^\pm)^{-1} g_b^\pm) J_i^{ab\pm} | j_{ab}^\pm, \vec{n}_{ab} \rangle. \quad (444)$$

Now we show that $Q_i^{ab\pm}$ is given by a function $A_i^{ab\pm}$ linear in the spin j_{ab}^\pm , times the quantity $P^{ab\pm}$ defined in (435),

$$Q_i^{ab\pm} = A_i^{ab\pm} P^{ab\pm}. \quad (445)$$

The function $A_i^{ab\pm}$ is determined as follows. The generator $J_i^{ab\pm}$ of $SU(2)$ in representation j_{ab}^\pm can be obtained as the derivative

$$i \frac{\partial}{\partial \alpha^i} D^{(j_{ab}^\pm)}(h(\alpha)) \Big|_{\alpha^i=0} = J_i^{ab\pm} \quad (446)$$

where the group element $h(\alpha)$ is defined via the canonical parametrization $h(\alpha) = \exp(-i\alpha^i \frac{\sigma_i}{2})$. Therefore, we can write $Q_i^{ab\pm}$ as

$$\begin{aligned} Q_i^{ab\pm} &= i \gamma \frac{\partial}{\partial \alpha^i} \left(\langle j_{ab}^\pm, -\vec{n}_{ba} | D^{(j_{ab}^\pm)} ((g_a^\pm)^{-1} g_b^\pm) D^{(j_{ab}^\pm)}(h(\alpha)) | j_{ab}^\pm, \vec{n}_{ab} \rangle \right) \Big|_{\alpha^i=0} \\ &= i \gamma \frac{\partial}{\partial \alpha^i} \left(\gamma \langle -\vec{n}_{ba} | (g_a^\pm)^{-1} g_b^\pm h(\alpha) | \vec{n}_{ab} \rangle \right)^{2j_{ab}^\pm} \Big|_{\alpha^i=0} \\ &= \gamma j_{ab}^\pm \langle -\vec{n}_{ba} | (g_a^\pm)^{-1} g_b^\pm \sigma^i | \vec{n}_{ab} \rangle \langle -\vec{n}_{ba} | (g_a^\pm)^{-1} g_b^\pm | \vec{n}_{ab} \rangle^{2j_{ab}^\pm - 1}. \end{aligned} \quad (447)$$

Comparing expression (447) with (445) and (435), we find that $A_i^{na\pm}$ is given by

$$A_i^{na\pm} = \gamma j_{na}^\pm \frac{\langle -\vec{n}_{an} | (g_a^\pm)^{-1} g_n^\pm \sigma^i | \vec{n}_{na} \rangle}{\langle -\vec{n}_{an} | (g_a^\pm)^{-1} g_n^\pm | \vec{n}_{na} \rangle}. \quad (448)$$

A vectorial expression for $A_i^{na\pm}$ can be given, introducing the rotation $R_a^\pm = D^{(1)}(g_a^\pm)$,

$$A_i^{na\pm} = \gamma j_{na}^\pm (R_n^\pm)^{-1} \frac{R_n^\pm n_{na} - R_a^\pm n_{an} - i(R_n^\pm n_{na} \times R_a^\pm n_{an})}{1 - (R_a^\pm n_{an}) \cdot (R_n^\pm n_{na})}. \quad (449)$$

Thanks to (443) and (445), we have that the expression for Q_i^{ab} simplifies to

$$Q_i^{ab} = A_i^{ab} P^{ab} \quad (450)$$

with

$$A_i^{ab} = A_i^{ab+} + A_i^{ab-}. \quad (451)$$

As a result, equation (441) reduces to

$$\langle W | E_n^a \cdot E_n^b | j, \Phi(\vec{n}) \rangle = \int \prod_{a=1}^5 dg_a^+ dg_a^- \delta^{ij} A_i^{na} A_j^{nb} \prod_{cd} P^{cd}(g^+, g^-), \quad (452)$$

which is of the form (436) with the insertion $A^{na} \cdot A^{nb}$. Therefore, comparing with equation (438), we have that

$$q_n^{ab}(g^+, g^-) = A^{na} \cdot A^{nb} \quad (453)$$

for $a \neq b$. The case with $a = b$ can be computed using a similar technique but the result is rather simple and expected, thus we just state it

$$q_n^{aa}(g^+, g^-) = \gamma^2 j_{na}(j_{na} + 1). \quad (454)$$

As far as $\langle E_n^a \cdot E_n^b E_m^c \cdot E_m^d \rangle$ a similar result can be found. In particular, for $n \neq m$ and $a, b, c, d \neq n, m$ the result is stated at the beginning of this section, equation (439), with the same expression for the insertion $q_n^{ab}(g^+, g^-)$ as in equation (453) and equation (454).

Substituting (438)-(439) in (430) we obtain a new expression for the propagator in terms of group integrals:

$$G_{nm}^{abcd} = \frac{\sum_j \mu(j) \psi(j) \int dg^\pm q_n^{ab} q_m^{cd} e^S}{\sum_j \mu(j) \psi(j) \int dg^\pm e^S} - \frac{\sum_j \mu(j) \psi(j) \int dg^\pm q_n^{ab} e^S}{\sum_j \mu(j) \psi(j) \int dg^\pm e^S} \frac{\sum_j \mu(j) \psi(j) \int dg^\pm q_m^{cd} e^S}{\sum_j \mu(j) \psi(j) \int dg^\pm e^S}. \quad (455)$$

This expression with metric operators written as insertions in an integral is the starting point for the large j_0 asymptotic analysis of next section.

10.6 LQG propagator: stationary phase approximation

The correlation function (455) depends on the scale j_0 fixed by the boundary state. We are interested in computing its asymptotic expansion for large j_0 . The technique we use is an (extended) stationary phase approximation of a multiple integral over both spins and group elements. In 10.7 we put expression (455) in a form to which this approximation can be applied. Then in 10.8 we recall a standard result in asymptotic analysis regarding connected two-point functions and in 10.9-10.10 we apply it to our problem.

10.7 The total action and the extended integral

We introduce the ‘‘total action’’ defined as $S_{\text{tot}} = \log \psi + S$ or more explicitly as

$$\begin{aligned} S_{\text{tot}}(j_{ab}, g_a^+, g_a^-) = & -\frac{1}{2} \sum_{ab, cd} \alpha^{(ab)(cd)} \frac{j_{ab} - j_{0ab}}{\sqrt{j_{0ab}}} \frac{j_{cd} - j_{0cd}}{\sqrt{j_{0cd}}} - i \sum_{ab} \phi_0^{ab} (j_{ab} - j_{0ab}) \\ & + S^+(j_{ab}, g_a^+) + S^-(j_{ab}, g_a^-). \end{aligned} \quad (456)$$

Notice that the action $S^+ + S^-$ is a homogeneous function of the spins j_{ab} therefore, rescaling the spins j_{0ab} and j_{ab} by an interger λ so that $j_{0ab} \rightarrow \lambda j_{0ab}$ and $j_{ab} \rightarrow \lambda j_{ab}$, we have that the total action goes to $S_{\text{tot}} \rightarrow \lambda S_{\text{tot}}$. We recall also that $q_n^{ab} \rightarrow \lambda^2 q_n^{ab}$. In the large λ limit, the sums over spins in expression (455) can be approximated with integrals over continuous spin variables¹⁸:

$$\sum_j \mu \int d^5 g^\pm q_n^{ab} e^{\lambda S_{\text{tot}}} = \int d^{10} j d^5 g^\pm \mu q_n^{ab} e^{\lambda S_{\text{tot}}} + O(\lambda^{-N}) \quad \forall N > 0. \quad (457)$$

¹⁸The remainder, i.e. the difference between the sum and the integral, can be estimated via Euler-Maclaurin summation formula. This approximation does not affect any finite order in the computation of the LQG propagator.

Moreover, notice that the action, the measure and the insertions in (455) are invariant under a $SO(4)$ symmetry that makes an integration $dg^+ dg^-$ redundant. We can factor out one $SO(4)$ volume, e.g. putting $g_1^+ = g_1^- = 1$, so that we end up with an integral over $d^4 g^\pm = \prod_{a=2}^5 dg_a^+ dg_a^-$.

As a result we can re-write expression (455) in the following integral form

$$G_{nm}^{abcd} = \lambda^4 \left(\frac{\int d^{10} j d^4 g^\pm \mu q_n^{ab} q_m^{cd} e^{\lambda S_{\text{tot}}}}{\int d^{10} j d^4 g^\pm \mu e^{\lambda S_{\text{tot}}}} - \frac{\int d^{10} j d^4 g^\pm \mu q_n^{ab} e^{\lambda S_{\text{tot}}}}{\int d^{10} j d^4 g^\pm \mu e^{\lambda S_{\text{tot}}}} \frac{\int d^{10} j d^4 g^\pm \mu q_m^{cd} e^{\lambda S_{\text{tot}}}}{\int d^{10} j d^4 g^\pm \mu e^{\lambda S_{\text{tot}}}} \right). \quad (458)$$

To this expression we can apply the standard result stated in the following section.

10.8 Asymptotic formula for connected two-point functions

Consider the integral

$$F(\lambda) = \int dx f(x) e^{\lambda S(x)} \quad (459)$$

over a region of \mathbb{R}^d , with $S(x)$ and $f(x)$ smooth complex-valued functions such that the real part of S is negative or vanishing, $\text{Re}S \leq 0$. Assume also that the stationary points x_0 of S are isolated so that the Hessian at a stationary point $H = S''(x_0)$ is non-singular, $\det H \neq 0$. Under these hypothesis an asymptotic expansion of the integral F for large λ is available: it is an extension of the standard stationary phase approximation that takes into account the fact that the action S is complex [?]. A key role is played by *critical points*, i.e. stationary points x_0 for which the real part of the action vanishes, $\text{Re}S(x_0) = 0$. Here we assume that there is a unique critical point. Then the asymptotic expansion of $F(\lambda)$ for large λ is given by

$$F(\lambda) = \left(\frac{2\pi}{\lambda} \right)^{\frac{d}{2}} \frac{e^{i \text{Ind} H} e^{\lambda S(x_0)}}{\sqrt{|\det H|}} \left(f(x_0) + \frac{1}{\lambda} \left(\frac{1}{2} f''_{ij}(x_0) (H^{-1})^{ij} + D \right) + \mathcal{O}\left(\frac{1}{\lambda^2}\right) \right) \quad (460)$$

with $f''_{ij} = \partial^2 f / \partial x^i \partial x^j$ and $\text{Ind} H$ is the index¹⁹ of the Hessian. The term D does not contain second derivatives of f , it contains only²⁰ $f(x_0)$ and $f'_i(x_0)$. Now we consider three smooth complex-valued functions g , h and μ . A connected 2-point function relative to the insertions g and h and w.r.t. the measure μ is defined as

$$G = \frac{\int dx \mu(x) g(x) h(x) e^{\lambda S(x)}}{\int dx \mu(x) e^{\lambda S(x)}} - \frac{\int dx \mu(x) g(x) e^{\lambda S(x)}}{\int dx \mu(x) e^{\lambda S(x)}} \frac{\int dx \mu(x) h(x) e^{\lambda S(x)}}{\int dx \mu(x) e^{\lambda S(x)}}. \quad (462)$$

Using (460) it is straightforward to show that the (leading order) asymptotic formula for the connected 2-point function is simply

$$G = \frac{1}{\lambda} (H^{-1})^{ij} g'_i(x_0) h'_j(x_0) + \mathcal{O}\left(\frac{1}{\lambda^2}\right). \quad (463)$$

¹⁹The index is defined in terms of the eigenvalues of h_k of the Hessian as $\text{Ind} H = \frac{1}{2} \sum_k \arg(h_k)$ with $-\frac{\pi}{2} \leq \arg(h_k) \leq \frac{\pi}{2}$.

²⁰More explicitly, the term D is given by

$$D = f'_i(x_0) R'''_{jkl}(x_0) (H^{-1})^{ij} (H^{-1})^{kl} + \frac{5}{2} f(x_0) R'''_{ijk}(x_0) R'''_{mnl}(x_0) (H^{-1})^{im} (H^{-1})^{jn} (H^{-1})^{kl} \quad (461)$$

with $R(x) = S(x) - S(x_0) - \frac{1}{2} H_{ij}(x_0) (x - x_0)^i (x - x_0)^j$.

Notice that both the measure function μ and the disconnected term D do not appear in the leading term of the connected 2-point function; nevertheless they are present in the higher orders (loop contributions). The reason we are considering the quantity G , built from integrals of the type (459), is that the LQG propagator has exactly this form. Specifically, in sections 10.9 we determine the critical points of the total action, in 10.10 we compute the Hessian of the total action and the derivative of the insertions evaluated at the critical points, and in 10.12 we state our result.

10.9 Critical points of the total action

The real part of the total action is given by

$$\operatorname{Re}S_{\text{tot}} = - \sum_{ab,cd} (\operatorname{Re} \alpha)^{(ab)(cd)} \frac{j_{ab} - j_{0ab}}{\sqrt{j_{0ab}}} \frac{j_{cd} - j_{0cd}}{\sqrt{j_{0cd}}} + \quad (464)$$

$$+ \sum_{ab} j_{ab}^- \log \frac{1 - (R_a^- n_{ab}) \cdot (R_b^- n_{ba})}{2} + \sum_{ab} j_{ab}^+ \log \frac{1 - (R_a^+ n_{ab}) \cdot (R_b^+ n_{ba})}{2} . \quad (465)$$

Therefore, having assumed that the matrix α in the boundary state has positive definite real part, we have that the real part of the total action is negative or vanishing, $\operatorname{Re}S_{\text{tot}} \leq 0$. In particular the total action vanishes for the configuration of spins j_{ab} and group elements g_a^\pm satisfying

$$j_{ab} = j_{0ab} , \quad (466)$$

$$g_a^\pm \text{ such that } R_a^\pm n_{ab}(j) = -R_b^\pm n_{ba}(j) . \quad (467)$$

Now we study the stationary points of the total action and show that there is a unique stationary point for which $\operatorname{Re}S_{\text{tot}}$ vanishes.

The analysis of stationary points of the action $S^+ + S^-$ with respect to variations of the group variables g_a^\pm has been performed in full detail by Barrett et al. in [147]. Here we briefly summarize their result as they apply unchanged to the total action. We invite the reader to look at the original reference for a detailed derivation and a geometrical interpretation of the result.

The requirement that the variation of the total action with respect to the group variables g_a^\pm vanishes, $\delta_g S_{\text{tot}} = 0$, leads to the two sets of equations (respectively for the real and the imaginary part of the variation):

$$\sum_{b \neq a} j_{ab}^\pm \frac{R_a^\pm n_{ab} - R_b^\pm n_{ba}}{1 - (R_a^\pm n_{ab}) \cdot (R_b^\pm n_{ba})} = 0 \quad , \quad \sum_{b \neq a} j_{ab}^\pm \frac{(R_a^\pm n_{ab}) \times (R_b^\pm n_{ba})}{1 - (R_a^\pm n_{ab}) \cdot (R_b^\pm n_{ba})} = 0 . \quad (468)$$

When evaluated at the maximum point (467), these two sets of equations are trivially satisfied. Infact the normals \vec{n}_{ab} in the boundary state are chosen to satisfy the closure condition (406) at each node. Therefore the critical points in the group variables are given by all the solutions of equation (467).

For normals \vec{n}_{ab} which define non-degenerate tetrahedra and satisfy the continuity condition (410), the equation $R_a n_{ab} = -R_b n_{ba}$ admits two distinct sets of solutions, up to global rotations. These two sets are related by parity. The two sets can be lifted to $SU(2)$. We call them \bar{g}_a^+ and \bar{g}_a^- . Out of them, four classes of solutions for the couple (g_a^+, g_a^-) can be found. They are given by

$$(\bar{g}_a^+, \bar{g}_a^-), (\bar{g}_a^-, \bar{g}_a^+), (\bar{g}_a^+, \bar{g}_a^+), (\bar{g}_a^-, \bar{g}_a^-) . \quad (469)$$

The geometrical interpretation is the following. The couples $(j_{ab}\vec{n}_{ab}, j_{ab}\vec{n}_{ab})$ are interpreted as the selfdual and anti-selfdual parts (with respect to some “time” direction, e.g. $(0, 0, 0, 1)$) of area bivectors associated to triangles in 4-dimensions; since these bivectors are diagonal, they live in the 3-dimensional subspace of \mathbb{R}^4 orthogonal to the chosen “time” direction. Because of the closure condition (406), for a fixed n the four bivectors $(j_{na}\vec{n}_{na}, j_{na}\vec{n}_{na})$ define an embedding of a tetrahedron in \mathbb{R}^4 . The two group elements g_a^+ and g_a^- of the action (437) define an $\text{SO}(4)$ element which rotates the “initial” tetrahedron. The system (467) is a gluing condition between tetrahedra. The first two classes of solutions in (469) glue five tetrahedra into two Euclidean non-degenerate 4-simplices related by a reflection, while the second two classes correspond to degenerate configurations with the 4-simplex living in the three-dimensional plane orthogonal to the chosen “time” direction.

The evaluation of the action $S(j_{ab}, g_a^+, g_a^-) = S^+(j_{ab}, g_a^+) + S^-(j_{ab}, g_a^-)$ on the four classes of critical points gives

$$S(j_{ab}, \bar{g}_a^+, \bar{g}_a^-) = + S_{\text{Regge}}(j_{ab}), \quad (470)$$

$$S(j_{ab}, \bar{g}_a^-, \bar{g}_a^+) = - S_{\text{Regge}}(j_{ab}), \quad (471)$$

$$S(j_{ab}, \bar{g}_a^+, \bar{g}_a^+) = + \gamma^{-1} S_{\text{Regge}}(j_{ab}), \quad (472)$$

$$S(j_{ab}, \bar{g}_a^-, \bar{g}_a^-) = - \gamma^{-1} S_{\text{Regge}}(j_{ab}), \quad (473)$$

where $S_{\text{Regge}}(j_{ab})$ is Regge action for a single 4-simplex with triangle areas $A_{ab} = \gamma j_{ab}$ and dihedral angles $\phi_{ab}(j)$ written in terms of the areas

$$S_{\text{Regge}}(j_{ab}) = \sum_{ab} \gamma j_{ab} \phi_{ab}(j). \quad (474)$$

Now we focus on stationarity of the total action with respect to variations of the spin labels j_{ab} . We fix the group elements (g_a^+, g_a^-) to belong to one of the four classes (469). For the first class we find

$$0 = \left. \frac{\partial S_{\text{tot}}}{\partial j_{ab}} \right|_{(\bar{g}_a^+, \bar{g}_a^-)} = - \sum_{cd} \frac{\alpha^{(ab)(cd)}(j_{cd} - j_{0cd})}{\sqrt{j_{0ab}}\sqrt{j_{0cd}}} - i\phi_0^{ab} + i \frac{\partial S_{\text{Regge}}}{\partial j_{ab}}. \quad (475)$$

The quantity $\partial S_{\text{Regge}}/\partial j_{ab}$ is γ times the extrinsic curvature at the triangle f_{ab} of the boundary of a 4-simplex with triangle areas $A_{ab} = \gamma j_{ab}$. As the phase ϕ_0^{ab} in the boundary state is chosen to be exactly γ times the extrinsic curvature, we have that equation (475) vanishes for $j_{ab} = j_{0ab}$. Notice that, besides being a stationary point, this is also a critical point of the total action as stated in (466).

On the other hand, if equation (475) is evaluated on group elements belonging to the classes $(\bar{g}_a^-, \bar{g}_a^+)$, $(\bar{g}_a^-, \bar{g}_a^-)$, $(\bar{g}_a^+, \bar{g}_a^+)$, we have that there is no cancellation of phases and therefore no stationary point with respect to variations of spins. This is the feature of the phase of the boundary state: it selects a classical contribution to the asymptotics of a spin foam model, a fact first noticed by Rovelli for the Barrett-Crane model in [91].

10.10 Hessian of the total action and derivatives of the insertions

Here we compute the Hessian matrix of the total action S_{tot} at the critical point $j_{ab} = j_{0ab}$, $(g_a^+, g_a^-) = (\bar{g}_a^+, \bar{g}_a^-)$. We introduce a local chart of coordinates $(\bar{p}_a^+, \bar{p}_a^-)$ in a neighborhood of the point $(\bar{g}_a^+, \bar{g}_a^-)$ on

$SU(2) \times SU(2)$. The parametrization is defined as follows: we introduce

$$g_a^\pm(p_a^\pm) = h(p_a^\pm) \bar{g}_a^\pm \quad (476)$$

with $h(p_a^\pm) = \sqrt{1 - |\vec{p}_a^\pm|^2} + i\vec{p}_a^\pm \cdot \vec{\sigma}$. The vector \vec{p}_a^\pm is assumed to be in a neighborhood of the origin, which corresponds to the critical point \bar{g}_a^\pm . We introduce also the notation n_a^\pm

$$n_a^\pm = \bar{R}_a^\pm n_a \quad (477)$$

where \bar{R}_a^\pm is the rotation associated to the $SU(2)$ group element \bar{g}_a^\pm . The bivectors $(j_{ab}n_{ab}^+, j_{ab}n_{ab}^-)$ have the geometrical interpretation of area bivectors associated to the triangles of a 4-simplex with faces of area proportional to j_{ab} .

The Hessian matrix is obtained computing second derivatives of the total action with respect to j_{ab} , p_a^+ and p_a^- , and evaluating it at the point $j_{ab} = j_{0ab}$ and $p_a^\pm = 0$. With this definitions we have that the (gauge-fixed) Hessian matrix is a $(10 + 12 + 12) \times (10 + 12 + 12)$ matrix (as it does not contain derivatives w.r.t. g_1^\pm) and has the following structure:

$$S''_{\text{tot}} = \begin{pmatrix} \frac{\partial^2 S_{\text{tot}}}{\partial j \partial j} & 0_{10 \times 12} & 0_{10 \times 12} \\ 0_{12 \times 10} & \frac{\partial^2 S_{\text{tot}}}{\partial p^+ \partial p^+} & 0_{12 \times 12} \\ 0_{12 \times 10} & 0_{12 \times 12} & \frac{\partial^2 S_{\text{tot}}}{\partial p^- \partial p^-} \end{pmatrix} \quad (478)$$

as

$$\left. \frac{\partial^2 S_{\text{tot}}}{\partial p_a^{i\pm} \partial p_b^{j\mp}} \right|_{\vec{p}=0} = 0, \quad \left. \frac{\partial^2 S_{\text{tot}}}{\partial j_{ab} \partial p_c^{j\mp}} \right|_{\vec{p}=0} = 0. \quad (479)$$

For the non-vanishing entries we find

$$Q_{(ab)(cd)} = \left. \frac{\partial^2 S_{\text{tot}}}{\partial j_{ab} \partial j_{cd}} \right|_{\vec{p}=0} = -\frac{\alpha^{(ab)(cd)}}{\sqrt{j_{0ab}} \sqrt{j_{0cd}}} + (S''_{\text{Regge}})_{(ab)(cd)}, \quad (480)$$

$$H_{(ai)(bj)}^\pm = \left. \frac{\partial^2 S_{\text{tot}}}{\partial p_a^{i\pm} \partial p_b^{j\pm}} \right|_{\vec{p}=0} = 2i\gamma^\pm j_{0ab} (\delta^{ij} - n_{ab}^{i\pm} n_{ab}^{j\pm} + i\epsilon^{ijk} n_{ab}^{k\pm}), \quad (481)$$

$$H_{(ai)(aj)}^\pm = \left. \frac{\partial^2 S_{\text{tot}}}{\partial p_a^{i\pm} \partial p_a^{j\pm}} \right|_{\vec{p}=0} = -2i\gamma^\pm \sum_{b \neq a} j_{0ab} (\delta^{ij} - n_{ab}^{i\pm} n_{ab}^{j\pm}), \quad (482)$$

where we have defined the 10×10 matrix of second derivatives of the Regge action

$$(S''_{\text{Regge}})_{(ab)(cd)} = \left. \frac{\partial^2 S_{\text{Regge}}}{\partial j_{ab} \partial j_{cd}} \right|_{j_{0ab}}. \quad (483)$$

We report also the first derivatives of the insertion $q_n^{ab}(g^+, g^-)$ evaluated at the critical point:

$$\left. \frac{\partial q_n^{ab}}{\partial \vec{p}_a^\pm} \right|_{\vec{p}=0} = i\gamma^2 \gamma^\pm j_{0na} j_{0nb} (\vec{n}_{nb}^\pm - \vec{n}_{na} \cdot \vec{n}_{nb} \vec{n}_{na}^\pm + i \vec{n}_{na}^\pm \times \vec{n}_{nb}^\pm), \quad (484)$$

$$\left. \frac{\partial q_n^{ab}}{\partial \vec{p}_n^\pm} \right|_{\vec{p}=0} = -i\gamma^2 \gamma^\pm j_{0na} j_{0nb} (\vec{n}_{na}^\pm + \vec{n}_{nb}^\pm) (1 - \vec{n}_{na} \cdot \vec{n}_{nb}), \quad (485)$$

$$\left. \frac{\partial q_n^{ab}}{\partial j_{cd}} \right|_{\vec{p}=0} = \gamma^2 \frac{\partial (j_{na} \vec{n}_{na} \cdot j_{nb} \vec{n}_{nb})}{\partial j_{cd}} \Big|_{j_{0ab}}. \quad (486)$$

We recall that in all these expressions the normals \vec{n}_{ab} are functions of j_{ab} as explained in section 10.1. These expressions will be used in section 10.12 to compute the leading order of the LQG propagator.

10.11 Expectation value of metric operators

Before focusing on the LQG propagator, i.e. on the two-point function, here we briefly discuss the one-point function $\langle E_n^a \cdot E_n^b \rangle$. Its meaning is the dynamical expectation value of the metric operator. The fact that it is non-vanishing provides the background for the propagator. Using the technique developed in the previous sections we can compute it at the leading order in the large spin expansion. We use the integral formula for the metric operator (438)-(439) and the stationary phase analysis of section 10.6 and find that the expectation value of the metric operator is simply given by the evaluation of the insertion $q_n^{ab}(g^+, g^-)$ at the critical point

$$\langle E_n^a \cdot E_n^b \rangle = q_n^{ab}(g^+, g^-) \Big|_{j_{0ab}, \vec{g}^+, \vec{g}^-} + \mathcal{O}(j_0). \quad (487)$$

For the diagonal components $a = b$ we have that the insertion is simply given by $q_n^{aa} = (\gamma j_{na})^2$ so that its evaluation at the critical point gives the area square of the triangle f_{na} . For the off-diagonal components we have that $q_n^{ab} = A_n^a \cdot A_n^b$ where A_n^{ai} is given in equation (449). Its evaluation at the critical point can be easily found using equation (467) in expression (449). We find

$$\vec{A}^{na} \Big|_{j_{0ab}, \vec{g}^+, \vec{g}^-} = \vec{A}^{na+} \Big|_{j_{0ab}, \vec{g}^+} + \vec{A}^{na-} \Big|_{j_{0ab}, \vec{g}^-} = \gamma j_{0na}^+ \vec{n}_{na}(j_0) + \gamma j_{0na}^- \vec{n}_{na}(j_0) = \gamma j_{0na} \vec{n}_{na}(j_0) \quad (488)$$

so that \vec{A}^{na} at the critical point evaluates to the classical value $\vec{E}_{ncl}^a = \gamma j_{0na} \vec{n}_{na}(j_0)$, the normal to the face a of the tetrahedron n (normalized to the area of the face). It is the classical counterpart of the operator $(E_n^a)^i$. Therefore we have that at the leading order the expectation value of the off-diagonal components is given by the dihedral angle between two faces of a tetrahedron

$$\begin{aligned} \langle E_n^a \cdot E_n^b \rangle &= \vec{E}_{ncl}^a \cdot \vec{E}_{ncl}^b + \mathcal{O}(j_0) \\ &= \gamma^2 j_{0na} j_{0nb} \vec{n}_{na}(j_0) \cdot \vec{n}_{nb}(j_0) + \mathcal{O}(j_0). \end{aligned} \quad (489)$$

They have the expected geometrical meaning. We observe that the same quantities computed with the Barrett-Crane spinfoam dynamics do not show the right behavior when the off-diagonal components of the metric operator are considered.

Using the same technique we can evaluate the leading order of the two-point function. We have that

$$\langle E_n^a \cdot E_n^b E_m^c \cdot E_m^d \rangle = E_{n_{\text{cl}}}^a \cdot E_{n_{\text{cl}}}^b E_{m_{\text{cl}}}^c \cdot E_{m_{\text{cl}}}^d + \mathcal{O}(j_0^3). \quad (490)$$

The quantity we are specifically interested in in this chapter is the *connected* two-point function. It is of order $\mathcal{O}(j_0^3)$, therefore it requires the next-to-leading orders in equations (489) and (490). Such orders depend on the measure $\mu(j)$. However in the computation of the connected part, these contributions cancel. The technique we use in next section for the calculation of the connected two-point function is the one introduced in section (10.8) and captures directly the leading order.

10.12 LQG propagator: the leading order

We have defined the LQG propagator as the connected two-point function $G_{nm}^{abcd} = \langle E_n^a \cdot E_n^b E_m^c \cdot E_m^d \rangle - \langle E_n^a \cdot E_n^b \rangle \langle E_m^c \cdot E_m^d \rangle$. Using the integral formula (438)-(439) and the result (463) for the asymptotics of connected two-point functions, we can compute the LQG propagator in terms of (the inverse of) the Hessian of the total action and of the derivative of the metric operator insertions at the critical point. These two ingredients are computed in section 10.10. Using them, we find that the LQG propagator is given by

$$\begin{aligned} G_{nm}^{abcd}(\alpha) &= \sum_{p,q,r,s} Q_{(pq)(rs)}^{-1} \frac{\partial q_n^{ab}}{\partial j_{pq}} \frac{\partial q_m^{cd}}{\partial j_{rs}} + \\ &+ \sum_{r,s=2}^5 \sum_{i,k=1}^3 \left((H^+)_{(ri)(sk)}^{-1} \frac{\partial q_n^{ab}}{\partial p_r^{i+}} \frac{\partial q_m^{cd}}{\partial p_s^{k+}} + (H^-)_{(ri)(sk)}^{-1} \frac{\partial q_n^{ab}}{\partial p_r^{i-}} \frac{\partial q_m^{cd}}{\partial p_s^{k-}} \right) \\ &+ \mathcal{O}(j_0^2) \end{aligned} \quad (491)$$

where all the terms appearing in this expression are defined in section 10.10. From this expression we can extract the dependence on the boundary spin j_0 and on the Immirzi parameter γ . We notice that the combinations

$$R_{nm}^{abcd} = \frac{1}{\gamma^3 j_0^3} \sum_{p<q,r<s} Q_{(pq)(rs)}^{-1} \frac{\partial q_n^{ab}}{\partial j_{pq}} \frac{\partial q_m^{cd}}{\partial j_{rs}}, \quad (492)$$

$$X_{nm}^{abcd} = \frac{1}{2\gamma^4 j_0^3} \sum_{r,s=2}^5 \sum_{i,k=1}^3 \left(\frac{1}{\gamma^+} (H^+)_{(ri)(sk)}^{-1} \frac{\partial q_n^{ab}}{\partial p_r^{i+}} \frac{\partial q_m^{cd}}{\partial p_s^{k+}} + \frac{1}{\gamma^-} (H^-)_{(ri)(sk)}^{-1} \frac{\partial q_n^{ab}}{\partial p_r^{i-}} \frac{\partial q_m^{cd}}{\partial p_s^{k-}} \right), \quad (493)$$

$$Y_{nm}^{abcd} = \frac{1}{2\gamma^4 j_0^3} \sum_{r,s=2}^5 \sum_{i,k=1}^3 \left(\frac{1}{\gamma^+} (H^+)_{(ri)(sk)}^{-1} \frac{\partial q_n^{ab}}{\partial p_r^{i+}} \frac{\partial q_m^{cd}}{\partial p_s^{k+}} - \frac{1}{\gamma^-} (H^-)_{(ri)(sk)}^{-1} \frac{\partial q_n^{ab}}{\partial p_r^{i-}} \frac{\partial q_m^{cd}}{\partial p_s^{k-}} \right), \quad (494)$$

are in fact independent from j_0 and from γ . In terms of these quantities we have that the LQG propagator has the following structure

$$G_{nm}^{abcd}(\alpha) = (\gamma j_0)^3 (R_{nm}^{abcd}(\alpha) + \gamma X_{nm}^{abcd} + \gamma^2 Y_{nm}^{abcd}) + \mathcal{O}(j_0^2) \quad (495)$$

where the dependence on γ and on j_0 has been made explicit now. The matrices R_{nm}^{abcd} , X_{nm}^{abcd} and Y_{nm}^{abcd} can be evaluated algebraically. Only the matrix R_{nm}^{abcd} depends on the three parameters $\alpha_0, \alpha_1, \alpha_2$ appearing on the boundary state. We find that

$$R_{nm}^{abcd} = \begin{pmatrix} \begin{pmatrix} c_1 & c_3 & c_3 \\ c_3 & c_2 & c_4 \\ c_3 & c_4 & c_2 \end{pmatrix} & \begin{pmatrix} c_3 & c_5 & c_6 \\ c_5 & c_3 & c_6 \\ c_6 & c_6 & c_4 \end{pmatrix} & \begin{pmatrix} c_3 & c_6 & c_5 \\ c_6 & c_4 & c_6 \\ c_5 & c_6 & c_3 \end{pmatrix} \\ \begin{pmatrix} c_3 & c_5 & c_6 \\ c_5 & c_3 & c_6 \\ c_6 & c_6 & c_4 \end{pmatrix} & \begin{pmatrix} c_2 & c_3 & c_4 \\ c_3 & c_1 & c_3 \\ c_4 & c_3 & c_2 \end{pmatrix} & \begin{pmatrix} c_4 & c_6 & c_6 \\ c_6 & c_3 & c_5 \\ c_6 & c_5 & c_3 \end{pmatrix} \\ \begin{pmatrix} c_3 & c_6 & c_5 \\ c_6 & c_4 & c_6 \\ c_5 & c_6 & c_3 \end{pmatrix} & \begin{pmatrix} c_4 & c_6 & c_6 \\ c_6 & c_3 & c_5 \\ c_6 & c_5 & c_3 \end{pmatrix} & \begin{pmatrix} c_2 & c_4 & c_3 \\ c_4 & c_2 & c_3 \\ c_3 & c_3 & c_1 \end{pmatrix} \end{pmatrix} \quad (496)$$

where

$$c_1 = 4\beta_1, \quad c_2 = 4\beta_2, \quad c_3 = -\frac{2}{3}(2\beta_0 - 3\beta_1 + 3\beta_2), \quad (497)$$

$$c_4 = \frac{1}{3}(8\beta_0 - 12\beta_1), \quad c_5 = \frac{1}{9}(49\beta_0 - 93\beta_1 + 48\beta_2), \quad c_6 = -\frac{1}{9}(23\beta_0 - 42\beta_1 + 15\beta_2), \quad (498)$$

and²¹

$$\beta_0 = \frac{1}{10} \left(-\frac{1}{\alpha_0 + 6\alpha_1 + 3\alpha_2} + \frac{32}{-8\alpha_0 - 8\alpha_1 + 16\alpha_2 + i\sqrt{15}} - \frac{5}{\alpha_0 - 2\alpha_1 + \alpha_2 + i\sqrt{15}} \right), \quad (501)$$

$$\beta_1 = \frac{1}{30} \left(-\frac{3}{\alpha_0 + 6\alpha_1 + 3\alpha_2} + \frac{16}{-8\alpha_0 - 8\alpha_1 + 16\alpha_2 + i\sqrt{15}} + \frac{5}{\alpha_0 - 2\alpha_1 + \alpha_2 + i\sqrt{15}} \right), \quad (502)$$

$$\beta_2 = \frac{1}{30} \left(-\frac{3}{\alpha_0 + 6\alpha_1 + 3\alpha_2} - \frac{64}{-8\alpha_0 - 8\alpha_1 + 16\alpha_2 + i\sqrt{15}} - \frac{5}{\alpha_0 - 2\alpha_1 + \alpha_2 + i\sqrt{15}} \right). \quad (503)$$

The matrices X_{nm}^{abcd} and Y_{nm}^{abcd} turn out to be proportional

$$X_{nm}^{abcd} = \frac{7}{36} Z_{nm}^{abcd}, \quad Y_{nm}^{abcd} = -i \frac{\sqrt{15}}{36} Z_{nm}^{abcd}, \quad (504)$$

²¹We notice that the inverse of the matrix $Q_{(ab)(cd)}$ can be written in terms of the parameters β_k using the formalism (421) introduced in section 10.1,

$$(Q^{-1})^{(ab)(cd)} = \sum_{k=0}^2 j_0 \beta_k P_k^{(ab)(cd)}. \quad (499)$$

The matrix $Q_{(ab)(cd)}$ is defined in equation (480) and is given by

$$Q^{(ab)(cd)} = \frac{1}{j_0} \sum_{k=0}^2 (ih_k - \alpha_k) P_k^{(ab)(cd)}, \quad (500)$$

with $h_0 = -\frac{9}{4}\sqrt{\frac{3}{5}}$, $h_1 = \frac{7}{8}\sqrt{\frac{3}{5}}$, $h_2 = -\sqrt{\frac{3}{5}}$.

with the matrix Z_{nm}^{abcd} given by

$$Z_{nm}^{abcd} = \begin{pmatrix} \begin{pmatrix} 0 & 0 & 0 \\ 0 & 0 & 0 \\ 0 & 0 & 0 \end{pmatrix} & \begin{pmatrix} 0 & -1 & e^{i\frac{\pi}{3}} \\ -1 & 0 & e^{-i\frac{\pi}{3}} \\ e^{i\frac{\pi}{3}} & e^{-i\frac{\pi}{3}} & 0 \end{pmatrix} & \begin{pmatrix} 0 & e^{-i\frac{\pi}{3}} & -1 \\ e^{-i\frac{\pi}{3}} & 0 & e^{i\frac{\pi}{3}} \\ -1 & e^{i\frac{\pi}{3}} & 0 \end{pmatrix} \\ \begin{pmatrix} 0 & -1 & e^{i\frac{\pi}{3}} \\ -1 & 0 & e^{-i\frac{\pi}{3}} \\ e^{i\frac{\pi}{3}} & e^{-i\frac{\pi}{3}} & 0 \end{pmatrix} & \begin{pmatrix} 0 & 0 & 0 \\ 0 & 0 & 0 \\ 0 & 0 & 0 \end{pmatrix} & \begin{pmatrix} 0 & e^{i\frac{\pi}{3}} & e^{-i\frac{\pi}{3}} \\ e^{i\frac{\pi}{3}} & 0 & -1 \\ e^{-i\frac{\pi}{3}} & -1 & 0 \end{pmatrix} \\ \begin{pmatrix} 0 & e^{-i\frac{\pi}{3}} & -1 \\ e^{-i\frac{\pi}{3}} & 0 & e^{i\frac{\pi}{3}} \\ -1 & e^{i\frac{\pi}{3}} & 0 \end{pmatrix} & \begin{pmatrix} 0 & e^{i\frac{\pi}{3}} & e^{-i\frac{\pi}{3}} \\ e^{i\frac{\pi}{3}} & 0 & -1 \\ e^{-i\frac{\pi}{3}} & -1 & 0 \end{pmatrix} & \begin{pmatrix} 0 & 0 & 0 \\ 0 & 0 & 0 \\ 0 & 0 & 0 \end{pmatrix} \end{pmatrix}. \quad (505)$$

This is the main result of the chapter, the scaling and the tensorial structure of metric correlations in LQG. In the following we collect some remarks on this result:

- The LQG propagator scales as j_0^3 , as expected for correlations of objects with dimensions of area square, $E_n^a \cdot E_n^b \sim (\gamma j_0)^2$.
- The off-diagonal components are not suppressed as happened for the Barrett-Crane model [79, 94] and have the same scaling as the diagonal ones.
- The contribution R_{nm}^{abcd} in (495) matches exactly with the matrix of correlations of areas and angles computed in perturbative quantum Regge calculus with a boundary state as done in [135].
- On the other hand, the ‘ γ -terms’ in (495), $\gamma X_{nm}^{abcd} + \gamma^2 Y_{nm}^{abcd}$, are new and proper of the spin foam model. They come from $SU(2) \times SU(2)$ “group” fluctuations. They don’t contribute to area-area correlations, nor to area-angle correlations. On the other hand, their contribution to angle-angle correlations is non-trivial.
- In the limit $\gamma \rightarrow 0$ and $j_0 \rightarrow \infty$ with $\gamma j_0 = \text{const} = A_0$, only the Regge contribution survives. It is interesting to notice that the same limit was considered in [?] in the context of loop quantum cosmology.
- The ‘ γ -terms’ have an interesting feature that we now describe. Let us focus on the tensorial components $G_4 = G_{12}^{(34)(45)}$ and $G_5 = G_{12}^{(35)(45)}$. They are related by a permutation of the vertices 4 and 5, keeping the other three vertices fixed. The ‘Regge-term’ is invariant under this permutation, $R_{12}^{(34)(45)} = R_{12}^{(35)(45)}$. On the other hand the ‘ γ -terms’ are not. In particular we have that

$$\gamma X_{12}^{(35)(45)} + \gamma^2 Y_{12}^{(35)(45)} = e^{i\frac{2\pi}{3}} \left(\gamma X_{12}^{(34)(45)} + \gamma^2 Y_{12}^{(34)(45)} \right). \quad (506)$$

It would be interesting to identify the origin of the phase $\frac{2\pi}{3}$. We notice that the permutation of the vertex 4 with the vertex 5 of the boundary spin-network corresponds to a parity transformation of the four-simplex. In this sense the ‘ γ -terms’ are parity violating.

In next section we investigate the relation of the result found with the graviton propagator computed in perturbative quantum field theory.

10.13 Comparison with perturbative quantum gravity

The motivation for studying the LQG propagator comes from the fact that it probes a regime of the theory where predictions can be compared to the ones obtained perturbatively in a quantum field theory of gravitons on flat space [132, 133, 134]. Therefore it is interesting to investigate this relation already at the preliminary level of a single spin foam vertex studied in this chapter. In this section we investigate this relation within the setting discussed in [79, 94, 95].

In perturbative quantum gravity²², the graviton propagator in the harmonic gauge is given by

$$\langle h_{\mu\nu}(x)h_{\rho\sigma}(y) \rangle = \frac{-1}{2|x-y|^2}(\delta_{\mu\rho}\delta_{\nu\sigma} + \delta_{\mu\sigma}\delta_{\nu\rho} - \delta_{\mu\nu}\delta_{\rho\sigma}). \quad (507)$$

Correlations of geometrical quantities can be computed perturbatively in terms of the graviton propagator. For instance the angle at a point x_n between two intersecting surfaces f_{na} and f_{nb} is given by²³

$$q_n^{ab} = g_{\mu\nu}(x_n)g_{\rho\sigma}(x_n)B_{na}^{\mu\rho}(x_n)B_{nb}^{\nu\sigma}(x_n) \quad (508)$$

where $B^{\mu\nu}$ is the bivector associated to the surface²⁴. As a result the angle fluctuation can be written in terms of the graviton field

$$\delta q_n^{ab} = h_{\mu\nu}(x_n) (T_n^{ab})^{\mu\nu}, \quad (510)$$

where we have defined the tensor $(T_n^{ab})^{\mu\nu} = 2\delta_{\rho\sigma}B_{na}^{\mu\rho}(x_n)B_{nb}^{\nu\sigma}(x_n)$. The angle correlation $(G_{nm}^{abcd})_{\text{qft}}$ is simply given by

$$(G_{nm}^{abcd})_{\text{qft}} = \langle h_{\mu\nu}(x_n)h_{\rho\sigma}(x_m) \rangle (T_n^{ab})^{\mu\nu} (T_m^{cd})^{\rho\sigma}. \quad (511)$$

In particular, this quantity can be computed for couples of surfaces identified by triangles of area A_0 living on the boundary of a regular Euclidean 4-simplex. This quantity has been computed in [94] and we report it here for reference,

$$(G_{nm}^{abcd})_{\text{qft}} = \frac{-A_0^3}{18\sqrt{3} \times 512} \left(\begin{array}{ccc} \left(\begin{array}{ccc} -16 & 6 & 6 \\ 6 & -28 & 16 \\ 6 & 16 & -28 \end{array} \right) & \left(\begin{array}{ccc} 6 & 4 & -7 \\ 4 & 6 & -7 \\ -7 & -7 & 16 \end{array} \right) & \left(\begin{array}{ccc} 6 & -7 & 4 \\ -7 & 16 & -7 \\ 4 & -7 & 6 \end{array} \right) \\ \left(\begin{array}{ccc} 6 & 4 & -7 \\ 4 & 6 & -7 \\ -7 & -7 & 16 \end{array} \right) & \left(\begin{array}{ccc} -28 & 6 & 16 \\ 6 & -16 & 6 \\ 16 & 6 & -28 \end{array} \right) & \left(\begin{array}{ccc} 16 & -7 & -7 \\ -7 & 6 & 4 \\ -7 & 4 & 6 \end{array} \right) \\ \left(\begin{array}{ccc} 6 & -7 & 4 \\ -7 & 16 & -7 \\ 4 & -7 & 6 \end{array} \right) & \left(\begin{array}{ccc} 16 & -7 & -7 \\ -7 & 6 & 4 \\ -7 & 4 & 6 \end{array} \right) & \left(\begin{array}{ccc} -28 & 16 & 6 \\ 16 & -28 & 6 \\ 6 & 6 & -16 \end{array} \right) \end{array} \right)$$

The question we want to answer here is if the quantity $(G_{nm}^{abcd})_{\text{qft}}$ and the leading order of the LQG propagator given by equation (495) can match. As we can identify γj_0 with the area A_0 , we have that the

²²Here we consider the Euclidean case.

²³We thank E. Alesci for a discussion on this point.

²⁴To be more specific, we consider local coordinates (σ^1, σ^2) for a surface t and call $t^\mu(\sigma)$ its embedding in the $4d$ manifold. The bivector $B_t^{\mu\nu}(x)$ is defined as

$$B_t^{\mu\nu}(x) = \frac{\partial t^\mu}{\partial \sigma^\alpha} \frac{\partial t^\nu}{\partial \sigma^\beta} \varepsilon^{\alpha\beta}. \quad (509)$$

two have the same scaling. The non-trivial part of the matching is the tensorial structure. Despite the fact that we have 9×9 tensorial components, only six of them are independent as the others are related by symmetries of the configuration we are considering. On the other hand the semiclassical boundary state $|\Psi_0\rangle$ we used in the LQG calculation has only three free parameters, $\alpha_0, \alpha_1, \alpha_2$. Therefore we can ask if there is a choice of these 3 parameters such that we can satisfy the 6 independent equations given by the matching condition

$$\left(G_{nm}^{abcd}(\alpha)\right)_{\text{lqg}} = \left(G_{nm}^{abcd}\right)_{\text{qft}} . \quad (512)$$

We find that a solution in terms of the parameters α_k can be found only in the limit of vanishing Immirzi parameter, keeping constant the product $\gamma j_0 = A_0$. In this limit we find a unique solution for α_k given by

$$\alpha_0 = \frac{1}{100}(495616\sqrt{3} - 45\sqrt{15}i) , \quad (513)$$

$$\alpha_1 = \frac{1}{200}(-299008\sqrt{3} + 35\sqrt{15}i) , \quad (514)$$

$$\alpha_2 = \frac{1}{25}(31744\sqrt{3} - 5\sqrt{15}i) . \quad (515)$$

Therefore the matching condition (512) can be satisfied, at least in the specific limit considered. Having found a non-trivial solution, it is interesting to study the real part of the matrix $\alpha^{(ab)(cd)}$ in order to determine if it is positive definite. Its eigenvalues (with the associated degeneracy) are

$$\lambda_5 = 9216\sqrt{3} , \quad \text{deg} = 5 , \quad (516)$$

$$\lambda_4 = \frac{4608\sqrt{3}}{5} , \quad \text{deg} = 4 , \quad (517)$$

$$\lambda_1 = -\frac{1024\sqrt{3}}{5} , \quad \text{deg} = 1 . \quad (518)$$

We notice that all the eigenvalues are positive except one, λ_1 . The corresponding eigenvector represents conformal rescalings of the boundary state, $j_{0ab} \rightarrow \lambda j_{0ab}$. It would be interesting to determine its origin and to understand how the result depends on the choice of gauge made for the graviton propagator (507).

11 Conclusions and outlook

In this last part we want to discuss and put in the light of a future research some of the original results contained in this thesis. We have presented, unfortunately in a very concise and partial way, the theory of Loop Quantum Gravity and its tentative covariant version given by Spin Foams. We showed preliminary indications in favor of the good semiclassical limit of the new EPRL Spin Foam Model, through the new technique of the propagation of wave-packets and through the asymptotic analysis of the fusion coefficients. The main result in this thesis is the calculation of the graviton propagator in the new model and its comparison with the one of perturbative quantum gravity, but we would like to emphasize the importance of semiclassical states in the calculation, and start our discussion from these.

We have presented a proposal of coherent states for Loop Quantum Gravity and shown that, in a specific limit, they reproduce the states used in the Spin Foam framework. Moreover, these states coincide with Thiemann's complexifier coherent states with the natural choice of complexifier operator, a rather specific choice of heat-kernel time and a clear geometrical interpretation for their $SL(2, \mathbb{C})$ labels. Coherent spin-networks are candidate semiclassical states for full Loop Quantum Gravity. Given a space-time metric (for instance the Minkowski or de Sitter ones), we can identify an intrinsic and extrinsic metric on a spatial slice Σ . Then, we can consider a cellular decomposition of Σ and a graph Γ embedded in Σ and dual to the decomposition. The data captured by the graph is easy to determine: we can smear the Ashtekar-Barbero connection on links of the graph and the electric field on surfaces dual to links. This procedure determines a finite amount of data that can be used as labels for the coherent state. In the case of a simplicial decomposition, we know that this data correspond to a Regge geometry with dislocations. These geometries are studied in [100] and are called 'twisted'.

The remarkable fact that, in the large spin limit, the states we consider reproduce the Livine-Speziale coherent intertwiners on nodes guarantees that they are actually peaked on a classical expectation value of non-commuting geometric operators. For instance, we know that the expectation value of the volume of a region containing a 4-valent node is given by the classical volume of an Euclidean tetrahedron with the normals to faces and the areas as prescribed by the labels of the coherent spin-network. What needs to be better understood is the relation and the origin of the tension with the results of Flori and Thiemann [109, 110] where they claim that only nodes of valency 6 can have a semiclassical behavior.

Coherent spin-networks are coherent in the strict mathematical sense, because they form an overcomplete basis of the kinematical Loop Quantum Gravity Hilbert space \mathcal{K}_Γ on a fixed graph Γ , are eigenstates of suitable annihilation operators, and saturate Heisenberg uncertainty relations. An aspect that needs further investigation regards the redundancy of the labels of these states. The situation is analogous to the one of the labels of the Livine-Speziale coherent intertwiners (four unit-normals) [56] as opposed to the constrained labels of the same states obtained by Conradi and Freidel via geometric quantization of a classical tetrahedron [97, 98]. Similarly, it is possible that the coherent states obtained via geometric quantization of the phase space of LQG associated to a graph actually coincide with a subset of the coherent states introduced here via heat-kernel methods. This would be an instance of Guillemin-Sternberg's 'quantization commutes with reduction' statement. Notice that the situation here is slightly more involved: geometric quantization seemingly knows nothing about heat kernels. Nevertheless, explicit computations by Hall [115] show that amazingly the two approaches give precisely the same coherent states in all the studied cases. This aspect deserves to be understood better.

A surprising property of the states we have discussed is that they bring together so many (apparently

conflicting) ideas that have been proposed in the search for semiclassical states in Loop Quantum Gravity. We consider this convergence to be a measure of the robustness of the theory. In particular, the convergence makes stronger the semiclassical calculations done in Spin Foams.

Now we discuss our calculation of the correlation functions of metric operators in Loop Quantum Gravity. The analysis presented involves two distinct ingredients:

- The first is a setting for defining correlation functions. The setting is the general boundary formalism. It involves a boundary semiclassical state $|\Psi_0\rangle$ which identifies the regime of interest, LQG operators $E_n^a \cdot E_n^b$ which probe the quantum geometry on the boundary, a spin foam model $\langle W |$ which implements the dynamics. The formalism allows to define semiclassical correlation functions in a background-independent context.
- The second ingredient consists in an approximation scheme applied to the quantity defined above. It involves a vertex expansion and a large spin expansion. It allows to estimate the correlation functions explicitly. The explicit result can then be compared to the graviton propagator of perturbative quantum gravity. We focused on the lowest order in the vertex expansion and the leading order in the large spin expansion.

The results found can be summarized as follows:

1. In section 10.1 we have introduced a semiclassical state $|\Psi_0\rangle$ peaked on the intrinsic and the extrinsic geometry of the boundary of a regular Euclidean 4-simplex. The technique used to build this state is the following: (i) we use the coherent intertwiners introduced in [56, 97] to label spin-network nodes as in [147]; (ii) we choose the normals labelling intertwiners so that they are compatible with a simplicial 3-geometry (410). This addresses the issue of discontinuous lengths identified in [155]; (iii) then we take a gaussian superposition over coherent spin-networks in order to peak on extrinsic curvature as in [91, 92]. This state is an improvement of the ansatz used in [79, 94, 95], as it depends only on the three free parameters $\alpha_0, \alpha_1, \alpha_2$.
2. In section 10.3 we have defined expectation values of geometric observables on a semiclassical state. The LQG propagator is defined in equation (429) as a connected correlation function for the product of two metric operators

$$G_{nm}^{abcd} = \langle E_n^a \cdot E_n^b E_m^c \cdot E_m^d \rangle - \langle E_n^a \cdot E_n^b \rangle \langle E_m^c \cdot E_m^d \rangle . \quad (519)$$

This is the object that in principle can be compared to the graviton propagator on flat space: the background is coded in the expectation value of the geometric operators and the propagator measures correlations of fluctuations over this background.

3. In section 10.5 we have introduced a technique which allows to write LQG metric operators as insertions in a $SO(4)$ group integral. It can be interpreted as the covariant version of the LQG operators. The formalism works for arbitrary fixed triangulation. Having an integral formula for expectation values and correlations of metric operators allows to formulate the large spin expansion as a stationary phase approximation. The problem is studied in detail restricting attention to the lowest order in the vertex expansion, i.e. at the single-vertex level.

-
4. The analysis of the large spin asymptotics is performed in section 10.6. The technique used is the one introduced by Barrett et al in [147]. There, the large spin asymptotics of the boundary amplitude of a coherent spin-network is studied and four distinct critical points are found to contribute to the asymptotics. Two of them are related to different orientations of a 4-simplex. The other two come from selfdual configurations. Here, our boundary state is peaked also on extrinsic curvature. The feature of this boundary state is that it selects only one of the critical points, extracting $\exp iS_{\text{Regge}}$ from the asymptotics of the EPRL spin foam vertex. This is a realization of the mechanism first identified by Rovelli in [91] for the Barrett-Crane model.
 6. In 10.11 we compute expectation values of LQG metric operators at leading order and find that they reproduce the intrinsic geometry of the boundary of a regular 4-simplex.
 7. Computing correlations of geometric operators requires going beyond the leading order in the large spin expansion. In section 10.8 we derive a formula for computing directly the *connected* two-point correlation function to the lowest non-trivial order in the large spin expansion. The formula is used in section 10.10.
 8. The result of the calculation, the LQG propagator, is presented in section 10.12. We find that the result is the sum of two terms: a “Regge term” and a “ γ -term”. The Regge term coincides with the correlations of areas and angles computed in Regge calculus with a boundary state [135]. It comes from correlations of fluctuations of the spin variables and depends on the parameters α_k of the boundary state. The “ γ -term” comes from fluctuations of the $SO(4)$ group variables. An explicit algebraic calculation of the tensorial components of the LQG propagator is presented.
 9. The LQG propagator can be compared to the graviton propagator. This is done in section 10.13. We find that the LQG propagator has the correct scaling behaviour. The three parameters α_k appearing in the semiclassical boundary state can be chosen so that the tensorial structure of the LQG propagator matches with the one of the graviton propagator. The matching is obtained in the limit $\gamma \rightarrow 0$ with γj_0 fixed.

Now we would like to put these results in perspective with respect to the problem of extracting the low energy regime of Loop Quantum Gravity and Spin Foams (see in particular [160]).

Deriving the LQG propagator at the level of a single spin foam vertex is certainly only a first step. Within the setting of a vertex expansion, an analysis of the LQG propagator for a finite number of spinfoam vertices is needed. Some of the techniques developed generalize to this more general case. In particular superpositions of coherent spin-networks can be used to build semiclassical states peaked on the intrinsic and the extrinsic curvature of an arbitrary boundary Regge geometry. Moreover, the expression of the LQG metric operator in terms of $SO(4)$ group integrals presented here works for an arbitrary number of spin foam vertices and allows to derive an integral representation of the LQG propagator in the general case, analogous to the one of [146] but with non-trivial insertions. This representation is the appropriate one for the analysis of the large spin asymptotics along the lines discussed for Regge calculus in [83]. The non-trivial question which needs to be answered then is if the semiclassical boundary state is able to enforce semiclassicality in the bulk. Another feature identified which appears to be general is that, besides the expected Regge contribution, correlations of LQG metric operators have a non-Regge contribution which is proper of the spin foam model. It would be interesting to investigate if this contribution propagates when more than a single spin foam vertex is considered.

References

- [1] C. Rovelli, “The century of the incomplete revolution: Searching for general relativistic quantum field theory,” *J. Math. Phys.* **41** (2000) 3776–3800, [arXiv:hep-th/9910131](#).
- [2] J. Alfaro and G. Palma, “Loop Quantum Gravity and Ultra High Energy Cosmic Rays,” *Physical Review D* **67** (2003) 083003, [arXiv:hep-th/0208193](#).
- [3] R. Aloisio, P. Blasi, A. Galante, and A. F. Grillo, “Planck scale kinematics and the Pierre Auger Observatory,” *Lect. Notes Phys.* **669** (2005) 1–30.
- [4] G. Amelino-Camelia, “Introduction to quantum-gravity phenomenology,” *Lect. Notes Phys.* **669** (2005) 59–100, [arXiv:gr-qc/0412136](#).
- [5] G. Amelino-Camelia, J. R. Ellis, N. E. Mavromatos, D. V. Nanopoulos, and S. Sarkar, “Potential Sensitivity of Gamma-Ray Burster Observations to Wave Dispersion in Vacuo,” *Nature* **393** (1998) 763–765, [arXiv:astro-ph/9712103](#).
- [6] G. Amelino-Camelia and T. Piran, “Planck-scale deformation of Lorentz symmetry as a solution to the UHECR and the TeV-gamma paradoxes,” *Phys. Rev.* **D64** (2001) 036005, [arXiv:astro-ph/0008107](#).
- [7] C. Rovelli, *Quantum Gravity*. Cambridge University Press, 2004.
- [8] C. Rovelli and L. Smolin, “Discreteness of area and volume in quantum gravity,” *Nucl. Phys.* **B442** (1995) 593–622, [arXiv:gr-qc/9411005](#).
- [9] M. Bojowald and H. A. Morales-Tecotl, “Cosmological applications of loop quantum gravity,” *Lect. Notes Phys.* **646** (2004) 421–462, [arXiv:gr-qc/0306008](#).
- [10] C. Rovelli, “Black Hole Entropy from loop quantum gravity,” *Phys. Rev. Lett.* **77** (1996) 3288–3291.
- [11] A. Ashtekar, J. Baez, A. Corichi, and K. Krasnov, “Quantum geometry and black hole entropy,” *Phys. Rev. Lett.* **80** (1998) 904–907, [arXiv:gr-qc/9710007](#).
- [12] A. Ashtekar, J. C. Baez, and K. Krasnov, “Quantum geometry of isolated horizons and black hole entropy,” *Adv. Theor. Math. Phys.* **4** (2000) 1–94, [arXiv:gr-qc/0005126](#).
- [13] K. A. Meissner, “Black hole entropy in loop quantum gravity,” *Class. Quant. Grav.* **21** (2004) 5245–5252, [arXiv:gr-qc/0407052](#).
- [14] M. Bojowald, “Absence of a Singularity in Loop Quantum Cosmology,” *Phys. Rev. Lett.* **86** (2001) 5227–5230.
- [15] J. Engle, E. Livine, R. Pereira, and C. Rovelli, “LQG vertex with finite Immirzi parameter,” *Nucl. Phys.* **B799** (2008) 136–149, [arXiv:0711.0146 \[gr-qc\]](#).
- [16] K. Noui and A. Perez, “Three dimensional loop quantum gravity: Physical scalar product and spin foam models,” *Class. Quantum Grav* **22** (2005) 1739–1761.

-
- [17] R. Oeckl, “A general boundary formulation for quantum mechanics and quantum gravity,” *Phys. Lett.* **B575** (2003) 318–324, [arXiv:hep-th/0306025](#).
- [18] E. Alesci and C. Rovelli, “The complete LQG propagator: I. Difficulties with the Barrett-Crane vertex,” *Phys. Rev.* **D76** (2007) 104012, [arXiv:0708.0883 \[gr-qc\]](#).
- [19] E. Alesci, E. Bianchi, E. Magliaro, and C. Perini, “Asymptotics of LQG fusion coefficients,” (2008) , [arXiv:0809.3718](#).
- [20] E. Magliaro, C. Perini, and C. Rovelli, “Numerical indications on the semiclassical limit of the flipped vertex,” *Class. Quant. Grav.* **25** (2008) 095009, [arXiv:0710.5034 \[gr-qc\]](#).
- [21] E. Alesci, E. Bianchi, E. Magliaro, and C. Perini, “Intertwiner dynamics in the flipped vertex,” [arXiv:0808.1971](#).
- [22] P. A. M. Dirac, *Lectures on Quantum Mechanics*. Belfer Graduate School of Science Monograph Series. Belfer Graduate School of Science, Yeshiva University, New York, 1964.
- [23] P. Bergmann, “Conservation Laws in General Relativity as the Generators of Coordinate Transformations,” *Phys. Rev.* **112** (1958) 287.
- [24] P. Bergmann, “Observables in General Relativity,” *Rev. Mod. Phys.* **33** (1961) 510–514.
- [25] P. Bergmann and A. Komar, “The phase space formulation of general relativity and approaches towards quantization,” *Gen. Rel. Grav.* **1** (1981) 227–254.
- [26] A. Komar, “General relativistic observables via Hamilton Jacobi functionals,” *Phys. Rev.* **D4** (1971) 923–927.
- [27] P. A. M. Dirac, “The theory of gravitation in Hamiltonian form,” *Phys. Rev.* **114** (1959) 924.
- [28] R. M. Wald, *General Relativity*. University of Chicago Press, 1984.
- [29] R. L. Arnowitt, S. Deser, and C. W. Misner, “The dynamics of general relativity,” [arXiv:gr-qc/0405109](#).
- [30] A. Perez, “Introduction to Loop Quantum Gravity and Spin Foams,” *gr-qc/0409061* (2004) .
- [31] A. Ashtekar, “New Hamiltonian formulation of general relativity,” *Phys. Rev. D* **36** (Sep, 1987) 1587–1602.
- [32] J. F. Barbero, “From euclidean to lorentzian general relativity: The real way,” *Phys. Rev.* **D54** (1996) 1492–1499.
- [33] J. F. Barbero, “Real ashtekar variables for lorentzian signature space times,” *Phys. Rev.* **D51** (1995) 5507–5510.
- [34] J. F. Barbero, “A real polynomial formulation of general relativity in terms of connections,” *Phys. Rev.* **D49** (1994) 6935–6938.

-
- [35] G. Immirzi, “Real and complex connections for canonical gravity,” *Class. Quant. Grav.* **14** (1997) L177–L181.
- [36] A. Ashtekar and J. Lewandowski, “Projective techniques and functional integration,” *J. Math. Phys.* **36** (1995) 2170.
- [37] C. Rovelli and L. Smolin, “Spin Networks and quantum gravity,” *Phys. Rev.* **D52** (1995) 5742–5759.
- [38] J. Baez, “Spin network states in gauge theory,” *Adv. Math.* **117** (1996) 253–272.
- [39] N. Grott and c. Rovelli, “Moduli spaces structure of knots with intersections,” *J. Math. Phys* **37** (1996) 3014.
- [40] W. Fairbain and C. Rovelli, “Separable Hilbert space in loop quantum gravity,” *J. Math. Phys* **45** (2004) 2802.
- [41] N. Grott and C. Rovelli, “Moduli spaces structure of knots with intersections,” *J. Math. Phys* **37** (1996) 3014.
- [42] W. Fairbain and C. Rovelli, “Separable Hilbert space in loop quantum gravity,” *J. Math. Phys* **45** (2004) 2802.
- [43] A. Ashtekar and J. Lewandowski, “Quantum theory of gravity i: Area operators,” *Class. Quant. Grav.* **14** (1997) A55–A81.
- [44] A. Ashtekar and J. Lewandowski, “Quantum theory of gravity ii: Volume operators,” [arXiv:gr-qc/9711031](https://arxiv.org/abs/gr-qc/9711031).
- [45] R. Loll, “Simplifying the spectral analysis of the volume operator,” *Nucl. Phys. B* **B500** (1997) 405–420.
- [46] R. Loll, “Spectrum of the volume operator in quantum gravity,” *Nucl. Phys. B* **B460** (1996) 143–154.
- [47] R. Loll, “The volume operator in discretized quantum gravity,” *Phys. Rev. Lett.* **75** (1995) 3048–3051.
- [48] T. Thiemann, “Closed formula for the matrix elements of the volume operator in canonical quantum gravity,” *Nucl. Phys. B* **39** (1998) 3347–3371.
- [49] T. Thiemann, “Quantum spin dynamics (qsd),” *Class. Quant. Grav.* **15** (1998) 839–873.
- [50] T. Thiemann, “Anomaly-free formulation of non-perturbative, four-dimensional lorentzian quantum gravity,” *Phys. Lett. B* **380** (1998) 257.
- [51] T. Thiemann, “Gauge field theory coherent states (gcs) : I. general properties,” *Class. Quant. Grav.* **18** (2001) 2025.
- [52] T. Thiemann, “Quantum spin dynamics VIII. The Master Constraint,” *Class. Quant. Grav.* **23** (2006) 2249–2266.

-
- [53] A. Ashtekar and J. Lewandowski, “Background independent quantum gravity: A status report,” *Class. Quant. Grav.* **21** (2004) R53, [arXiv:gr-qc/0404018](#).
- [54] M. P. Reisenberger, “World sheet formulations of gauge theories and gravity,” [arXiv:gr-qc/9412035](#).
- [55] J. Engle, R. Pereira, and C. Rovelli, “Loop-Quantum-Gravity Vertex Amplitude,” *Phys. Rev. Lett.* **99** (2001) 161301.
- [56] E. R. Livine and S. Speziale, “A new spinfoam vertex for quantum gravity,” *Phys. Rev.* **D76** (2007) 084028, [arXiv:0705.0674 \[gr-qc\]](#).
- [57] L. Freidel and K. Krasnov, “A New Spin Foam Model for 4d Gravity,” *Class. Quant. Grav.* **25** (2008) 125018, [arXiv:0708.1595 \[gr-qc\]](#).
- [58] J. C. Baez, “Spin foam models,” *Class. Quant. Grav.* **15** (1998) 1827–1858.
- [59] A. Perez, “Spin foam models for quantum gravity,” *Class. Quant. Grav.* **20** (2003) R43, [arXiv:gr-qc/0301113](#).
- [60] J. Halliwell and J. B. Hartle, “Wave functions constructed from an invariant sum over histories satisfy constraints,” *Phys. Rev.* **D43** (1991) 1170–1194.
- [61] C. Rovelli and M. Reisenberger, “Spacetime states and covariant quantum theory,” *Phys. Rev. D* **65** (2002) 125016.
- [62] R. Livine, Etera, A. Perez, and C. Rovelli, “2d manifold-independent spinfoam theory,” *Class. Quant. Grav.* **20** (2003) 4425–4445.
- [63] W. J. Fairbairn and A. Perez, “Extended matter coupled to BF theory,” *Phys. Rev.* **D78** (2008) 024013, [arXiv:0709.4235 \[gr-qc\]](#).
- [64] C. Rovelli, “The projector on physical states in loop quantum gravity,” *Phys. Rev. D* **59** (1999) 104015.
- [65] M. Reisenberger and C. Rovelli, ““sum over surfaces” form of loop quantum gravity,” *Phys. Rev. D* **56** (1997) 3490–3508.
- [66] M. Reisenberger and C. Rovelli, “Spacetime as a feynman diagram: the connection formulation,” [arXiv:gr-qc/0002083](#).
- [67] c. Petronio and R. De Pietri, “Feynman diagrams of generalized matrix models and the associated manifolds in dimension 4,” *J. Math. Phys.* **41** (2000) 6671–6688.
- [68] A. Mikovic, “Quantum field theory of spin networks,” *Class. Quant. Grav.* **18** (2001) 2827–2850.
- [69] D. Oriti, “The group field theory approach to quantum gravity,” [arXiv:gr-qc/0607032](#).
- [70] T. Regge, “General relativity without coordinates,” *Nuovo Cim.* (1961) .

-
- [71] G. Ponzano and T. Regge, “Semiclassical limit of Racah coefficients,”. Spectroscopic and Group Theoretical Methods in Physics, edited by F. Block (North Holland, Amsterdam, 1968).
- [72] J. W. Barrett and L. Crane, “Relativistic spin networks and quantum gravity,” *J. Math. Phys.* **39** (1998) 3296–3302.
- [73] J. W. Barrett and L. Crane, “A lorentzian signature model for quantum general relativity,” *Class. Quant. Grav.* **17** (2000) 3101–3118.
- [74] L. Crane and D. N. Yetter, “On the Classical Limit of the Balanced State Sum,” [arXiv:gr-qc/9712087](https://arxiv.org/abs/gr-qc/9712087).
- [75] J. W. Barrett and R. M. Williams, “The asymptotics of an amplitude for the 4-simplex,” *Adv. Theor. Math. Phys.* **3** (1999) 209–215, [arXiv:gr-qc/9809032](https://arxiv.org/abs/gr-qc/9809032).
- [76] J. C. Baez, J. D. Christensen, and G. Egan, “Asymptotics of 10j symbols,” *Class. Quant. Grav.* **19** (2002) 6489, [arXiv:gr-qc/0208010](https://arxiv.org/abs/gr-qc/0208010).
- [77] L. Freidel and D. Louapre, “Asymptotics of 6j and 10j symbols,” *Class. Quant. Grav.* **20** (2003) 1267–1294, [arXiv:hep-th/0209134](https://arxiv.org/abs/hep-th/0209134).
- [78] J. W. Barrett and C. M. Steele, “Asymptotics of relativistic spin networks,” *Class. Quant. Grav.* **20** (2003) 1341–1362, [arXiv:gr-qc/0209023](https://arxiv.org/abs/gr-qc/0209023).
- [79] E. Alesci and C. Rovelli, “The complete LQG propagator: I. Difficulties with the Barrett-Crane vertex,” *Phys. Rev.* **D76** (2007) 104012, [arXiv:0708.0883](https://arxiv.org/abs/0708.0883) [gr-qc].
- [80] S. Holst, “Barbero’s Hamiltonian derived from a generalized Hilbert- Palatini action,” *Phys. Rev.* **D53** (1996) 5966–5969, [arXiv:gr-qc/9511026](https://arxiv.org/abs/gr-qc/9511026).
- [81] E. R. Livine, “Projected spin networks for Lorentz connection: Linking spin foams and loop gravity,” *Class. Quant. Grav.* **19** (2002) 5525–5542.
- [82] S. Alexandrov, “Spin foam model from canonical quantization,” *Phys. Rev. D* **77** (2008) 024009, [arXiv:0705.3892](https://arxiv.org/abs/0705.3892).
- [83] E. Bianchi and A. Satz, “Semiclassical regime of Regge calculus and spin foams,” *Nucl. Phys.* **B808** (2009) 546–568, [arXiv:0808.1107](https://arxiv.org/abs/0808.1107) [gr-qc].
- [84] F. Conrady and L. Freidel, “On the semiclassical limit of 4d spin foam models,” *Phys. Rev.* **D78** (2008) 104023, [arXiv:0809.2280](https://arxiv.org/abs/0809.2280) [gr-qc].
- [85] A. Yutsin, I. Levinson, and V. Vanagas, *Mathematical Apparatus of the Theory of Angular Momentum*. Israel Program for Scientific Translation, Jerusalem, Israel, 1962.
- [86] D. Varshalovich, A. N. Moskalev, and V. K. Khersonskii, “Quantum Theory of Angular Momentum,”. (World Scientific Pub., 1988).

-
- [87] C. Rovelli and S. Speziale, “A semiclassical tetrahedron,” *Class. Quant. Grav.* **23** (2006) 5861–5870, [arXiv:gr-qc/0606074](#).
- [88] J. Engle, R. Pereira, and C. Rovelli, “Flipped spinfoam vertex and loop gravity,” *Nucl. Phys.* **B798** (2008) 251–290, [arXiv:0708.1236 \[gr-qc\]](#).
- [89] J. D. Christensen and G. Egan, “An efficient algorithm for the Riemannian 10j symbols,” *Class. Quant. Grav.* **19** (2002) 1185, [arXiv:gr-qc/0110045](#).
- [90] I. Khavkine, “Evaluation of new spin foam vertex amplitudes,” [arXiv:0809.3190 \[gr-qc\]](#).
- [91] C. Rovelli, “Graviton propagator from background-independent quantum gravity,” *Phys. Rev. Lett.* **97** (2006) 151301, [arXiv:gr-qc/0508124](#).
- [92] E. Bianchi, L. Modesto, C. Rovelli, and S. Speziale, “Graviton propagator in loop quantum gravity,” *Class. Quant. Grav.* **23** (2006) 6989–7028, [arXiv:gr-qc/0604044](#).
- [93] E. R. Livine and S. Speziale, “Group integral techniques for the spinfoam graviton propagator,” *JHEP* **11** (2006) 092, [arXiv:gr-qc/0608131](#).
- [94] E. Alesci and C. Rovelli, “The complete LQG propagator: II. Asymptotic behavior of the vertex,” *Phys. Rev.* **D77** (2008) 044024, [arXiv:0711.1284 \[gr-qc\]](#).
- [95] E. Alesci, E. Bianchi, and C. Rovelli, “LQG propagator: III. The new vertex,” *Class. Quant. Grav.* **26** (2009) 215001, [arXiv:0812.5018 \[gr-qc\]](#).
- [96] E. Bianchi, E. Magliaro, and C. Perini, “LQG propagator from the new spin foams,” *Nucl. Phys.* **B822** (2009) 245–269, [arXiv:0905.4082 \[gr-qc\]](#).
- [97] F. Conrady and L. Freidel, “Quantum geometry from phase space reduction,” [arXiv:0902.0351 \[gr-qc\]](#).
- [98] L. Freidel, K. Krasnov, and E. R. Livine, “Holomorphic Factorization for a Quantum Tetrahedron,” [arXiv:0905.3627 \[hep-th\]](#).
- [99] S. Speziale, “Twisted geometries: a geometric parametrization of $SU(2)$ phase space,” *talk given at Loops 2009 in Beijing*.
- [100] L. Freidel and S. Speziale, “Twisted geometries: A geometric parametrisation of $SU(2)$ phase space,” [arXiv:1001.2748 \[gr-qc\]](#).
- [101] T. Thiemann, “Gauge field theory coherent states (GCS). I: General properties,” *Class. Quant. Grav.* **18** (2001) 2025–2064, [arXiv:hep-th/0005233](#).
- [102] T. Thiemann and O. Winkler, “Gauge field theory coherent states (GCS). II: Peakedness properties,” *Class. Quant. Grav.* **18** (2001) 2561–2636, [arXiv:hep-th/0005237](#).
- [103] T. Thiemann and O. Winkler, “Gauge field theory coherent states (GCS) III: Ehrenfest theorems,” *Class. Quant. Grav.* **18** (2001) 4629–4682, [arXiv:hep-th/0005234](#).

-
- [104] T. Thiemann and O. Winkler, “Gauge field theory coherent states (GCS). IV: Infinite tensor product and thermodynamical limit,” *Class. Quant. Grav.* **18** (2001) 4997–5054, [arXiv:hep-th/0005235](#).
- [105] H. Sahlmann, T. Thiemann, and O. Winkler, “Coherent states for canonical quantum general relativity and the infinite tensor product extension,” *Nucl. Phys.* **B606** (2001) 401–440, [arXiv:gr-qc/0102038](#).
- [106] T. Thiemann, “Complexifier coherent states for quantum general relativity,” *Class. Quant. Grav.* **23** (2006) 2063–2118, [arXiv:gr-qc/0206037](#).
- [107] B. Bahr and T. Thiemann, “Gauge-invariant coherent states for Loop Quantum Gravity I: Abelian gauge groups,” *Class. Quant. Grav.* **26** (2009) 045011, [arXiv:0709.4619 \[gr-qc\]](#).
- [108] B. Bahr and T. Thiemann, “Gauge-invariant coherent states for Loop Quantum Gravity II: Non-abelian gauge groups,” *Class. Quant. Grav.* **26** (2009) 045012, [arXiv:0709.4636 \[gr-qc\]](#).
- [109] C. Flori and T. Thiemann, “Semiclassical analysis of the Loop Quantum Gravity volume operator: I. Flux Coherent States,” [arXiv:0812.1537 \[gr-qc\]](#).
- [110] C. Flori, “Semiclassical analysis of the Loop Quantum Gravity volume operator: Area Coherent States,” [arXiv:0904.1303 \[gr-qc\]](#).
- [111] B. C. Hall, “The Segal-Bargmann Coherent State Transform for Compact Lie Groups,” *J. Funct. Anal.* **122** (1994) 103–151.
- [112] A. Ashtekar, J. Lewandowski, D. Marolf, J. Mourao, and T. Thiemann, “Coherent state transforms for spaces of connections,” *J. Funct. Anal.* **135** (1996) 519–551, [arXiv:gr-qc/9412014](#).
- [113] J. C. Baez and J. W. Barrett, “The quantum tetrahedron in 3 and 4 dimensions,” *Adv. Theor. Math. Phys.* **3** (1999) 815–850, [arXiv:gr-qc/9903060](#).
- [114] E. Bianchi, E. Magliaro, and C. Perini, “Coherent spin-networks,” [arXiv:0912.4054 \[gr-qc\]](#).
- [115] B. C. Hall, “Geometric quantization and the generalized Segal-Bargmann transform for Lie groups of compact type,” *Comm. Math. Phys.* **226** (2002) 233–268.
- [116] M. Carmeli, *Group Theory and General Relativity: Representations of the Lorentz Group and Their Applications to the Gravitational Field*. Imperial College Press, 2000.
- [117] E. Bianchi, “Loop Quantum Gravity a la Aharonov-Bohm,” [arXiv:0907.4388 \[gr-qc\]](#).
- [118] L. Modesto and C. Rovelli, “Particle Scattering in Loop Quantum Gravity,” *Phys. Rev. Lett.* **95** (2005) 191301.
- [119] F. Conrady and C. Rovelli, “Generalized Schroedinger equation in Euclidean field theory,” *Int. J. Mod. Phys.* **A19** (2004) 4037–4068, [arXiv:hep-th/0310246](#).

-
- [120] L. Doplicher, “Generalized Tomonaga-Schwinger equation from the Hadamard formula,” *Phys. Rev.* **D70** (2004) 064037, [arXiv:gr-qc/0405006](#).
- [121] F. Conrady, L. Doplicher, R. Oeckl, C. Rovelli, and M. Testa, “Minkowski vacuum in background independent quantum gravity,” *Phys. Rev.* **D69** (2004) 064019, [arXiv:gr-qc/0307118](#).
- [122] S. Speziale, “Towards the graviton from spinfoams: The 3d toy model,” *JHEP* **05** (2006) 039, [arXiv:gr-qc/0512102](#).
- [123] E. R. Livine, S. Speziale, and J. L. Willis, “Towards the graviton from spinfoams: Higher order corrections in the 3d toy model,” *Phys. Rev.* **D75** (2007) 024038, [arXiv:gr-qc/0605123](#).
- [124] D. Colosi *et al.*, “Background independence in a nutshell: The dynamics of a tetrahedron,” *Class. Quant. Grav.* **22** (2005) 2971–2990, [arXiv:gr-qc/0408079](#).
- [125] E. Magliaro, C. Perini, and C. Rovelli, “Compatibility of radial, Lorenz, and harmonic gauges,” *Phys. Rev.* **D76** (2007) 084031.
- [126] V. A. Fock, “Proper time in classical and quantum mechanics,” *Sov. Phys.* **12** (1937) 044.
- [127] J. Schwinger, “On gauge invariance and vacuum polarization,” *Phys. Rev.* **82** (1952) 684.
- [128] P. Menotti, G. Modanese, and D. Seminara, “The radial gauge propagators in quantum gravity,” *Ann. Phys.* **224** (1993) 110, [arXiv:hep-th/9209028](#).
- [129] G. Modanese, “The propagator in the radial gauge,” *J. Math. Phys.* **33** (1992) 1523.
- [130] S. Leupold and H. Weigert, “Radial propagators and Wilson loops,” *Phys. Rev.* **D54** (1996) 7695–7709, [arXiv:hep-th/9604015](#).
- [131] S. Leupold, “Feynman rules in radial gauge,” [arXiv:hep-th/9609222](#).
- [132] M. J. G. Veltman, “Quantum Theory of Gravitation,”. In *Les Houches 1975, Proceedings, Methods In Field Theory*, Amsterdam 1976, 265-327.
- [133] J. F. Donoghue, “General relativity as an effective field theory: The leading quantum corrections,” *Phys. Rev.* **D50** (1994) 3874–3888, [arXiv:gr-qc/9405057](#).
- [134] C. P. Burgess, “Quantum gravity in everyday life: General relativity as an effective field theory,” *Living Rev. Rel.* **7** (2004) 5, [arXiv:gr-qc/0311082](#).
- [135] E. Bianchi and L. Modesto, “The perturbative Regge-calculus regime of Loop Quantum Gravity,” *Nucl. Phys.* **B796** (2008) 581–621, [arXiv:0709.2051 \[gr-qc\]](#).
- [136] J. D. Christensen, E. R. Livine, and S. Speziale, “Numerical evidence of regularized correlations in spin foam gravity,” [arXiv:0710.0617 \[gr-qc\]](#).
- [137] S. Speziale, “Background-free propagation in loop quantum gravity,” *Adv. Sci. Lett.* **2** (2009) 280–290, [arXiv:0810.1978 \[gr-qc\]](#).

-
- [138] R. Oeckl, “General boundary quantum field theory: Foundations and probability interpretation,” *Adv. Theor. Math. Phys.* **12** (2008) 319–352, [arXiv:hep-th/0509122](#).
- [139] J. W. Barrett and L. Crane, “Relativistic spin networks and quantum gravity,” *J. Math. Phys.* **39** (1998) 3296–3302, [arXiv:gr-qc/9709028](#).
- [140] V. Bonzom, E. R. Livine, M. Smerlak, and S. Speziale, “Towards the graviton from spinfoams: the complete perturbative expansion of the 3d toy model,” [arXiv:0802.3983 \[gr-qc\]](#).
- [141] J. Engle, R. Pereira, and C. Rovelli, “The loop-quantum-gravity vertex-amplitude,” *Phys. Rev. Lett.* **99** (2007) 161301, [arXiv:0705.2388 \[gr-qc\]](#).
- [142] E. Magliaro, C. Perini, and C. Rovelli, “Numerical indications on the semiclassical limit of the flipped vertex,” *Class. Quant. Grav.* **25** (2008) 095009, [arXiv:0710.5034 \[gr-qc\]](#).
- [143] E. Alesci, E. Bianchi, E. Magliaro, and C. Perini, “Intertwiner dynamics in the flipped vertex,” *Class. Quant. Grav.* **26** (2009) 185003, [arXiv:0808.1971 \[gr-qc\]](#).
- [144] I. Khavkine, “Evaluation of new spin foam vertex amplitudes,” *Class. Quant. Grav.* **26** (2009) 125012, [arXiv:0809.3190 \[gr-qc\]](#).
- [145] I. Khavkine, “Evaluation of new spin foam vertex amplitudes with boundary states,” [arXiv:0810.1653 \[gr-qc\]](#).
- [146] F. Conrady and L. Freidel, “Path integral representation of spin foam models of 4d gravity,” [arXiv:0806.4640 \[gr-qc\]](#).
- [147] J. W. Barrett, R. J. Dowdall, W. J. Fairbairn, H. Gomes, and F. Hellmann, “Asymptotic analysis of the EPRL four-simplex amplitude,” *J. Math. Phys.* **50** (2009) 112504, [arXiv:0902.1170 \[gr-qc\]](#).
- [148] J. W. Barrett, R. J. Dowdall, W. J. Fairbairn, F. Hellmann, and R. Pereira, “Lorentzian spin foam amplitudes: graphical calculus and asymptotics,” [arXiv:0907.2440 \[gr-qc\]](#).
- [149] C. Rovelli and L. Smolin, “Discreteness of area and volume in quantum gravity,” *Nucl. Phys. B* **442** (1995) 593–619.
- [150] A. Ashtekar and J. Lewandowski, “Quantum theory of geometry. I: Area operators,” *Class. Quant. Grav.* **14** (1997) A55–A82, [arXiv:gr-qc/9602046](#).
- [151] A. Ashtekar and J. Lewandowski, “Quantum theory of geometry. II: Volume operators,” *Adv. Theor. Math. Phys.* **1** (1998) 388–429, [arXiv:gr-qc/9711031](#).
- [152] A. Ashtekar, A. Corichi, and J. A. Zapata, “Quantum theory of geometry. III: Non-commutativity of Riemannian structures,” **15** (1998) 2955–2972, [gr-qc/9806041](#).
- [153] S. A. Major, “Operators for quantized directions,” *Class. Quant. Grav.* **16** (1999) 3859–3877, [arXiv:gr-qc/9905019](#).

-
- [154] T. Thiemann, “A length operator for canonical quantum gravity,”
J. Math. Phys. **39** (1998) 3372–3392, [arXiv:gr-qc/9606092](#).
- [155] E. Bianchi, “The length operator in Loop Quantum Gravity,” [arXiv:0806.4710 \[gr-qc\]](#). to appear in *Nucl. Phys.* **B**.
- [156] T. Regge, “GENERAL RELATIVITY WITHOUT COORDINATES,”
Nuovo Cim. **19** (1961) 558–571.
- [157] J. W. Barrett, M. Rocek, and R. M. Williams, “A note on area variables in Regge calculus,”
Class. Quant. Grav. **16** (1999) 1373–1376, [arXiv:gr-qc/9710056](#).
- [158] L. Freidel, “Group field theory: An overview,” *Int. J. Theor. Phys.* **44** (2005) 1769–1783,
[arXiv:hep-th/0505016](#).
- [159] E. Alesci, E. Bianchi, E. Magliaro, and C. Perini, “Asymptotics of LQG fusion coefficients,”
[arXiv:0809.3718 \[gr-qc\]](#).
- [160] A. Ashtekar, L. Freidel, and C. Rovelli, “Recovering low energy physics: a discussion,”
International Loop Quantum Gravity Seminar (May 5th, 2009) .